Supervisor: Prof. Tapas Kumar Chatterjee
Co-supervisors: Prof. Jan van Bever Donker
Dr. Wasiu Adedayo Sonibare
Date: 15th June 2017

Source Rock Analysis, Thermal Maturation and Hydrocarbon Generation Modelling within the Southern Pletmos Basin, Offshore of South Africa

FRITZ A. AGBOR

UNIVERSITY *of the*
WESTERN CAPE

UNIVERSITY of the
WESTERN CAPE

THESIS PRESENTED TO THE DEPARTMENT OF EARTH SCIENCES

IN PARTIAL FULFILLMENT OF THE REQUIREMENTS

FOR THE DEGREE OF MASTER OF SCIENCE

IN PETROLEUM GEOLOGY

Declaration

I Fritz Ako Agbor confirm that to the best of my knowledge, except where reference is made herein, this thesis submitted for assessment is my own and expressed with my own words. Any uses within it if the works of other authors in any form (e.g. ideas, equations, figures, text, tables and programs) are properly acknowledge at point of their use. A list of references employed is also included. This thesis does not contain any material that has been written by another person or any previously published material that has been submitted to the University of the Western Cape or any other institution for the purpose of attaining a Master's degree.

Signed:

Date:

Copyright © 2017 University of Western Cape

All rights reserved

http://etd.uwc.ac.za/

Abstract

This study is a first attempt that integrates source rock geochemical evaluation, with analytic and numerical basin-modelling techniques to identify and ascertain the present-day configuration, spatial distributions, characteristics and hydrocarbon generative potentials of existing source rocks within the southern depocenter of the relatively frontier Pletmos sub-basin. Petroleum charge within the basin is proposed to have occurred during most of the Cenozoic Era. The investigation employed a forward modelling approach whereby models were calibrated through a combination of geological and geophysical datasets from 6 wells, and constrained by vitrinite reflectance and kinetic parameters.

Five Mesozoic source rocks ranging from Kimmeridgian to Turonian were identified based on results from Rock-Eval data analysis of 89 samples, performed by SOEKOR Ltd. The results demonstrate that TOC values range from 0.5 - 4.0 wt. % and is highest for the Aptian and lowest for the Kimmeridgian. HI values range from 23.7 – 499.5 (mg HC/g TOC) essentially indicating that they are predominated by type III (gas-prone) kerogens and, to a lesser extent contain mixed type II/I1I (oil/gas-prone). Thus, are considered as primarily gas-prone. Tmax values matched with recorded vitrinite reflectance (%VRo); they indicate that source rock maturities range from immature - late mature (dry gas).

Reconstructed burial and thermal histories permitted modelling of the thermal maturation and transformation ratios. Results show that maturity trends are in accordance with transformation ratios and they both increase away from the Superior High and generally attain a maximum at the southern portions of the modelled area. At present-day, maturities range from immature – late mature (dry gas) in accordance with the preliminary source rock evaluation results. As expected, the highest extent of kerogen transformation is exhibited by the deepest (oldest) buried Kimmeridgian source rock; the reverse is true for the youngest (mostly-immature) Turonian source rock. Three periods (i.e. ~98Ma, ~80Ma and ~60Ma) are predicted as critical moments for the Kimmeridgian, Valanginian/Hauterivan, and Aptian respectively, implying that hydrocarbon generation preceded charging and the modelled source rocks probably contributed to the hydrocarbons within the area.

Keywords: Basin Modelling**;** Rock–Eval pyrolysis; Kinetic parameters; Source rock evaluation; Burial history; Thermal maturation; Hydrocarbon generation

UNIVERSITY of the WESTERN CAPE

http://etd.uwc.ac.za/

Acknowledgements

First of all, I thank Prof. T.K Chatterjee and Prof. J.V.B Donker for their guidance and support dedicated towards me and the research project. Their understandings of my questions were always remarkable. Most especially I thank Dr. W.A. Sonibare and Mr. N.A. Teumahji of Schlumberger Ltd. Their expertise, ability to interpret information and solve problems, enthusiasm and guidance on the subject matter helped to make this study possible. I therefore, offer my sincere gratitude for their time. Working with them has been an honour!

My full-hearted gratitude goes to Ms. Sanelisiwe Mhlambi for her time, and the numerous fruitful discussions that aided in paving the way forwards during the technical difficulties. Moreover, for her patience, moral support, motivating spirit, and endless support which prevented this thesis research project from turning into a never ending story.

I also present my biggest thanks to the National Research Foundation (NRF) for its financial support, and the Petroleum Agency South Africa (PASA) and Petroleum Oil and Gas Corporation of South Africa (PetroSA) for providing the data used in the study.

Finally, I cannot be thankful enough to my family, especially my siblings who have given me endless support, love and encouragement throughout my life.

Above all, I thank God. Without whom, I would not be where I am today.

UNIVERSITY of the
WESTERN CAPE

"A pod of active source rock is the primary element of a petroleum system; staying close to a mature source rock where drilling success ratio is highest, best reduces risks ".

– Magoon and Dow, 1994

http://etd.uwc.ac.za/

Table of Contents

UNIVERSITY of the
WESTERN CAPE

http://etd.uwc.ac.za/

UNIVERSITY of the
WESTERN CAPE

http://etd.uwc.ac.za/

List of Figures

UNIVERSITY of the WESTERN CAPE

http://etd.uwc.ac.za/

UNIVERSITY of the
WESTERN CAPE

http://etd.uwc.ac.za/

List of Tables

UNIVERSITY of the
WESTERN CAPE

http://etd.uwc.ac.za/

CHAPTER 1

Introduction

1.1 Problem Definition and Rationale

In spite of its complex tectonic history, the relatively frontier Pletmos sub-basin remains a repository for some prominent organic-rich source rocks. These source rocks occur from the Kimmeridgian through to the Turonian (Mclachlan and McMillan, 1979; Davies et al., 1991; Brown et al., 1996 and McMillan et al., 1997). Hydrocarbon exploration success within the basin hinges on the characteristic organic matter (OM) contents, thermal maturity, generation potentials and expulsion efficiencies of these source rocks. Nonetheless, previous studies have mostly focused on the northern depocentre, and there exists paucity in published organic geochemical and modelling studies, particularly for the southern depocentre which constitutes the study area (Fig. 1.1).

The start of hydrocarbon exploration by Soekor (Pty) Ltd within the Pletmos sub-basin was in the 1970s (Brown et al., 1996) and has happened throughout recent decades. Accordingly, it has led to the discovery of gas and condensate, and the establishment of proven petroleum system(s) (McMillan et al., 1997; Roux, 1997). Albeit its proven potential, most drilled wells and targeted traps are found to be water-bearing and charging seems to have occurred preferentially within few selected layers and/or specific areas. These, along with the lack of information on the 3-D geometries and architectural configurations, subsurface spatial distributions, characteristics, geo-histories, maturity evolution, hydrocarbon generation potentials, and expulsion timing of the source rocks, which are yet to be established, constitute a major challenge, and are attributable to the unsuccessful exploration efforts within the basin.

This study attempts to integrate organic geochemistry (i.e. source rock analysis) and basin-modelling techniques, that have been successfully applied in the adjacent Bredasdorp Basin (e.g. Davies, 1997; Sonibare et al., 2015) to address the aforementioned problems. The focus is to establish the timing of hydrocarbon generation, to understand the source rock generative potential within the study area; which will aid in future play and prospect development.

UNIVERSITY of the WESTERN CAPE
http://etd.uwc.ac.za/

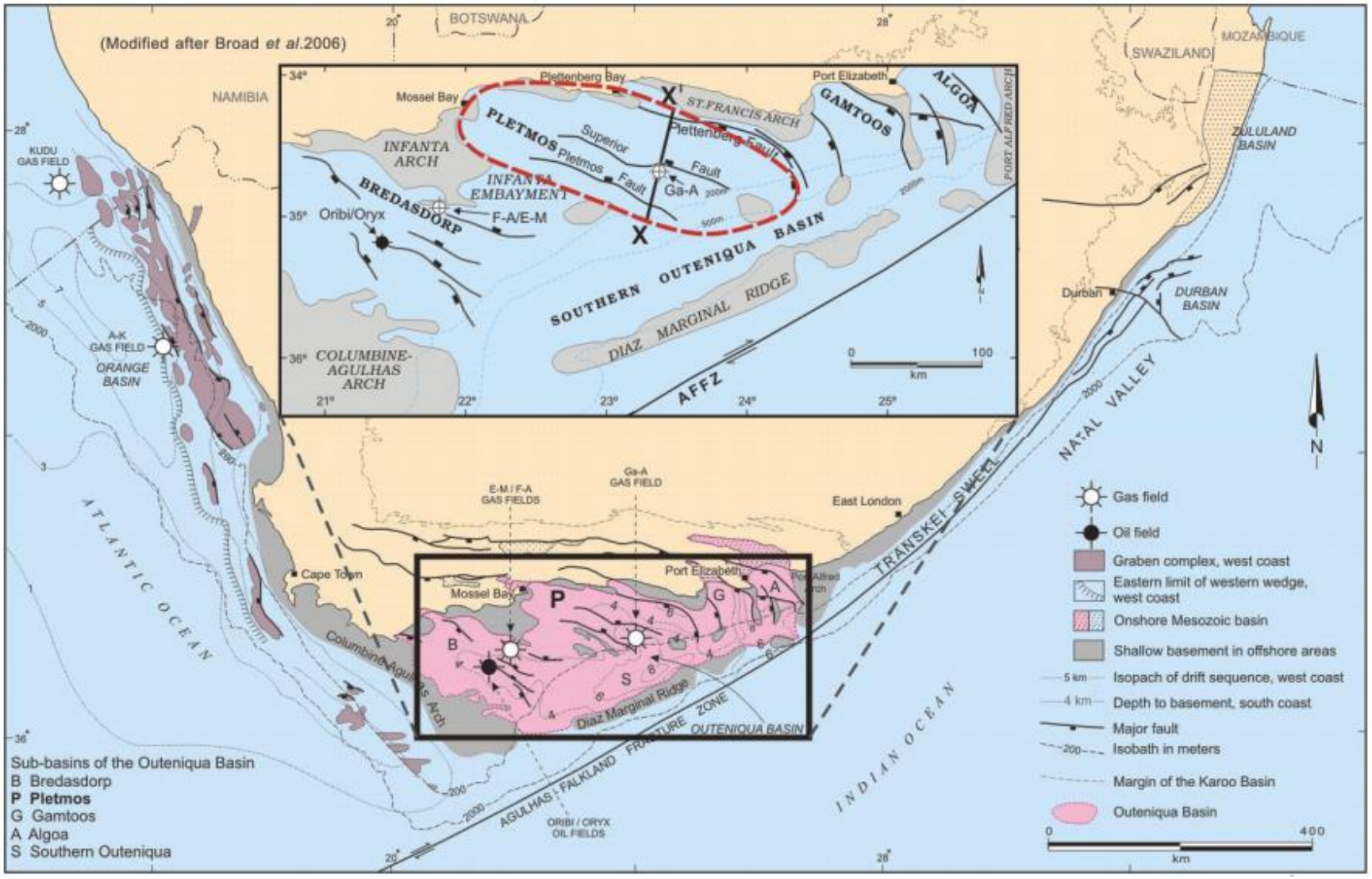

Figure 1.1: *Geological location map of the study area, encompassing the model location within the Pletmos Basin and tectonic province extents AFFZ – Agulhas-Falkland Fracture Zone adapted after* Roux and Davids, *(2009).*

http://etd.uwc.ac.za/

1.2 Thesis aims and Objectives

This current study has two main aims:

1. To provide a comprehensive understanding of the evolutionary histories and geographic extents of existing source rocks, and
2. To ascertain their organic richness, thermal maturity levels and hydrocarbon generative potentials.

As such, key study objectives are as follows;

- Evaluate the TOC, quality, burial extents, maturity, architectural configurations and spatial variations of the source rocks,
- Determine the thermal maturation histories, to establish the maturity trend distributions and cumulative source rock generation potentials,
- Determine the critical moments of hydrocarbon generation and expulsion, and
- Establish the impact of tectonism on the overall source rock potential within the area of study.

1.3 Thesis Organization

The thesis is organized into six mutually connected parts that lead to a conclusion. **Chapter 1** begins with a brief introduction and location of the study area. **Chapter 2** focuses on the reviews of previous works on the area; the geological setting, tectonic setting, sequence stratigraphy and depositional environments, petroleum system development, basin modelling & analytic tools, as well as related key geological principles. **Chapter 3** focuses on the research methodology (materials, methods and design). The result interpretations and discussions thereof are presented in **Chapter 4** and **Chapter 5,** respectively. **Chapter 6** has the conclusions, and ends with recommendations for future research.

UNIVERSITY of the
WESTERN CAPE

http://etd.uwc.ac.za/

Literature Review

2.1 Regional Tectonic Setting

The South-eastern continental margin, off the coast of South Africa encompasses a shelfal area of ~ 165000 km² across the southernmost tip of the African continent (Johnson et. al., 2006). This region of the margin is typified by an assemblage of taphrogenic (graben and half-graben rift) basin systems (Pletmos, Bredasdorp, Algoa, Gamtoos and Southern Outeniqua) collectively known as the Outeniqua Basin (Bally and Snelson, 1980; Dingle et al., 1983; McMillan et al., 1997; Broad et al., 2006; Fig. 2.1).

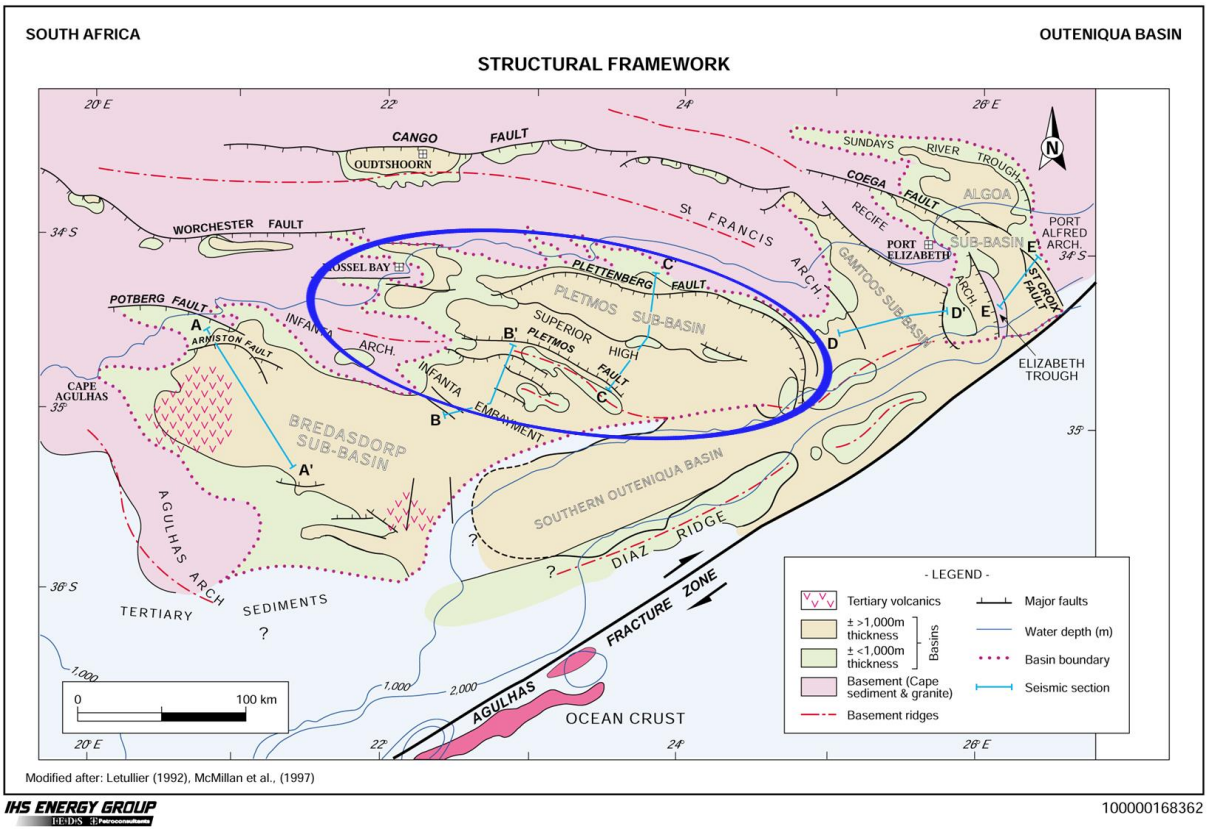

Figure 2.1: *Structural framework map of the Outeniqua basin, with blue circular line indicating the Pletmos sub-basin extends. Adapted from IHS basin report, (2010) and modified after Broad et al., (2006).*

The Outeniqua Basin is largely believed to have originated from the numerous lithospheric stretching, rift-and-drifting series of events (Gerrard and Smith, 1982; Edwards and Santogrossi, 1990) that are linked with the break-up of Gondwanaland. It is also thought to possess classic historic records of persistent right-lateral shear movements that characterized

http://etd.uwc.ac.za/

the mid-late Jurassic to early Cretaceous periods of the Early-Mesozoic era (Broad et al., 2006; Campher, 2010; Sonibare et al., 2014).

Moreover, the Outeniqua Basin is said to be underlain by pre-rift deposits (Dingle et al., 1983; Davies, 1997a; Sonibare et al., 2014), that are separated from each other by series of oblique normal faults (that transmutes to more listric faults eastwards) whose strike directions towards existing basement arches change gradually from east-west-trends in the Western sub-basins, to north-south-trends in the most Eastern sub-basins (McMillan et al., 1997; Thomson, 1998; Broad et al., 2006).

2.2 Tectonic Evolution

Particularly central to this study is the structural orientation within the Pletmos sub-basin (here onwards referred to as "the Basin"). The Basin, encompasses an area of ~ 190 km long and ~70km wide, and is structurally more intricate than its adjacent neighbouring Bredasdorp Basin (McMillan et al., 1997). It is sub-divided into two major local (northern and southern) depocenters by the complex Superior Fault (Fig.1.1; Fig. 2.1). These depocentres are mostly grabens bounded to the south and north by the Pletmos, Superior and Plettenberg Faults, respectively. Together, they are constrained to the North, by the highly faulted boundary parallel to the present shorelines, have a southern boundary that is ~ 200m southward of the deep isobathic southern Outeniqua Basin and extend towards the Agulhas-Falkland Fracture Zone (Fig. 2.1). It is bordered to the northeast and southwest, by the St. Francis Arch and Infanta Embayment respectively (Brown et al., 1996; Broad et al., 2004).

UNIVERSITY of the WESTERN CAPE

2.2.1 Syn-rift

In the Basin, associated rifting processes are largely believed to have been instigated in the south at ~136 Ma during the Middle–Late Jurassic (Brown et al., 1996; Broad et al., 2006), before propagating northwards at ~130 Ma. Initial rifting, began due to extension stresses initiating normal faulting which created the horst, graben and half-graben structures that are bordered by the Plettenberg, Superior, and Pletmos major normal faults, whose hanging wall movements are contemporaneous with sedimentation (Roux and Davids, 2009; McMillan et al., 1997). This rifting process was later supplemented by intense listric faulting, caused by dextral transtensional (strike-slip) movement along the AFFZ towards the north (e.g. Fig. 2.1; McMillan et al., 1997; Johnson et al., 2006). Terminations of substantial normal movements of the fault blocks associated with these faults were trailed by widespread uplift and enhanced subaerial erosion, during the Late Cretaceous which is marked by the second-order drift onset

http://etd.uwc.ac.za/

unconformity (6Atl). Even though subsequent strike-slip reactivation evident by facies changes is noted along the Superior Fault (Brown et al., 1996; McMillan et al., 1997), and in the north of this Fault, sedimentation rates declined substantially concurrently with the 6Atl phase of uplift subsequent to localized depositions at depocenters where fault-controlled subsidence continued to be the dominant tectonic control on sedimentation (McMillan et al., 1997; Roux and Davids, 2009).

2.2.2 Post-rift

Once the Falkland Plateau cleared the southern tip of the African plate, external stresses were released, and thermally driven subsidence began to dominate the basins' depocenters. Though, Late Cretaceous and Cenozoic extensional stresses, as well as minor perturbations, generated by the thermally driven subsidence processes at the time initiated many shallow normal faults. These faults locally reactivated movement along the major rift faults (McMillan et al., 1997; Broad et al., 2004). It is inferred in many cases that the 'post break-up' phase of the Basin (plus the other basins within the Outeniqua Basin), documented the passage of the African plate over the Shona and Bouvet mantle-related hotspots at ~ 80–60 Ma (Duncan, 1981; Martin, 1987; Gohl & Uenzelmann-Neben, 2001, cited in Sonibare et al., 2014). These mantle-related hotspot events have been alleged to have steered regional episodic uplifts and thermal variations during the late Cretaceous and early Tertiary periods (Bate and Malan, 1992; Davies, 1997b; Gohl & Uenzelmann-Ne-ben, 2001; Broad et al., 2006; Tinker et al., 2008). Similarly important was a plume development in Southern Africa, during late Miocene times; a post break-up event recognized as the 'African Superswell', and thought to have possibly instigated renewed lithospheric stretching of the basins (Nyblade and Robinson, 1994; Hartnady and Partridge, 1995; Nyblade, 2003; Sonibare et al., 2015), as well as resulting to the prominent Cenozoic tilting, uplift and basin erosion (Burden, 1992; Davies, 1997b; Roux, 2007).

Even so, previous studies by Davies (1997b) and Roux (2007) related to the above tectonic activities, advocate that eustatic fluctuations possibly instigated at least three main episodes of coastal retreat, coupled with a pause in active sedimentation, and dominant regional erosion during the early Paleocene, late Oligocene and late Miocene times (Dingle et al., 1983; McMillan et al., 1997; Davies, 1997a; Broad et al., 2006). It is interesting to note here that these Tertiary events are projected to have contributed significantly to the uplift, subsequent removal and deposition of considerable amount of sediments in different areas

http://etd.uwc.ac.za/

within the Basin (Burden, 1992; Davies, 1997b; Broad et al., 2006). Consequently, ensuing to a modern structural configuration, anticipated to have been designed from the amassed effects of mixed tectonic and sedimentary processes that range from continental break-up to uplift, subsidence, mantle dynamics, denudation, sediment dispersal and accretion (e.g. Sonibare et al., 2014) as detailed in Figure 2.2.

2.3 Basin Stratigraphy, Paleogeography and Depositional Environments

The absence of a complete drilled sequence, coupled with the rapid changes in earliest sediment facies of depocenter deeps, has hindered a full conception of the Basin's pre-rift history (McMillan et al. 1997). Nonetheless, based on drilled wells that extended into shallow basement, it is projected that the Ordovician to Devonian Cape Supergroup (Bokkeveld shales and slates) meta-clastics and metasandstones of the Table Mountain Group, lie beneath the syn-rift deposits (McMillan et al., 1997; Johnson et al., 2006).

Tectono-stratigraphically, the Basin consists mainly of two mega-sequences that can be linked to the syn-rift and post-rift tectonic phases. Existent syn-rift sequences have been delineated into the currently considered 'Syn-Rift 1' and 'Syn-Rift 2' packages (Roux and Davids, 2009). The 'Syn-Rift 1' package comprises sediments of a faulted block, which originated from rifting due to extensional reactivation of the Cape Fold Belt during the late Jurassic. Whereas 'Syn-Rift 2' package is regarded to have originated following the Valanginian transform processes along the Agulhas-Falkland Fracture Zone (AFFZ), during a second episode of rift tectonics that affected the western sub-basins, that is, Bredasdorp, Infanta Embayment and Pletmos (van der Merwe & Fouché, 1992; McMillan et al., 1997; Thomson, 1998).

UNIVERSITY of the
WESTERN CAPE

http://etd.uwc.ac.za/

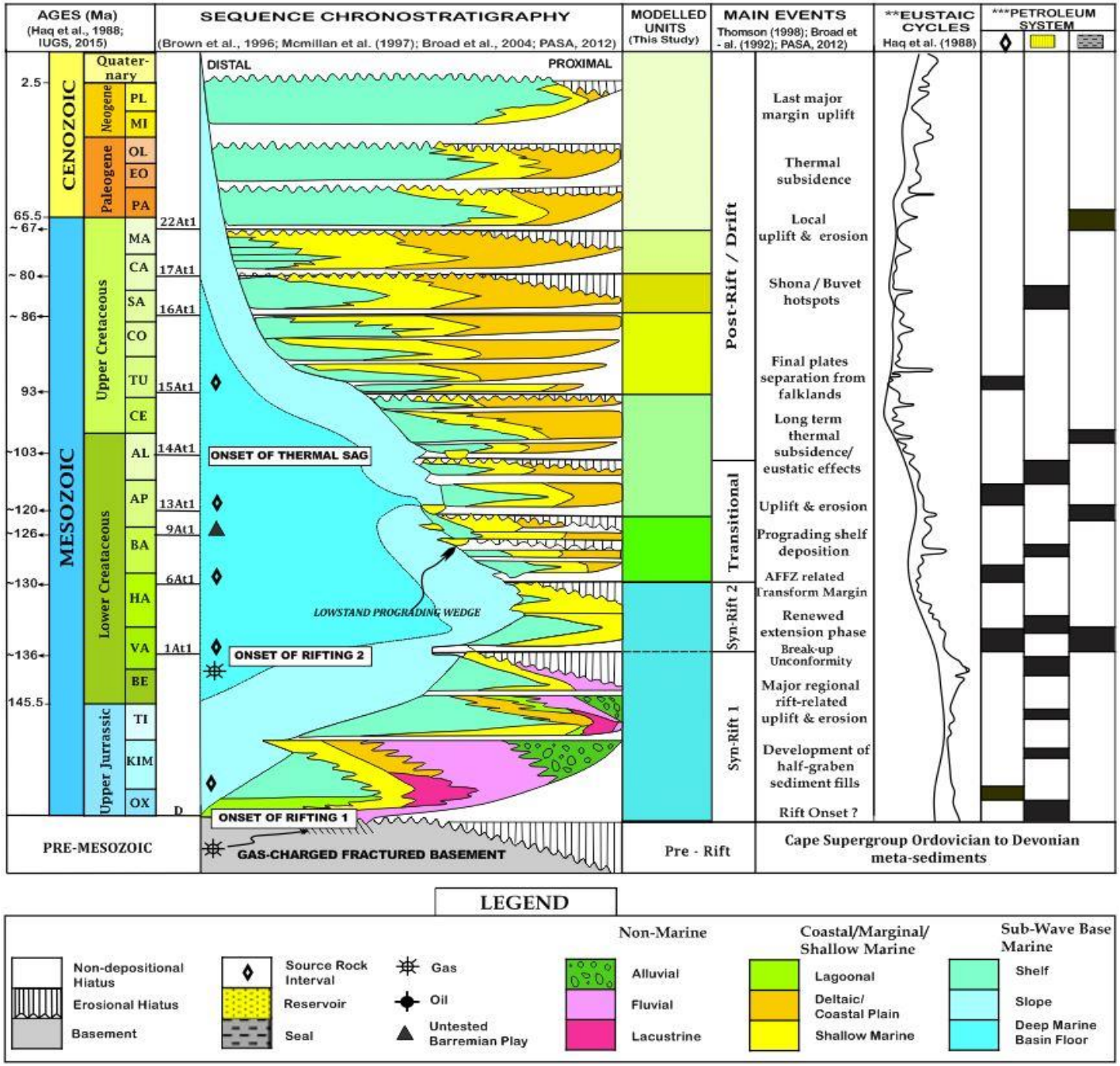

Figure 2.2: *Simplified chronostratigraphic and sequence chart of the Pletmos Basin detailing the ages and petroleum system elements incorporated in the numerical models.*

*** Haq et al. (1987); IUGS,(2015)*

**** Davies (1997a), Mc Millan et al. (1997), Thomson (1998), Broad et al. (1992, 2006), Roux (2007), PASA (2012) and this study*

http://etd.uwc.ac.za/

Initial sedimentation in the Basin occurred concurrently within the two major depocenters. Local extremely thick D-1Atl interval sediment accumulations notably occur in the most southern areas, such as: at the north of the Pletmos Fault, at the graben just south of the Plettenberg Fault and north of the Superior Fault (Fig.1.1; Fig. 2.1). These intervals are composed of shallow marine inner to outer shelf sandstones and claystones with localized non-marine (red and green) beds. Their deposition was followed by that of the 6A sequence, subsequent to the migration of sediment sources from the north to the northwest margin of the basin (Bate and Malan, 1992; McMillan et al., 1997; Broad et al., 2006; Roux, 2007). Above these intervals is the 6Atl unconformity, which marks a phase of uplift and erosion prior to deposition of a second, mainly deep marine, poorly oxygenated sequence (6Atl to 13Atl), that mainly consist of a mix of continental fluvio-lacustrine and shallow marine sediments (Dingle et al., 1983; Bate and Malan, 1992; McMillan et al., 1997; Broad et al., 2006).

The Syn-rift to post-rift transition phase of the basin began with the deposition of early post-rift sediments (Late Hauterivian – Mid Albian) above the 6At1 unconformity chiefly in intermediate marine environments (Brink et al., 1994). During this time most fluvial drainage systems were diverted, resulting to North-western and South-western high gradient streams, largely flowing southward towards the Northern (Plettenberg) graben depocenter due to the uplift. This happened concurrently with initially high but subsequently rapidly diminishing subsidence that permitted flooding along the Superior and Pletmos faults, which led to substantial expansion of the marine embayments within the depocenters. Simultaneously, transform movements along the AFFZ were still very prominent. This phase is characterized by the development of numerous basin floor fan complexes, during a major episode of drowning that resulted to the deposition a maximum flooding surface above the Early Aptian (13At) unconformity (Gouws, 1990; Brink et al., 1994; McMillan et al., 1997).

The Cretaceous post-rift paleogeography (Fig. 2.3) of the Basin was chiefly controlled by long-term tectonic phases that transpired between ~ 126 –117.5 Ma. Deposition during such period was mainly localized in the depocenters where fault subsidence continuously acted as the dominant tectonic control on sedimentation. The Post-rift successions (of Early Aptian (13At1) - Upper Cenomanian (15At1) and Upper Cenomanian (15At1) – Seafloor) that overlie the Syn-rift are comprised of deltaic and shallow – deep marine siliciclastics. These sequences displayed distinctive changes in their stacking geometries in response to a continued subsidence that resulted from post-rift thermal relaxation and possible eustatic

UNIVERSITY of the WESTERN CAPE
http://etd.uwc.ac.za/

effects during the late Albian to Cenozoic times. Episodic events that ensued fluctuations in depositions resulting from dynamics such as: increasing rates of subsidence and accommodation, plus to a lesser extent, variable rates of sediment supply and open marine activities. Producing accommodation space for the progradation and aggradation of interbedded argillaceous sediments of the typical passive margin shelf and slope deposits in the deltaic to shallow marine environments (McMillan et al., 1997; Broad et al., 2006; Roux, 2007; Roux and Davids, 2009).

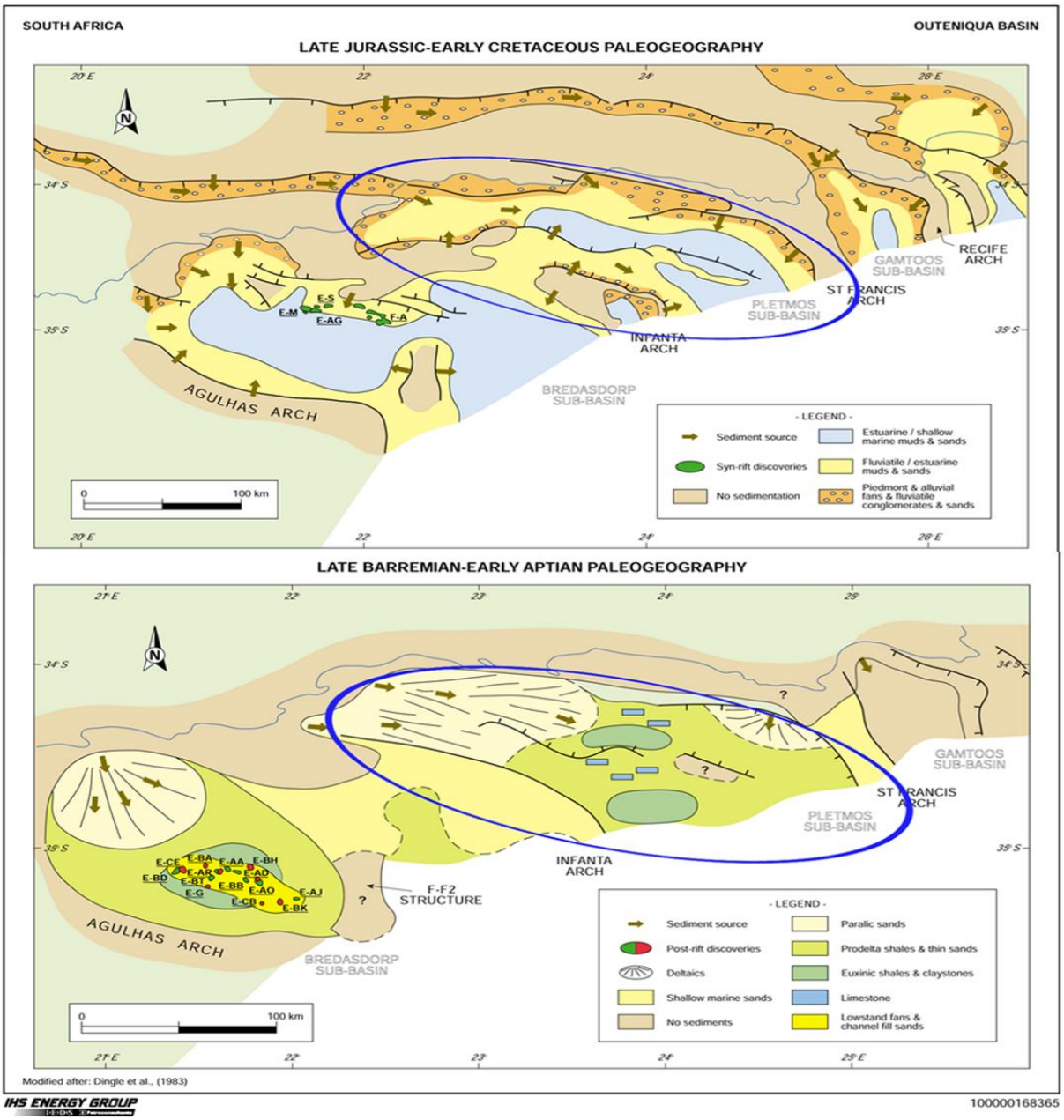

Figure 2.3: *Paleogeography orientations of the Outeniqua Basin, adapted from IHS basin report, (2010), with the blue circular line indicating the locating extent of the Pletmos sub-basin, modified after Dingle et al., (1983).*

http://etd.uwc.ac.za/

2.4 Source Rocks within the Pletmos basin

Usually source rocks are known to be formed by means of a combination between rapid sedimentation and upwelling, in anoxic to dysaerobic areas, where high organic matter productivity is preserved (Chinn, 1991). Drilling results within the Basin largely infer multiple existing shales with fair to good quality and varying kerogen types (Roux, 1997). These shales are generally considered to be the potential source rocks in the Pletmos Basin and generally follow an established regional trend (Roux, 1997; Roux and Davids, 2009; Fig. 2.4).

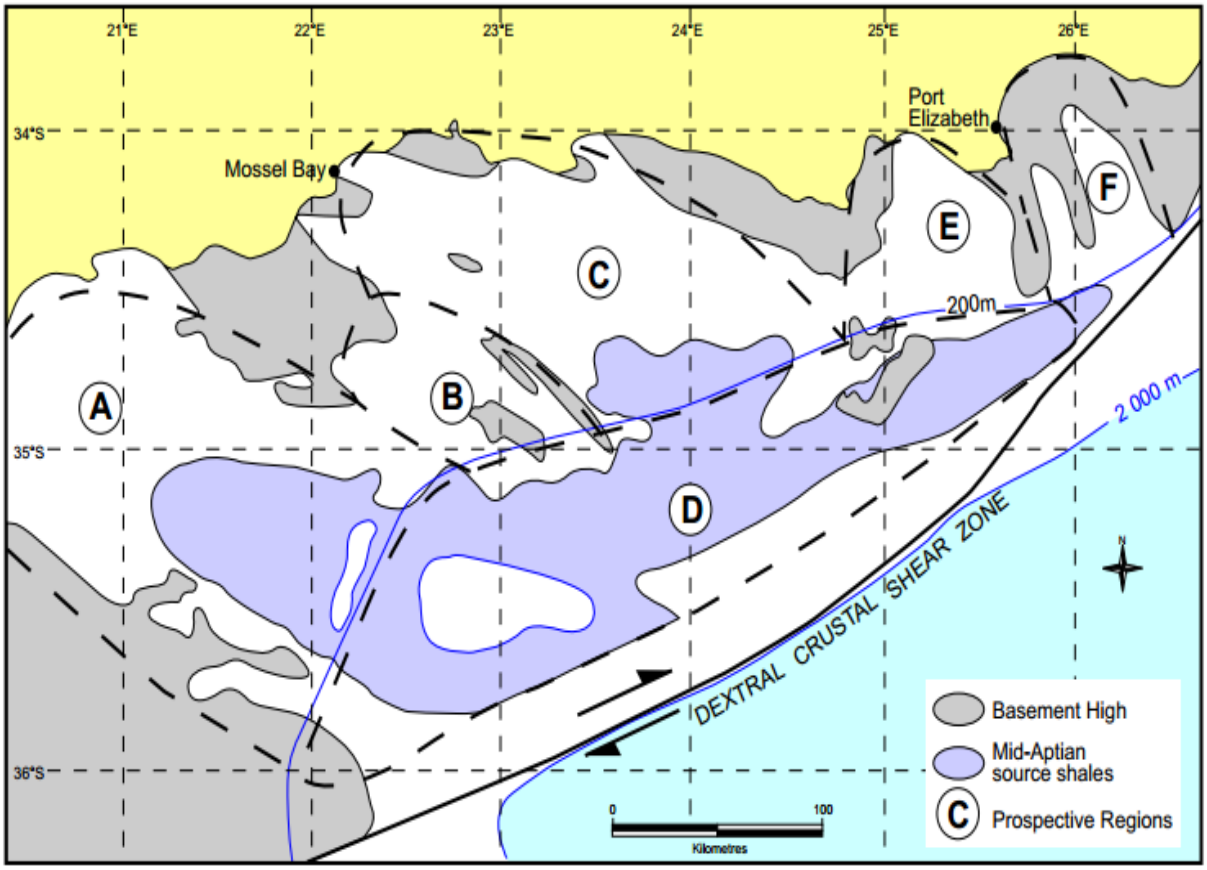

Figure 2.4: *Mid–Aptian source rock distribution across the Outeniqua Basin based on seismic profiles and well data, adapted from PASA (2010) after Broad et al., (2006).*

The conceptualized models for the region based on the available geological and geophysical data allude to the existence of various source rock formations to be in existence within the basin. These include the Kimmeridgian, Valanginian, Hauterivian - Barremian, Aptian and Turonian (Burden, 1992; Malan, 1993; Roux, 1997; Mclachlan and McMillan, 1979; Davies et al., 1991). A summary of the potential source characteristics of these intervals in the basin is presented in table 1.

http://etd.uwc.ac.za/

***Table 1**: Pletmos Basin source rocks, adapted and modified from Roux, (1997)*

Interval (sequence)	Source Rock Name	Kerogen Type	Thickness (m)
15A	Turonian	I/II (wet gas) - oil	10-15
13A	Late Aptian	II wet gas - oil	40-60
9A	Early Aptian	(II)/III wet gas - oil	50-100
6A East	Hauterivian	II/III wet gas - oil	40-60
6A West	Barremian	III dry gas	30-50
1A	Valanginian	II/III wet gas - oil	40-80
Pre-horizon 'Ó'	Kimmeridgian	?	?

Evidences supporting the regional occurrence of the Kimmeridgian lacustrine shales within the early rift-related sediments of the Syn-rift 1 interval are relatively minimal due to limited penetrating depths of wells (Davies, 1997; McMillan et al., 1997; Roux, 2007). Yet, the most prominent is assumed to be the widespread ~ 60m thick, early Aptian (13A sequence) organic-rich shales that occur above the mid-Aptian unconformity (13At1). This shale stratum is proposed to have been deposited under deep marine anoxic conditions during major flooding events that favoured sand starvation.

Nonetheless, it is worth noting that the presence, thicknesses, lateral variations, kerogen compositions and parameters of the potential source rocks, still need to be confirmed within this study area.

UNIVERSITY of the
WESTERN CAPE

http://etd.uwc.ac.za/

CHAPTER 3

Methodology

3.1. Data

The study utilized integrated geophysical, geological and geochemical subsurface datasets, which were obtained from PASA. These comprise:

- A 3D seismic coverage of ~ 1288.05km² acquired in 2000 by PetroSA,
- Well logs such as gamma ray (GR), resistivity (RHOB), sonic (DT), density (DRHO) and neutron (NPHI) and checkshot data,
- well (or formation) tops,
- Conventional core analysis reports – with information on parameters such as porosity, permeability, water saturation and formation (pore) pressures and temperatures, and
- Well completion and engineering reports.
- Geochemical data (Rock-Eval pyrolysis, TOC, VRo) analysis results. Note that ALL lab measurements were done by Soekor, and only the results formed part of the dataset.

UNIVERSITY of the
WESTERN CAPE

The well data were from six exploration and appraisal wells (Ga-A4, Ga-E1, Ga-E2, Ga-H1, Ga-Q1, and Ga-Q2) whose locations are revealed in Figure 3.1. These wells (Fig. 3.1) were chosen because they are thought to assist in understanding the proximal to distal paleo-depositional environment grading and contained hydrocarbon shows. Moreover, they were: (1) drilled to depths that penetrated a significant part of the geologic section of interest, and (2) had sample availability which allowed for information from the geochemical analysis results such as TOC%, HI, and VRo values to be utilized in calibrating maturation models.

These were supplemented by information on the lithologies and their periods of deposition and erosion from Brown et al., (1996) and McMillan et al., (1997). In addition to the sedimentary section ages used to evaluate the evolution of the basin from the International Union of Geological Sciences (IUGS) 2015.

http://etd.uwc.ac.za/

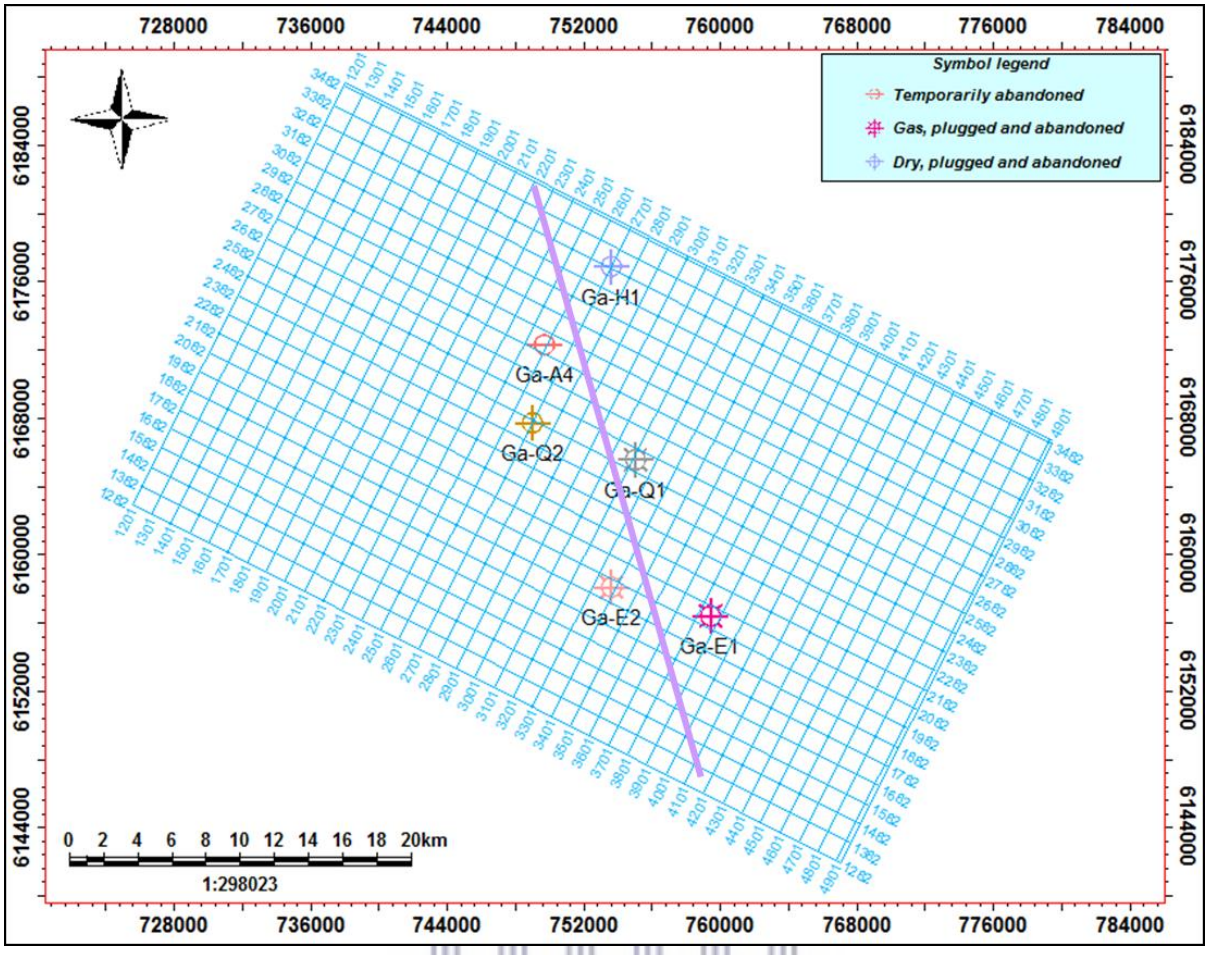

Figure 3.1: *Map encompassing the modelled extent of the study area, with locations of the wells whose data were utilized, and a cross-sectional seismic line used to demonstrate the key basin-wide unconformities and major faults within the study area.*

UNIVERSITY of the
WESTERN CAPE

3.2. Research Design

Schlumberger's PETREL® and PetroMod® 2014.1 suites of software were used in the study. The Petrel platform was used for seismic interpretation and allowed the integration of different geologic data into the creation of a structural framework. Dynamic modelling of the petroleum system was done with PetroMod. To achieve the said aims of the study, a multi-step integrated modelling workflow was employed as summarised in Figure 3.2.

http://etd.uwc.ac.za/

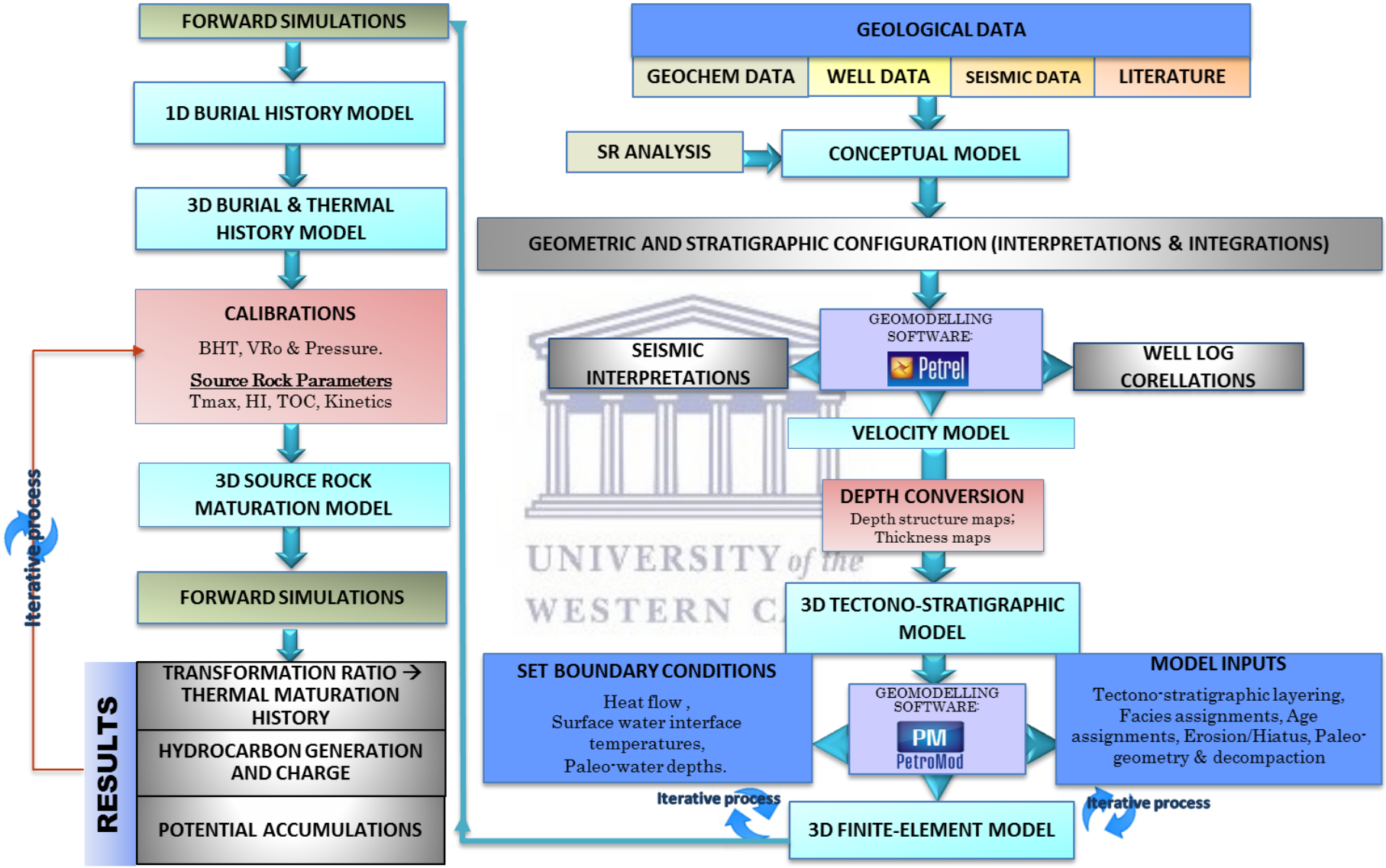

***Figure 3.2**: The integrated workflow and/or sequence of methodology utilized for the study.*

http://etd.uwc.ac.za/

3.3. Methods

3.3.1 Present-day Basin-fill Configuration

3.3.1.1. Conceptual geological Model

The detailed mapping of this study furnished the conceptual model, which was required for reconstructing the geo-history in order to quantify the maximum burial depth and temperature. This was achieved based on the chronology of events and processes as detailed in Section 2.3 (Fig. 2.2). It allowed for the definition of the lithologies, depositional ages and thicknesses of lithological units.

3.3.1.2. Structural and stratigraphic interpretation (Framework)

As a prerequisite to constructing the present-day 3D model, a tectono-stratigraphic framework was created. This was possible through the integration of various existing well and seismic data in order to establish a time-depth relationship. Initially this involved relating horizon tops that were identified at wells with specific reflections on seismic profiles through an integrated seismic-to-well tie (Fig. 3.3) using the convolutional model.

This was followed by the mapping of major faults and the identification and interpretation of key stratigraphic horizons (i.e. significant basin-wide unconformities) during seismic interpretation. In total, eight seismic reflectors (seven of which are key basin-wide unconformities) in addition to the seafloor, and approximately 60 faults have been interpreted including the major regional faults within the 3D seismic cube. It is imperative to note here that within the field, secondary unconformities (such as 9At1, 12At1 and 14At1) were only seismically resolved or traceable along limited few high-quality seismic lines of the cube, hence were not considered as components of the identified seismic horizons.

A velocity model (Fig. 2; Appendix A) was then constructed using a Simple Layer Cake method. The approach, created a simple model where the $\mathbf{V_0}$ (interval velocity between two horizons) was obtained from a compressional sonic log to represent the interval velocity at the top of the modelled formations. This (velocity model) was then calibrated to well tops. To patent depths and envisage a good level of certainty, the interpreted faults and stratigraphic surfaces (constructed from the interpreted horizons) were then domain-converted using the velocity model to allow for the creation of the depth-structure maps.

UNIVERSITY of the WESTERN CAPE
http://etd.uwc.ac.za/

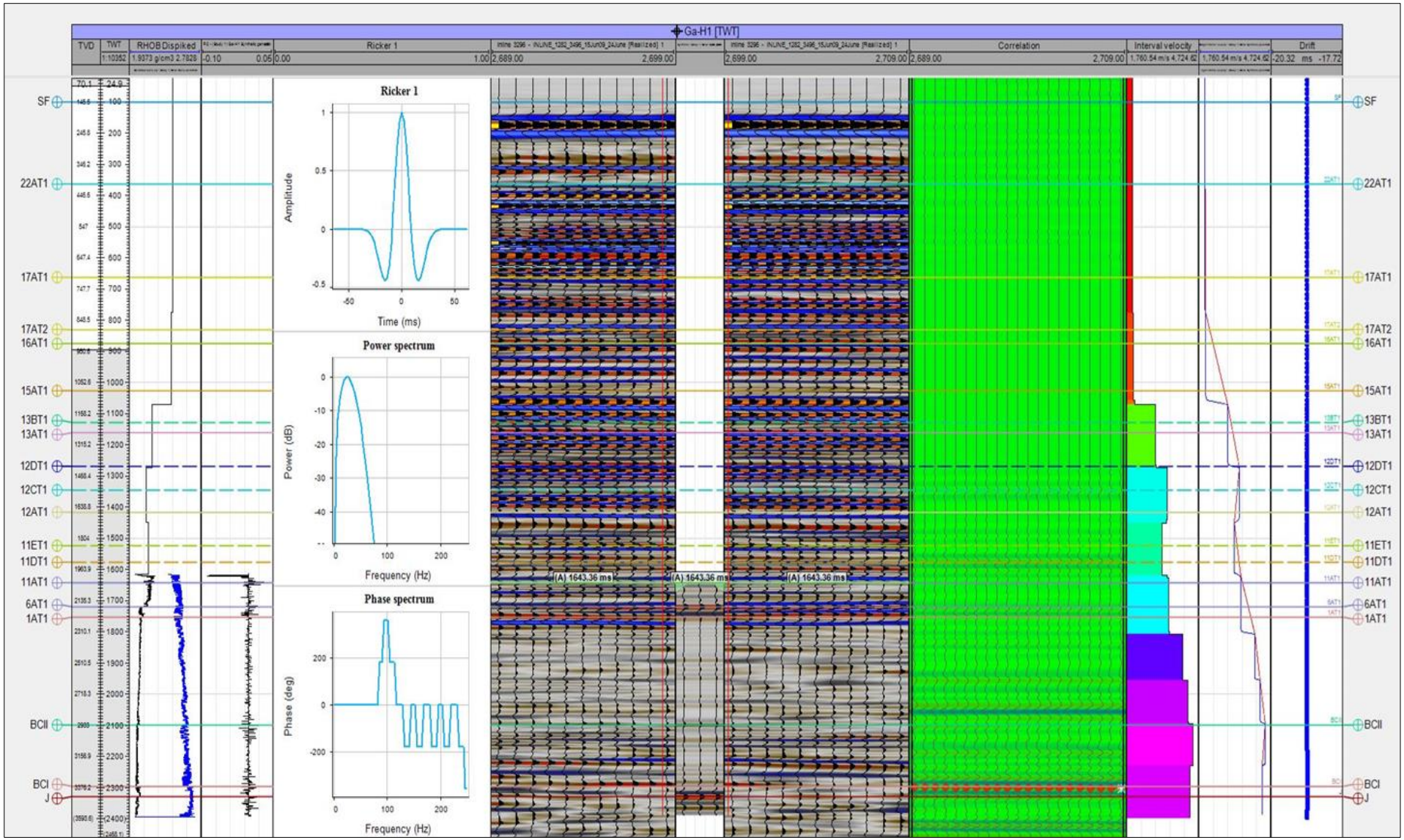

Figure 3.3: *Integrated seismic to well tie correlation panel displaying computed synthetic seismograms from well log that have been linked to the corresponding events of the seismic section. Note; most of the traces (both seismic and synthetic) are stacked near the well, and the very poor resolution of the representative seismic interval.*

http://etd.uwc.ac.za/

Furthermore, to aid in understanding the possible variations in structural regimes and main tectonic phases within the study area, the depth-converted surfaces along with faults, were modelled and incorporated to construct the 3D tectonostratigraphic framework.

The 3D tectonostratigraphic framework (Fig. 3.4) served as an input for subsequent construction of the 3D dynamic basin model. The final 3D model comprised of 28 stratigraphic layers. Hence, it provided insights to the geometry of the study area. This in turn allowed for the determination of the (potential) petroleum system units, particularly the associated source rock formations in the area.

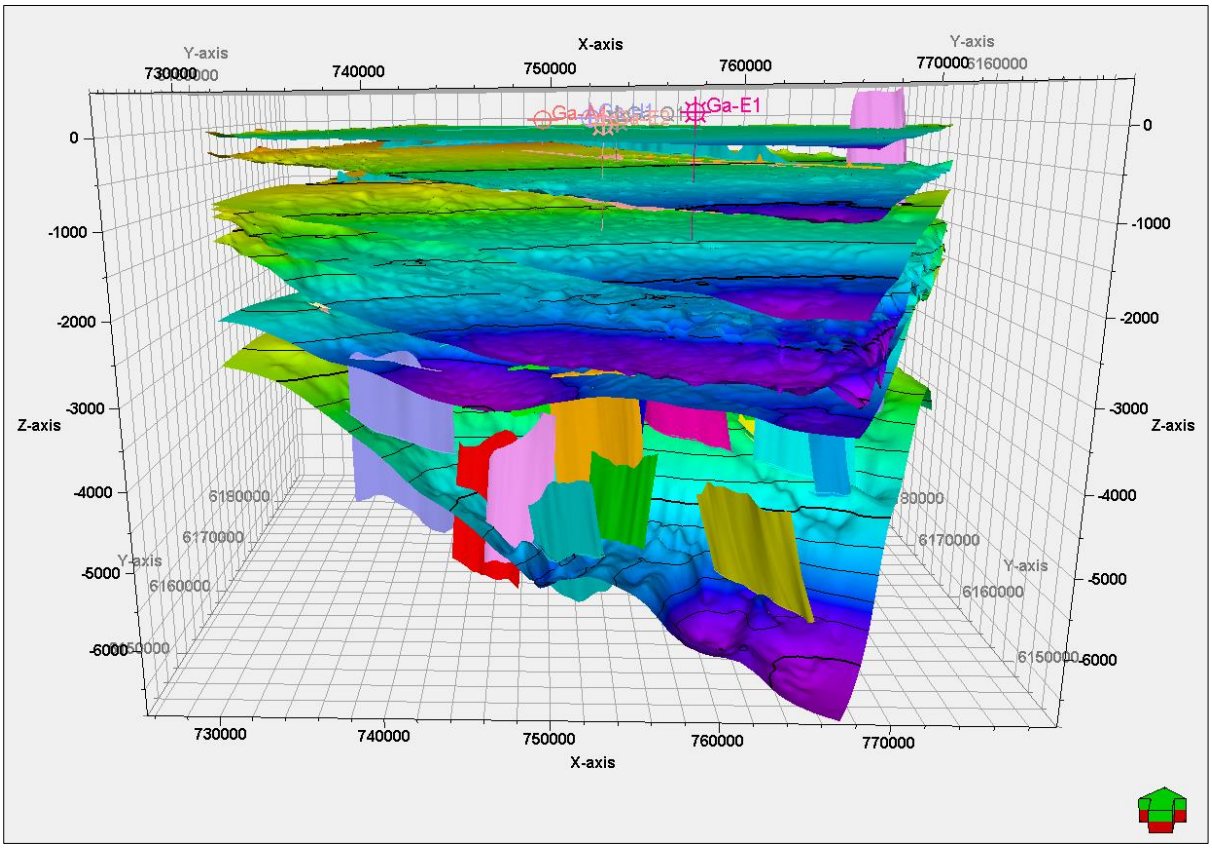

Figure 3.4: *A representation of the 3D tectonostratigraphic framework for the area established from detailed analyses of seismic and well data.*

Although seismic interpretations provided vital insights to satisfy basin modelling, especially regarding lithological characterisation, seismic resolution is in the order of several tens of meters and it is better at shallower depths than at greater depths. This poses a challenge in identifying potential source rocks that are deeply buried. Similarly, thin source rock units, important for petroleum generation, are often missed in seismic interpretation. Well logs, on the other hand, provide information in the range of meters thus enabling resolution of potential source rock units that might have been unresolved during seismic interpretation.

http://etd.uwc.ac.za/

Hence, well logs (mainly GR) (Fig. 3.5) were interpreted to offer complementary information on the lithology, and they also provided a basis for the visual assessment of thickness variations from the proximal to the distal locations.

3.3.2 Geochemical data Analysis

Laboratory Total Organic Carbon (TOC) analysis and Rock-eval pyrolysis carried out by SOEKOR Ltd. are presented in Tables 1- 3 of Appendix B. The results thereof were utilized in this study in order to determine the source rock characteristics.

The quantity of the organic matter (OM) present was determined by a measure of the organic carbon (TOC) content. For this study, a minimum organic content of 0.5% TOC was considered as adequate (Table 1; Appendix C). Notably, high TOC values alone are not necessarily indicative of good quality source rocks. The source rock quality was determined by means of the kerogen types present. This was carried out by plotting HI against OI on a modified van Krevelen diagram. The thermal maturity was estimated from pyrolysis Tmax and vitrinite reflectance measurements (Hunt, 1996). Because carbon is a vital component of all organic compounds, and the hydrocarbon potential of a formation is related to its percentage composition, the carbon content value has been a key factor in evaluating the organic richness and ability of a source rock to generate hydrocarbons (Jarvie, 1991). For this, TOC values were plotted against HI. The representative cut-offs used during the procedures of this section, are presented by the tables in Appendix C.

UNIVERSITY of the
WESTERN CAPE

3.3.3 3D Modelling: workflow, Inputs and Calibrations

Essentially, the thermal modelling and calibration proceeding required an initial model set-up that involved parameter definitions such as described below;

- ***Paleo-geometries***

In order to properly model the thermal evolution and lithologic decompaction, estimated paleo geometries (paleo water depth) were incorporated in the (1D and 3D) models. The Paleo-water depths were established from a combination of data from literature (Brown et al., 1996) and approximations following interpretations from well completion reports, well-correlation and facies relationships determined from cores and depositional environmental inferences of the sedimentary successions. Assigned values ranged between ~ 40 to 300m demonstrating the varying and shallow paleo water depths, with maximum water-depths occurring during the Hauterivian, Aptian and Albian times.

http://etd.uwc.ac.za/

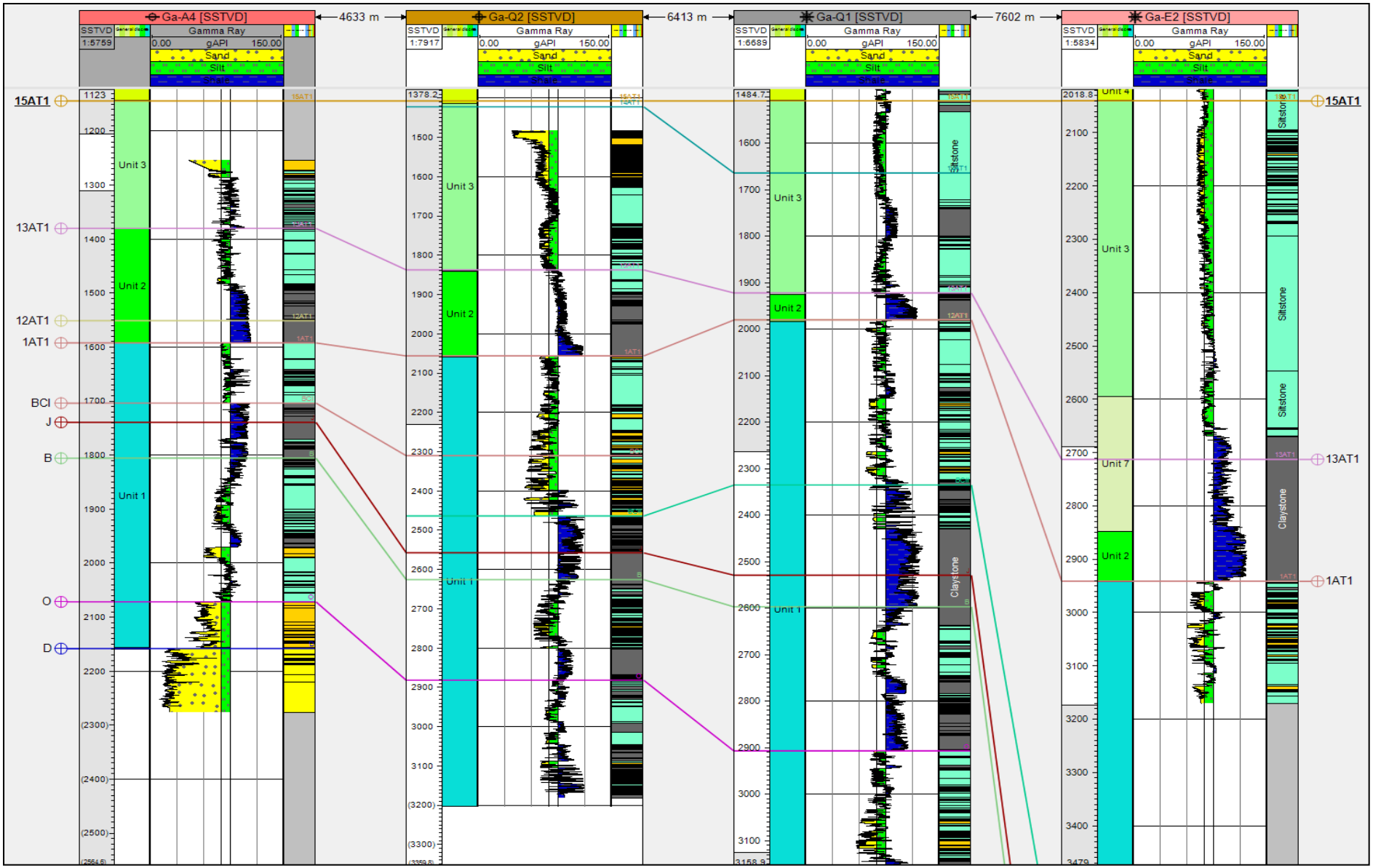

Figure 3.5: *NW–SE well correlation panel displaying stratigraphic horizons with representative vertical superposition of lithofacies, and shaliness estimation based on gamma ray log interpretation indicating possible source rock intervals for selected wells within the study area.*

http://etd.uwc.ac.za/

During the modeling process, the estimated erosion magnitudes throughout the sedimentary sequence contradicted the measured maturity trends. Therefore, they were initially implemented instead as hiatuses. Nonetheless, their effects were considerably negligible on the present-day maturity and temperature trends upon final calibration.

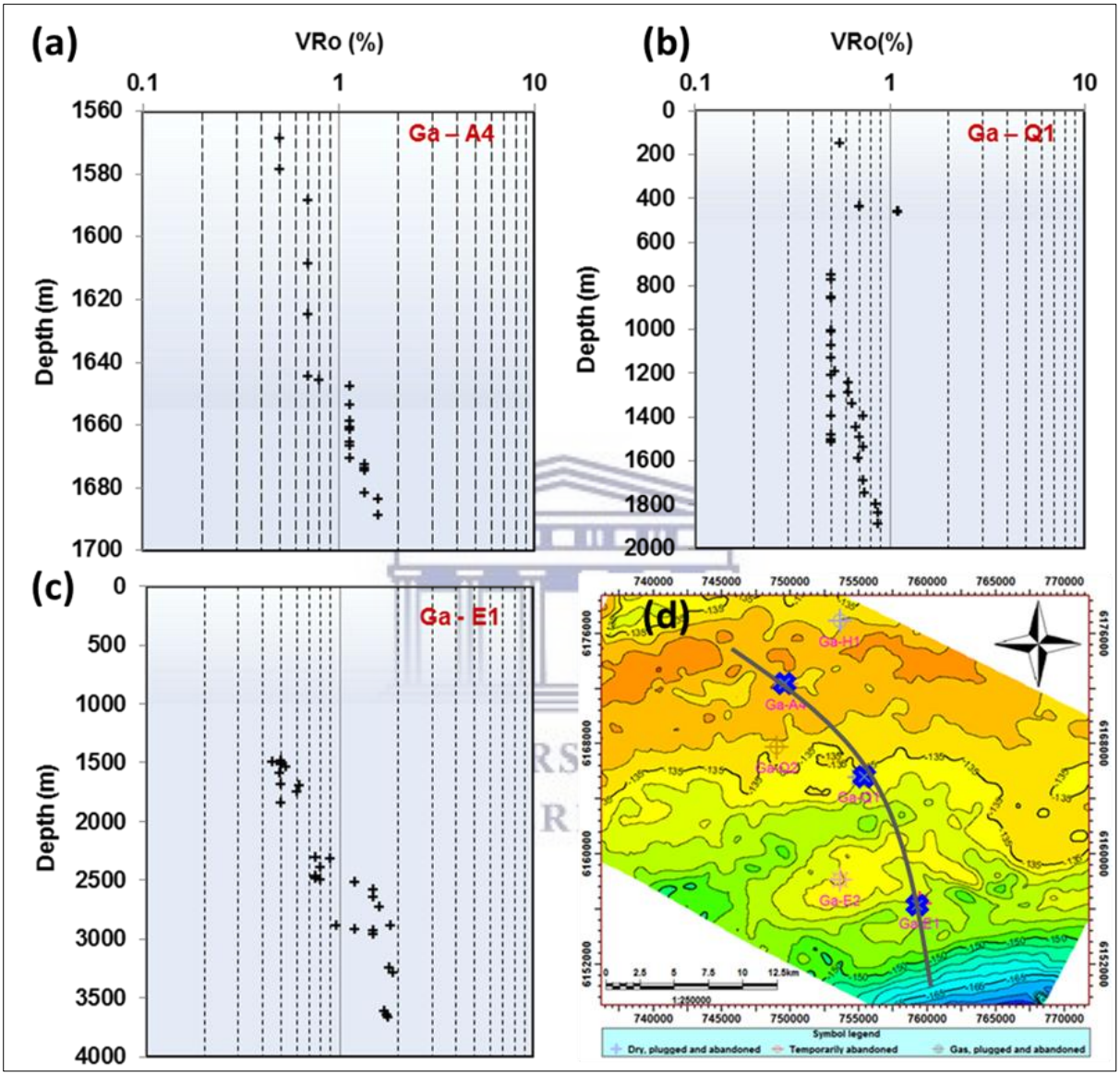

Figure 3.6: *Measured vitrinite reflectance data plots for three studied wells utilized for the thermal calibration, displaying the N-S paleo-geothermal gradient evolution trends. Note the general decrease in sublinearity of the VR trends from N-S.*

Boundary conditions

In PetroMod, Basal Heat Flow (HF), Paleo Water Depth (PWD) and Sediment Water Interface Temperatures (SWIT), were the three boundary conditions implemented for the forward modelling process. These were vital in defining the basic kinetic conditions for thermal development and maturation through time.

http://etd.uwc.ac.za/

Varying paleoclimates and the SWIT controlled upper boundary conditions for the forward modelling. Hence, for this area, upper boundary surface temperatures through time, were automatically assigned (in PetroMod) following the approach of Wygrala (1989) that assimilated paleo-latitude variations. The incorporated surface temperature profile provided a present-day SWIT value of ~ 17^0C, which almost corresponds to the estimated temperature derived by Goutorbe et al. (2008) for the Southern African seafloor.

Similarly, the lower boundary condition for various time intervals were defined using values of basal sediment heat inflows which corresponded to laterally varying heat flux maps of present-day depths.

Initially, due to the lack of derived regional published values of paleo-geothermal gradients at locations within the basin, simulations using a constant basal heat flux distributions through-time (that were identical to calculated values of present-day) were assumed. Nonetheless, a range of paleo-geothermal values of mantle heat flow at the Southern African continental interior (Goutorbe et al., 2008) were later factored in, based on the major paleo-tectonic history as evident by vitrinite reflectance fluctuations. These in essence were later compared with the data values utilized by Davies (1997) to equate the heat flux with the measured borehole temperatures.

- ***Kinetics***

Kinetic calculations were a key factor on which computational modelling was based. In this study, for kerogen to hydrocarbon conversion reaction rates, the default compositional kinetic model of Sweeney and Burnham (1989) was assumed. This model is a first-order reaction model based on Arrhenius Laws and operates similar to conventional models that are used in calculating kerogen transformation ratios in source rocks. Moreover, its kinetic model parameters are based on stratigraphic age and depositional environments and they presume primary cracking, by validating the thermal history with the available vitrinite reflectance depth information. To compare the relative influence of the default kinetic models to other variables on simulation output, the Pepper & Corvi (1995) kinetic model was utilized for the sensitivity tests. This is because the organofacies of the Pepper and Corvi kinetic model parameters mostly relates to terrigenous, non-marine and coastal environments belonging to the late Palaeozoic and younger ages.

Initial hydrocarbon generation simulation scenario (1) utilised the Burnham (1989) _TII kinetic model for simulating the Kimmeridgian and Aptian source rock units whilst the

UNIVERSITY of the WESTERN CAPE
http://etd.uwc.ac.za/

Burnham (1989) _TIII kinetic model was used for the Valanginian, Hauterivian and Turonian Formations. The second simulation scenario (2) for these source rocks utilized the Pepper & Corvi (1995) _TII (B) and Pepper & Corvi (1995) _IIIH (DE) kinetic models. These simulations used the same boundary conditions (SWIT, PWD and basal heat flow evolutions) with the defined source rocks parameters established from the Rock-eval analysis results interpretations presented in Section 4.2.

- ***Thermal calibration***

This procedure, fully integrated radiogenic heat produced by sediments of various assigned facies, along with that from the basement into all stages. The process validated model predictions through the use of available present-day borehole temperatures (Section 4.3) and vitrinite reflectance data (Fig. 3.6; Section 4.2). This was followed by the thermal evolution-model calibration process, using predicted present-day geothermal field gradients (Fig. 3.6) as boundary conditions.

This was performed in two stages;

- by reconstructing the present-day temperatures based on well temperatures, and
- by reconstructing the paleo-temperature distributions using vitrinite reflectance values obtained from a time and temperature function of the EASY% Ro chemical kinetic equations of Sweeney and Burnham (1990).

3.3.4 Source rock thermal maturation and petroleum generation modelling

To investigate the timing of source rock maturation, and subsequent petroleum generation, a 3D forward modelling evolution approach was employed. The 3D modelling encompassed the use of aforementioned database, and many unified iterative steps enumerated in Figure 3.2. Based on the calibration process employed during the geo-history and maturity evolution stages, the timing of source rock maturation, and subsequent generation were examined by means of widely-accepted forward modelling techniques (Tissot and Welte, 1984; Poelchau et al., 1997; Al-Hajeri et al., 2009; Hantschel and Kauerauf, 2009; Fig. 3.2).

The critical moment of generation was assumed to relate to the age during which ~50% of the kerogen contained by the source rocks had been converted to hydrocarbons (Hantschel and Kaurerauf, 2009; Hadad et al., 2016; Makeen et al., 2016). Transformation ratios greater than 50% were assumed to represent the likelihood of expulsion from the source rocks. Lastly, the expulsion efficiency for each source rock was defined as the ratio of expelled hydrocarbons in relation to the total generated (Duran et al., 2013).

UNIVERSITY of the WESTERN CAPE
http://etd.uwc.ac.za/

CHAPTER 4

Results

This chapter details the results from the analyses/interpretations carried out during the study. It starts with the sedimentary basin fill configuration, followed by the results from the source rock characterization and lastly the present-day thermal evolution and source rock maturation modelling.

4.1 Seismic Interpretation

As mentioned previously, the primary impetus was to understand the present-day structural configuration of the study area. A representative cross section that best reflects the spatial distribution of the principal structural elements is shown in Figure 4.1.

As can be observed in Figure 4.1, the most essentially diagnostic seismo-stratigraphic feature is the thinning of the stratal units above the Mid Valanginian (1At1) unconformity towards the North-western portion of the modelled area. The mapped major fault geometries are generally normal in nature, with notably the main Superior fault being largely listric as is believed to have been modified by as a result reactivational strike-slip movements, discussed in Chapter 2. The associated minor faults are mainly antithetic and synthetic, indicating depth related increasing displacements towards the South with a North-west to South-east trend. Their propagations are largely localised, though some are contiguous to the Pre-Mesozoic Basement and typically traverse from syn-rift to post-rift sequences with upward decreasing offsets (Fig. 4.1). Of all the mapped faults, the Superior growth fault is observed to have caused the most displacement with upward decreasing offsets above the 13At1 horizon.

Presented in Figure 4.2 are the established depth-structure maps constructed from seismic interpretation (in the time domain) and the subsequent velocity modelling (depth-conversion), respectively. Figure 4.3 provides the relative thickness and spatial sediment distributions of the modelled sedimentary sequence units of interest. The depth-structure maps and thicknesses served as some of the main input parameters into the modelling process, as they essentially provided the morphology of the Upper Jurassic – Cenozoic basin infill (Figs. 4.4 and 4.5).

UNIVERSITY of the
WESTERN CAPE

http://etd.uwc.ac.za/

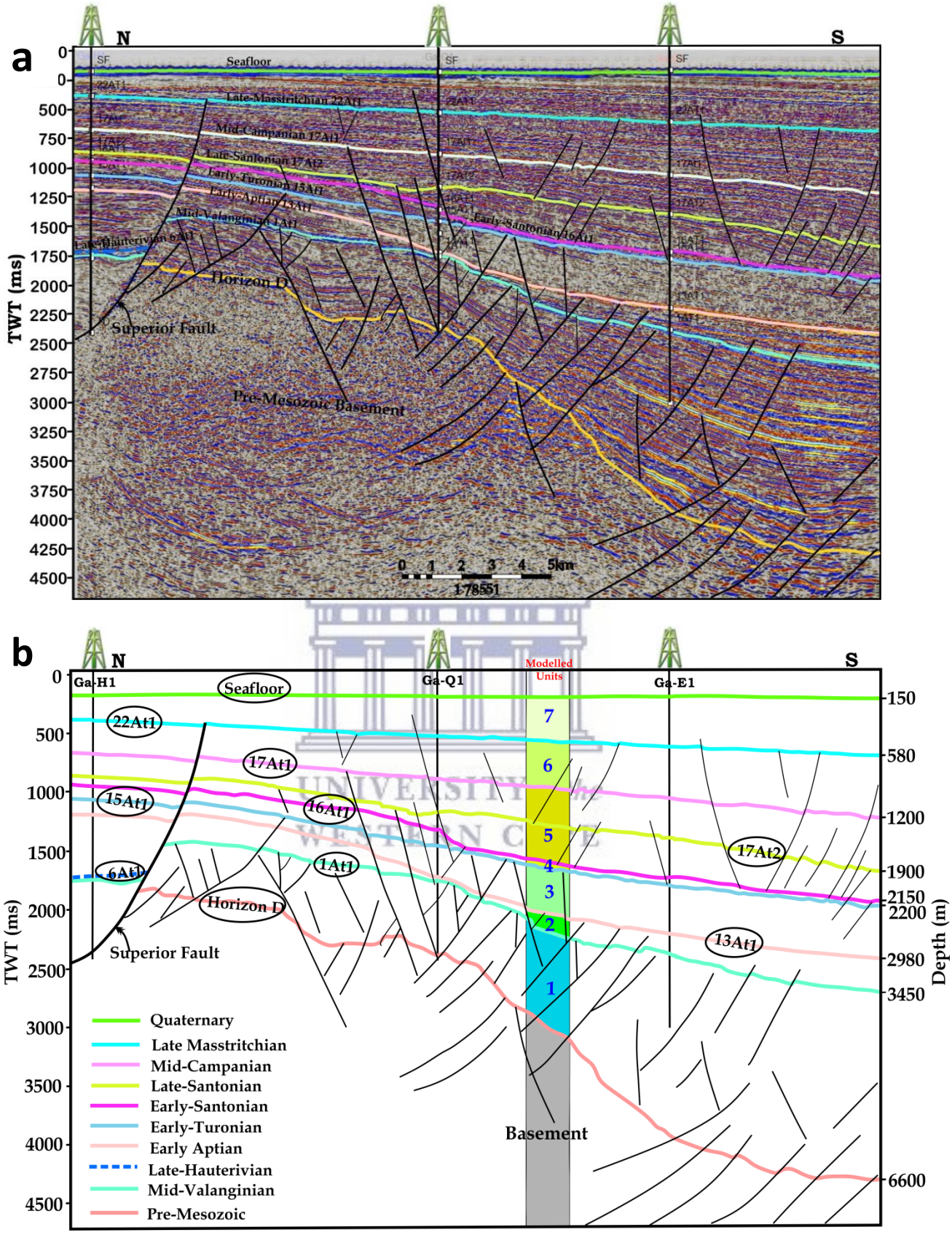

Figure 4.1: a) *An interpreted N–S seismic arbitrary line profile extracted from the 3D seismic survey, and* ***b)*** *schematic cross-section showing key basin-wide unconformities, major faults and modelled units. Note the overall thinning towards the North and thickening towards the South of interval layers.*

http://etd.uwc.ac.za/

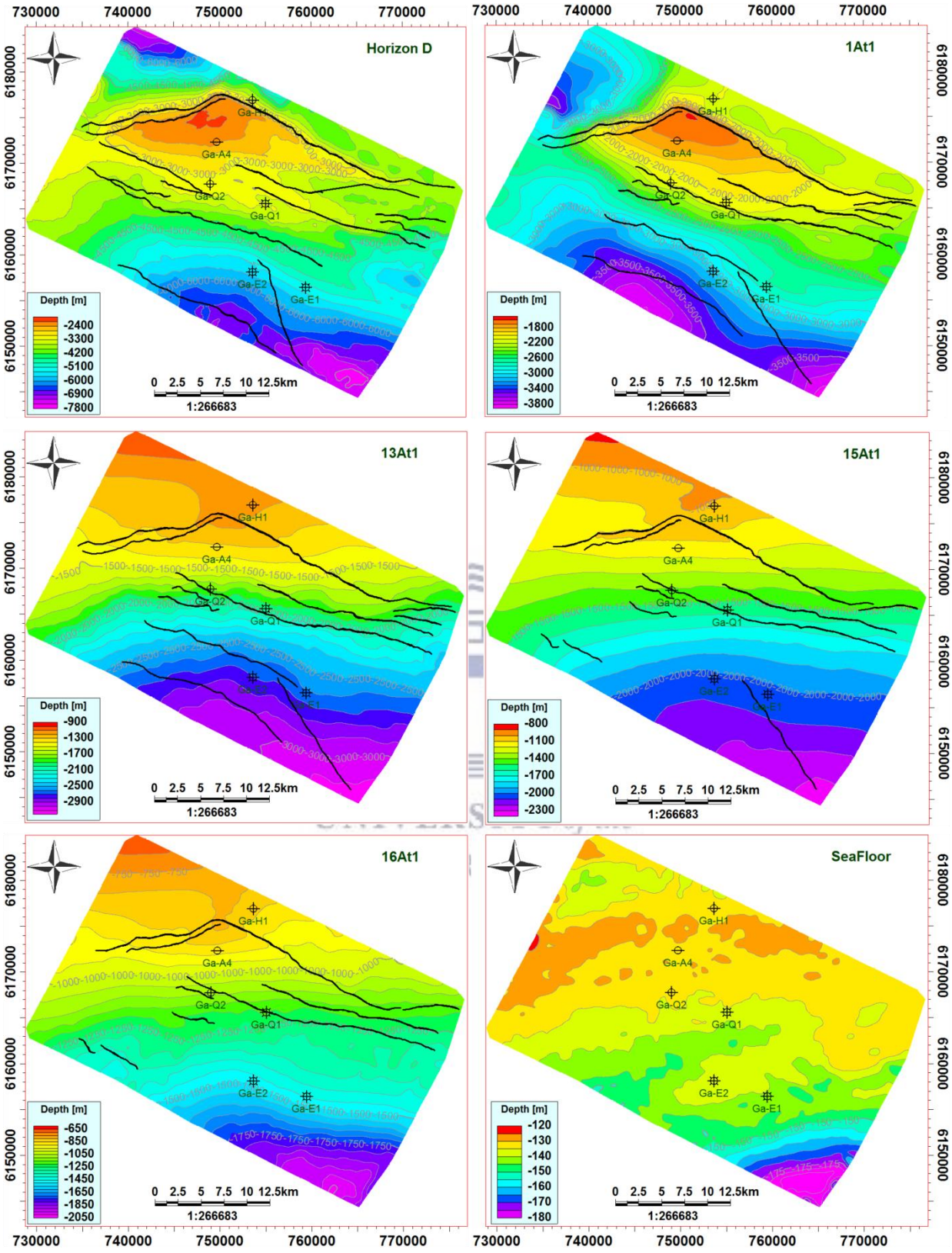

Figure 4.2: *Constructed depth structure maps of top horizons of the representative modelled units with mapped major faults.*

The Superior High is seen by closed contours adjacent to the Superior Fault (Fig 4.2a and b). The most notable feature that can be observed on the structure maps (Fig. 4.2 and 4.3) is the

http://etd.uwc.ac.za/

southward tilting of post-rift (above 1At1) sedimentary units away from the Superior High. This is evidenced by the warmer colours which generally grade into colder colours (i.e. from red to purple/magenta) towards the South. This is indicative of the creation of more accommodation space in the southwards direction at the time of deposition.

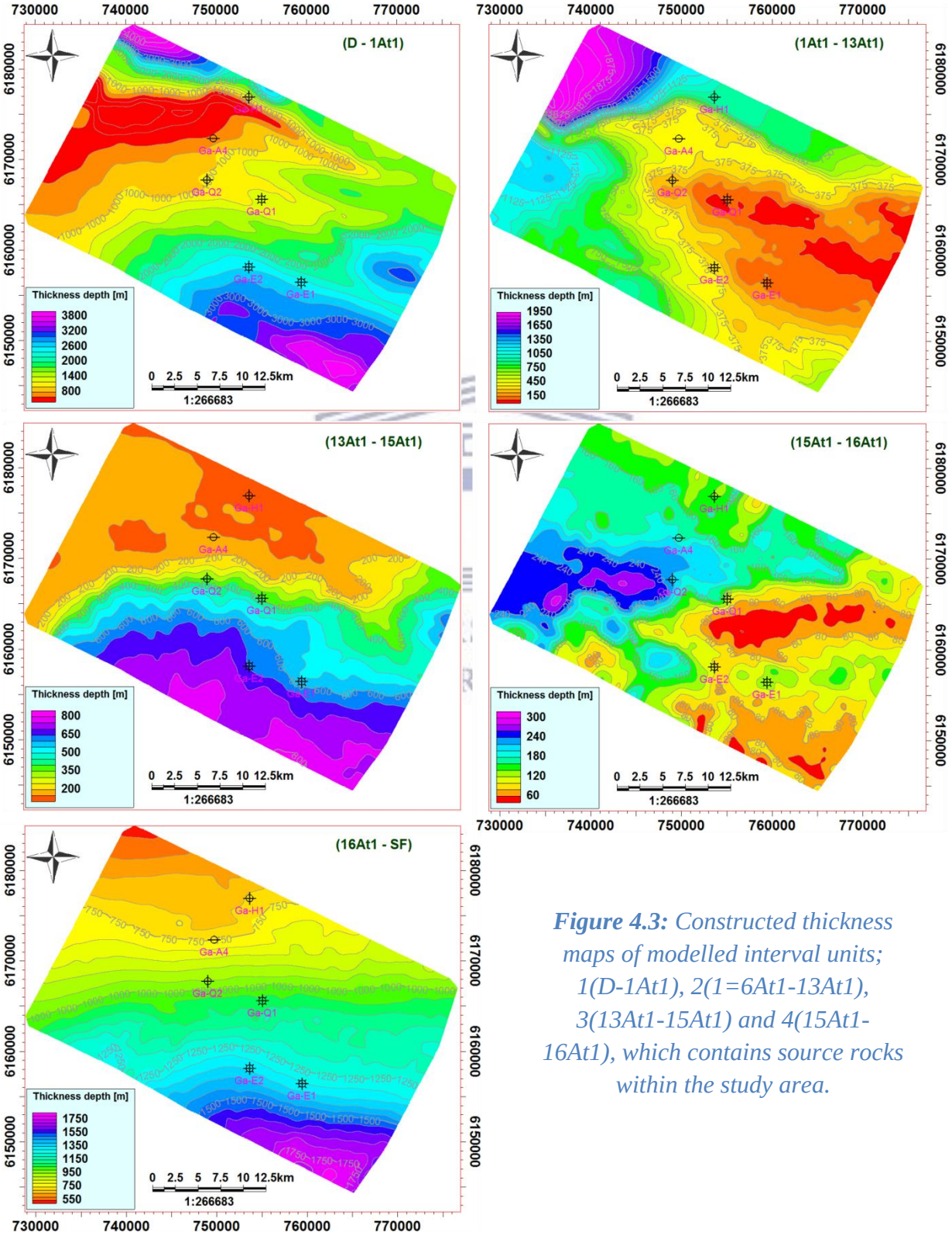

Figure 4.3: *Constructed thickness maps of modelled interval units; 1(D-1At1), 2(1=6At1-13At1), 3(13At1-15At1) and 4(15At1-16At1), which contains source rocks within the study area.*

http://etd.uwc.ac.za/

Notable on the thickness maps is the general thinning of the Unit 1 and 3 sequences (i.e. Figs. 4.3a and 4.3c) towards the Superior High. This can be attributed to the outstripping of sediments on the High during the regional uplift events in each episode. This led to the deposition of these sediments in the tectonically subsided parts of the basin, most of which were towards the South and North of the Superior Fault, i.e. the two sediment depocentres of the Pletmos Basin. The overburden thickness shows a comparable thickness distribution trend which can also be attributed to the tilting of units above the 1At1 unconformity (Figs. 4.1 and 4.2a-b), as stated above.

Further, Unit 2 and 4 (i.e. Figs. 4.3b and 4.3d) display no clear trend. Overall, the two units show a general thinning towards the South-East direction. This thickness distribution can be ascribed to the tectonically enhanced erosion events of the associated regional unconformities. Moreover, below is the three-dimensional configuration of the basin derived from the interpretation.

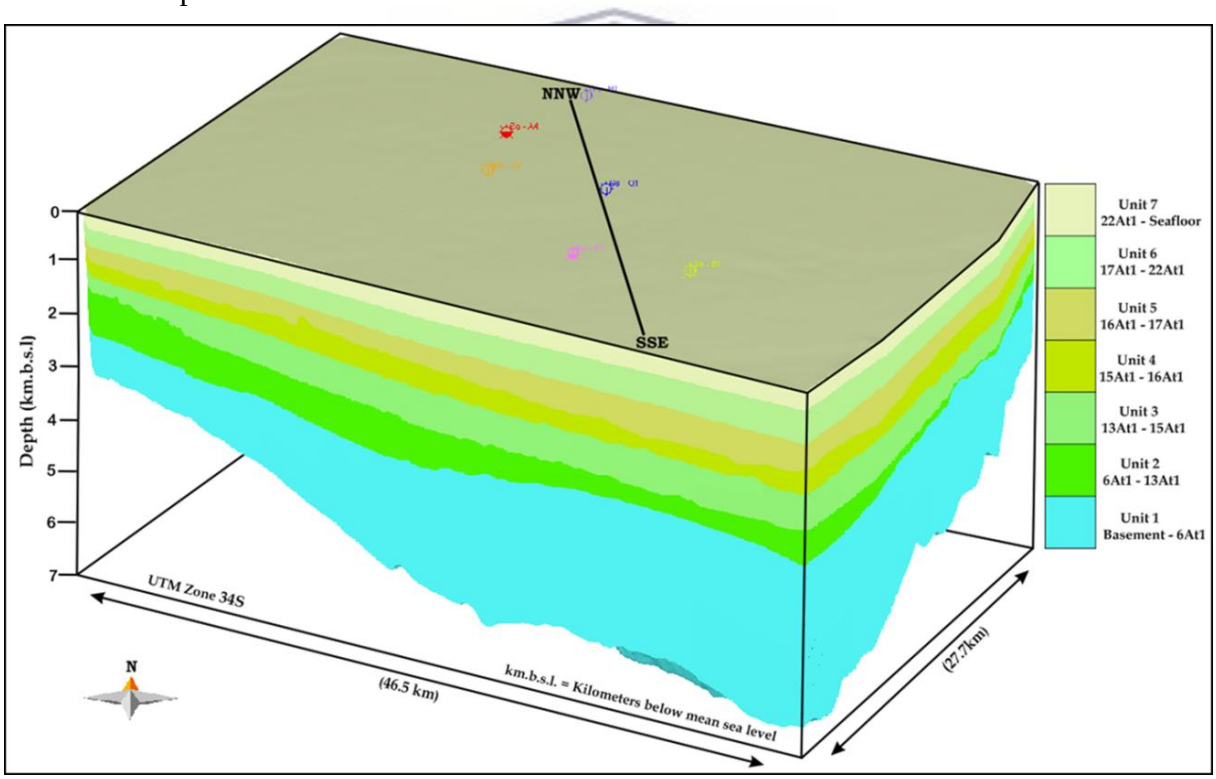

Figure 4.4: *A consistent 3D structural model of the Upper Jurassic – Cenozoic basin-fill*

A cross-section through the structural model, revealing the modelled units, vertical and lateral lithofacies variation, major unconformities and chronologic arrangement at present-day is presented in Figure 4.5. This essentially reveals the spatial layer thicknesses as the number of defined stratigraphic events based on the geological ages, which are in accordance with the related timing of erosion and hiatuses that separate the main modelled units.

http://etd.uwc.ac.za/

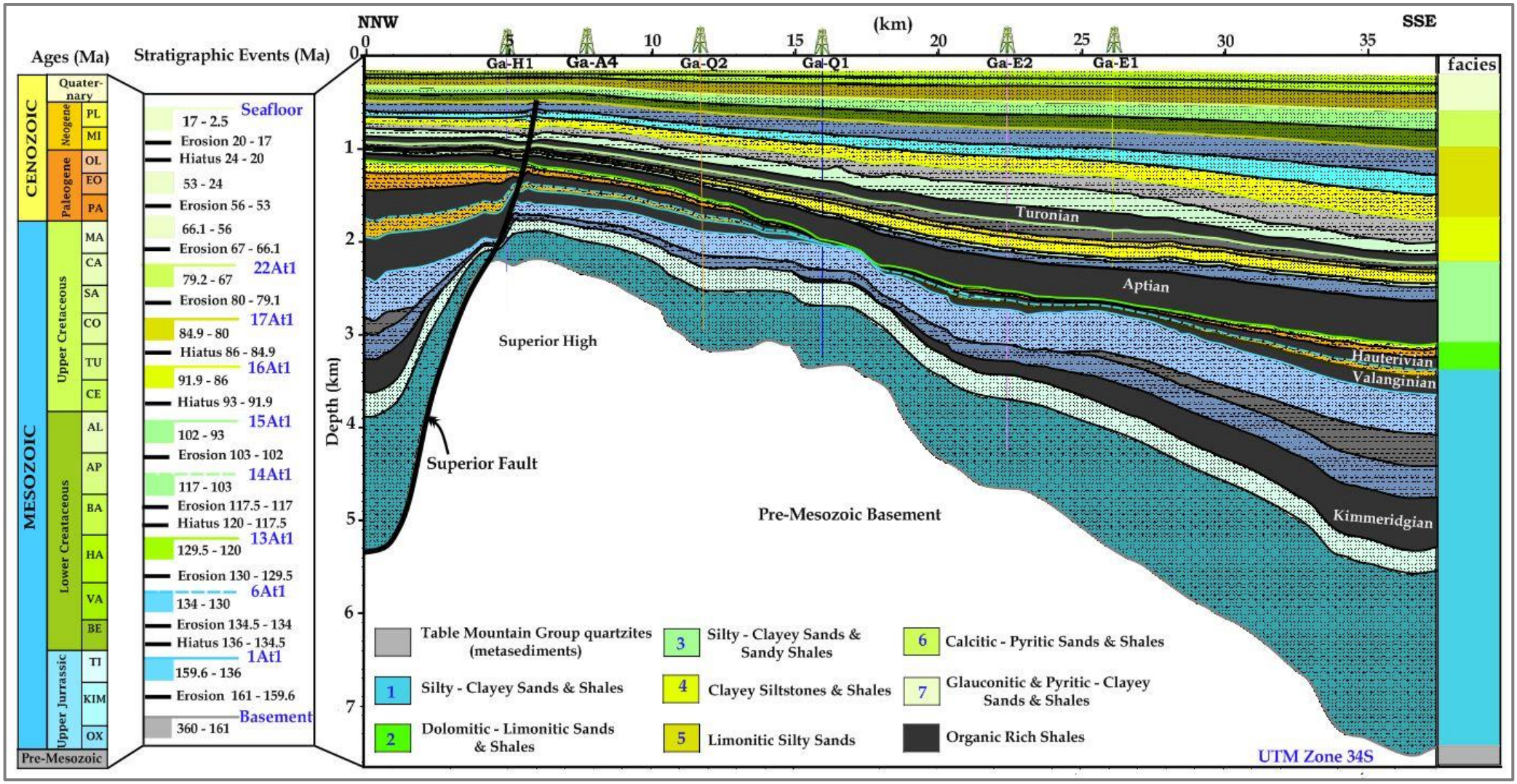

Figure 4.5: *Present-day model set-up utilized for the thermal modelling, displaying the defined stratigraphic events, major unconformities and vertical and lateral lithofacies variation and modelled units. Note the colour-coded facies are based on the modelled units.*

http://etd.uwc.ac.za/

4.2 Source Rocks Evaluation

In order to properly model the timing of maturation and generation, it was essential to recognize the kinds of source rock systems present. These usually include: potential, effective, relic effective and spent source rocks (see Glossary for definitions). This section focused on the determination of the potential source rock characteristics to classify them accordingly prior to modelling. It presents interpretations of Rock-Eval pyrolysis data and other geochemical data from six wells (see Fig. 3.1 for location) using graphical representations.

4.2.1 Source Rock Quantity (Organic Richness)

Well bore depths range from 2,300 to 5,100 m covering the Mesozoic - Cenozoic interval. Figure 4.6 illustrates a depth versus TOC (weight %) plots for various samples. The plot shows samples from various source rocks within the basin, differentiated by the different colours. The shale units display variable degrees of richness, with TOC contents ranging from approximately 0.5 to 5wt. % at subsurface depths ranging from 1500 – 4000m. A majority of the source rock samples contain organic matter with TOC wt. % values above the accepted threshold of 0.5 wt% for potential source rocks. The variation of TOC content can be attributed to combined effects of the environment of deposition and burial depth.

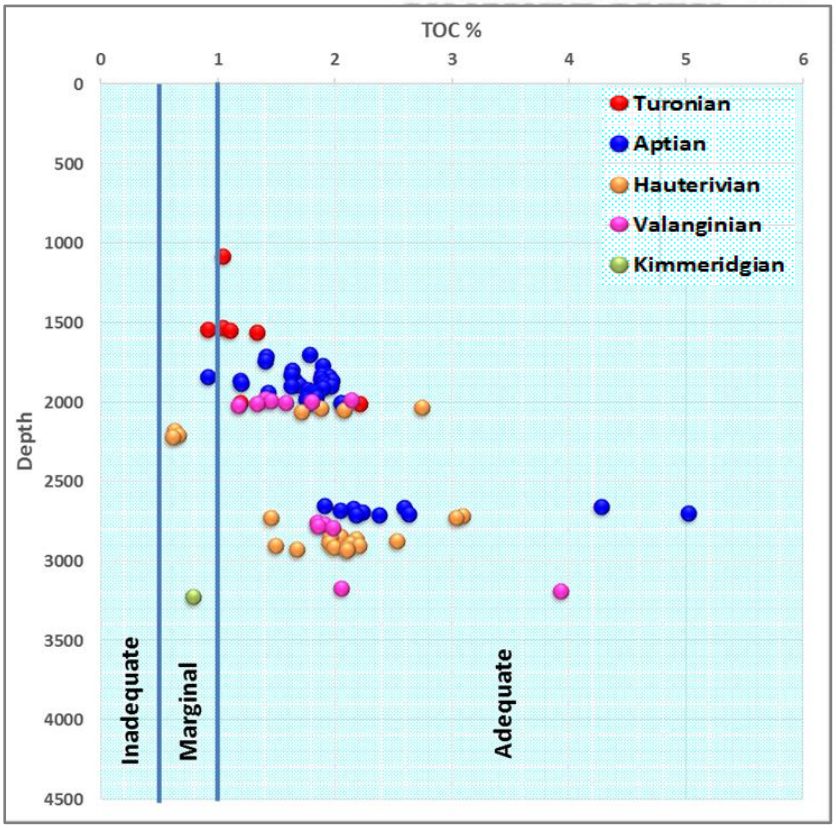

Figure 4.6: *Analysed sample distribution plots demonstrating the Total Organic Carbon (wt. percent) content versus depth.*

http://etd.uwc.ac.za/

4.2.2 Source Rock Quality

Having analysed the TOC content of the source rock samples in the previous section, presented below are Rock Eval HI and OI values plotted on a modified Van Krevelen diagram (Fig. 4.7) as a way of screening the samples for source rock quality and - type.

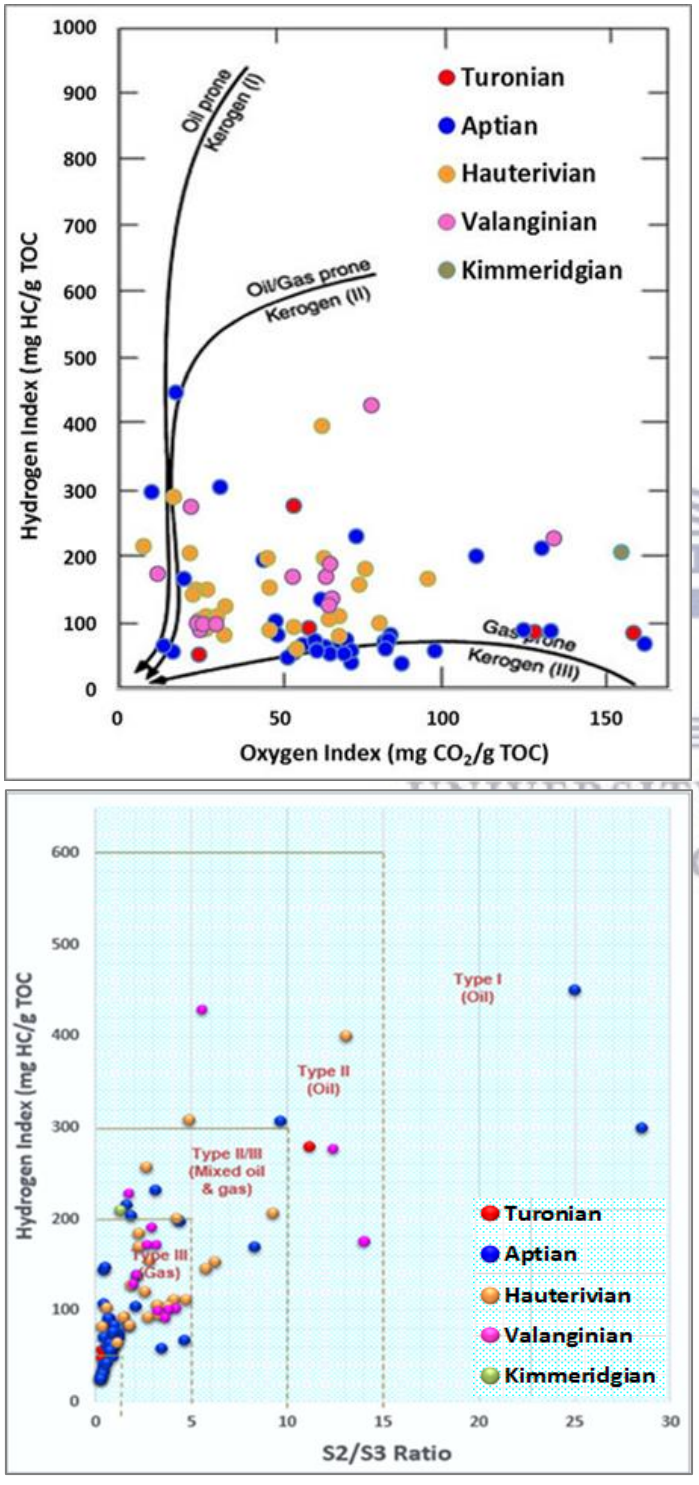

Figure 4.7: *Modified Van-Krevelen diagram (a) of analysed sample distribution showing various kerogen types (quality) with character of expelled products during peak maturity for the various stratigraphic source rock units (b).*

The general trend reveals that the majority of samples from all the source rocks are predominantly Type III kerogens with some Type II (Fig. 4.7). As can be seen, the Type III kerogens are characteristically gas-prone (Fig. 4.7b). This is typified by low HI (<200) and high OI. Note that the Kimmeridgian source displays a low TOC and HI. However, this is largely due to the fact that only a single sample value was analysed. On the basis of these characteristics, this source rock can very well be able to generate hydrocarbons provided that the interval is thick and the organic matter concentration is high. The Aptian source rock displays some significantly high S2/S3 values indicative of the likelihood of oil as

http://etd.uwc.ac.za/

the expelled product during peak maturity. Note however, that some samples plot within Type IV (Fig 4.7b) which may imply reworking and/or deposition a highly oxidizing environment.

The respective HI and OI ranges, and approximate S2/S3 ratio values obtained from Soekor lab analyses for the various source rocks are summarised in Table 2.

Table 2: *Organic matter quality and nature of expelled product at peak for the different source rock intervals*

Source Rock	Depositional Environments	Quality of Organic Matter				Main Product Expelled at peak maturity
		Kerogen Type	HI (mg HC/g TOC)	OI (mg CO2/g TOC)	S2/S3 Ratio	
Turonian	Inner Shelf	III	47.3 – 278.3	24.9 – 184.6	0.3 – 11.2	Gas
Aptian	Slope – Deep Marine	II-III	23.7 – 499.5	10.5 – 315.0	0.3 – 28.5	Gas
Hauterivian	Deep Marine (abyssal plain)	II/III	63.2 – 399.2	22.2 – 204.9	0.4 – 13.1	Gas
Valanginian	Deep Marine (abyssal plain)	II/III	91 – 429	12.4 – 133.8	1.7 – 14.1	Gas
Kimmeridgian	Lacustrine	II	> 200	~ 160	~ 1.4	Mixed Oil and Gas

UNIVERSITY of the WESTERN CAPE

In general, HI values of the analysed samples vary from 23.7 to 499.5 (mgHC/g TOC) (Table 2). Although the organic matter is in general composed of Type III and Type II kerogens, it appears to be getting increasingly gas-prone from the Turonian Formation (that contains mainly Type III) to Aptian, Hauterivian and the Valanginian formations that contain gradually increasing Type IIs (with limited Type I samples in the Aptian). A fact pointing to predominance of gas-prone source rocks with wet gas/condensate and dry gas produced, depending on maturity. The Kimmerdigian source rock, though with a Type III kerogen based on the HI and OI analysis, will likely produce a mixture of oil and gas due largely to its depositional environment revealed in Table 2.

Figure 4.8 reveals a fair to excellent generation potential collectively for the source rocks. As illustrated most of the sampled values fall within the 'good' and 'very good' range of values (Fig. 4.8) illustrated by HI values between 250 and 480 (mgHC/gTOC) with corresponding TOC contents between 1 and 2.5 wt %. The Kimmeridgian sample has TOC and HI values of 0.78 wt% and 208.86 (mgHC/gTOC), respectively that indicate a fair potential (e.g. Peters

http://etd.uwc.ac.za/

and Cassa, 1994). Upon maturation, the prospective source rocks within the study area given their current TOC contents and HI indices will generally be characterised by very good petroleum generation potentials (Fig. 4.8).

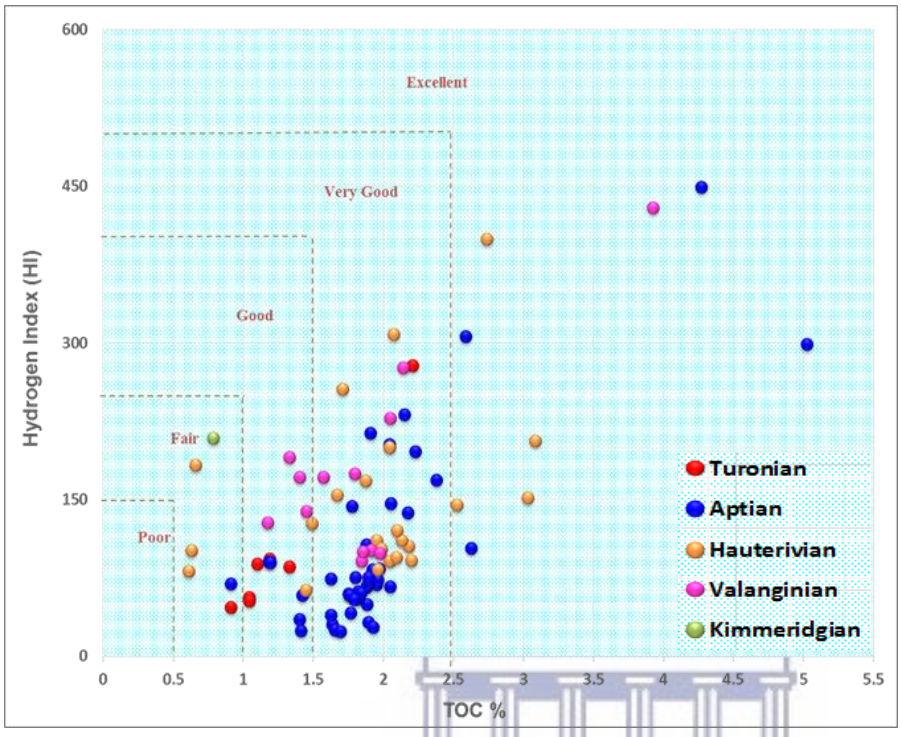

Figure 4.8: *Plot of analysed sample distribution demonstrating the petroleum generation potential of the various stratigraphic units*

4.2.3 Thermal maturity level

In the last section, the types of source rocks were analysed and it was established that they generally range between type II and III kerogens. Plotting T_{max} versus HI further validates this finding and illustrates the different maturation paths of various kerogen types (Fig. 4.9).

Figure 4.9 shows that the analysed samples range between 425 and 455 °C. In addition, there exists a relatively uniform variation in the T_{max} values throughout the sample set. Most samples of the Aptian and Turonian source rocks are in the immature stage of hydrocarbon generation, characterized by low T_{max} (< 435ºC) values, whereas those of the Hauterivian, Valanginian and Kimmeridgian show Early – Late maturity stages for hydrocarbon generation, characterized by higher T_{max} (435- 465 ºC) values (Table 3; Appendix C). The T_{max} values are further matched with recorded vitrinite reflectance (%VRo) maturity values (0.5 – 1.60 %) of the study area to authenticate the results (Fig. 4.10).

The vitrinite reflectance generally increases with the depth of burial (Fig 4.10). Conversely, it has also been observed that the %VRo values for the Valanginian increase marginally from 0.70 %VRo to 1.60 %VRo at roughly the same depth level across the studied wells.

http://etd.uwc.ac.za/

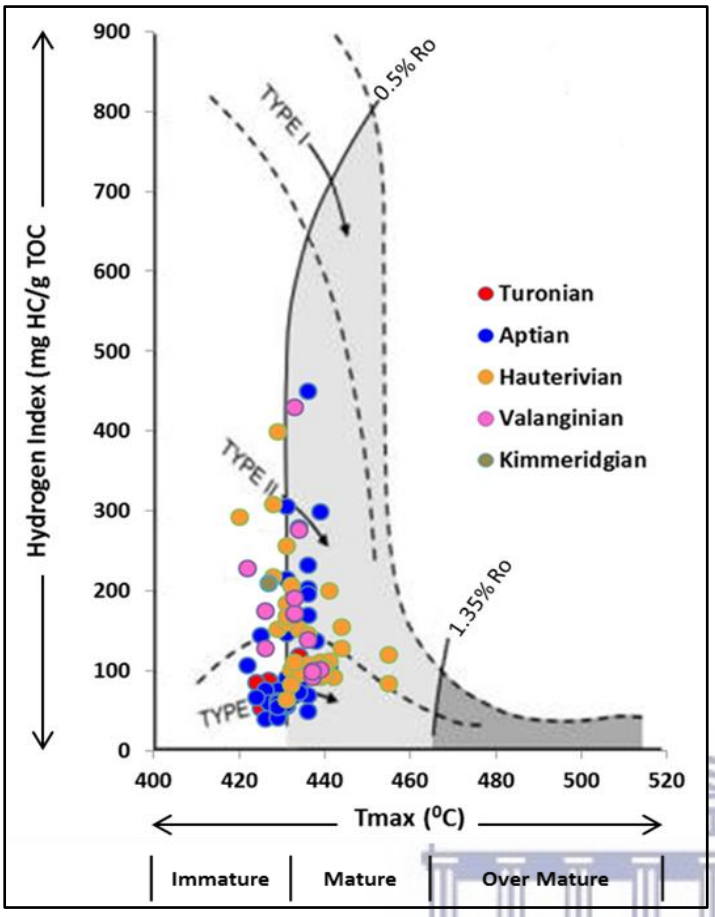

Figure 4.9: *Plot of Hydrogen Index versus T_{max} defining kerogen types of the source rock samples, showing kerogen thermal maturity stages.*

This could be attributed to the fact that the sedimentary units get deeper and thicker towards the South (Figs. 4.1, 4.2, 4.3 and 4.5). Similarly, the Tertiary sediments also range from Immature to Post-mature. The possible reason for this may be a rapid transition in lithofacies and/or burial. Another possible reason would be contamination of the samples due to cavings from even shallower well intervals.

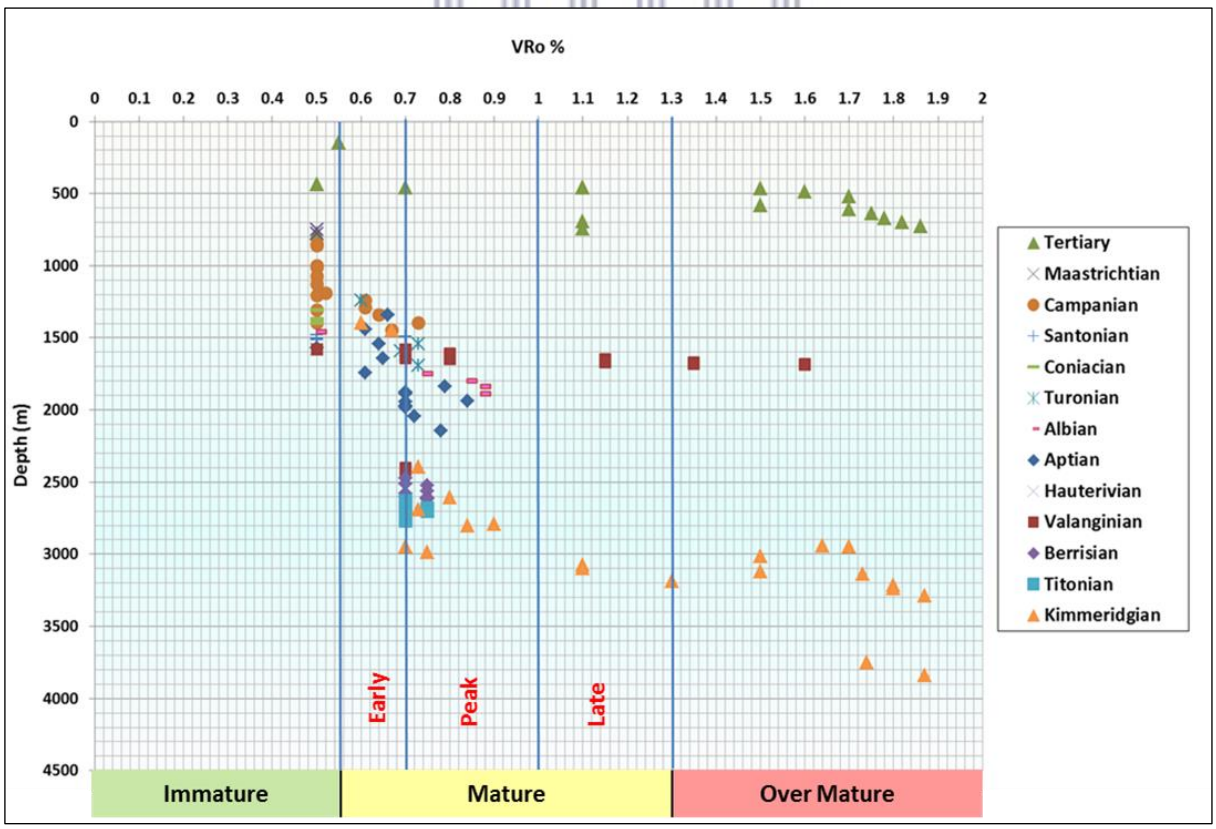

Figure 4.10: *Vitrinite Reflectance as it varies with depth (expressed as mean Ro value) for individual sample values for the different ages.*

http://etd.uwc.ac.za/

Furthermore, the study area is highly faulted and fractured which would mean that areas that are more fractured might have experienced more basal heat flow.

The summary of the characteristic stage of thermal maturity, and corresponding ranges for Tmax, Vitrinite reflectance values of the source rock units are provided in Table 3.

Table 3: *Characteristic stage of thermal maturity and range values, for Tmax and Vitrinite reflectance for the different source rock intervals.*

Source Rock	Stage of thermal maturity	Maturation	
		Ro (%)	**Tmax** (°C)
Turonian	Immature – Early mature	0.6 – 0.73	424 – 435
Aptian	Immature – Peak mature	0.5 – 0.84	424 – 441
Hauterivian	Immature – Peak mature	0.5 – 0.70	428 – 455
Valanginian	Peak mature – Late mature	0.7 – 1.60	426 – 429
Kimmeridgian	Peak mature – Post mature?	0.7 – 1.10	~ > 424

A representative log that graphically reveals the geochemical information of the well is presented by Figure 4.11. This plot exemplifies the identification of the potential effective source rock intervals in this study. It summarizes and simplifies the visualization of lithologies and formations that were possible source rocks at present maturation levels for one of the study wells. The established source rock strata were considered for organic matter maturation and petroleum generation. Accordingly, a summary of their defined parameters that were assigned/input into the maturation and generation models are thus provided in Table 4.

UNIVERSITY of the WESTERN CAPE

Table 4: *Input parameters based on the thermally immature samples for the modelled source rock intervals in the 3D model*

Source Rock Interval	Kerogen Type	Thickness Range [m]	TOC Value [%]	HI Value [mgHC/gTOC]	Kinetics
Kimmeridgian	II	65 - 200	1.80	320	Burnham (1989)_TII
Valanginian	II-III	30 - 120	1.35	205	Burnham (1989)_TIII
Hauterivian	II/III	80 - 140	1.70	210	Burnham (1989)_TIII
Aptian	II/III	30 - 250	4.00	440	Burnham (1989)_TII
Turonian	III	20 - 85	1.50	135	Burnham (1989)_TIII

The results thus far, obtained in this section were integrated into the source rock maturation and petroleum generation modelling of the area (Section 4.4).

http://etd.uwc.ac.za/

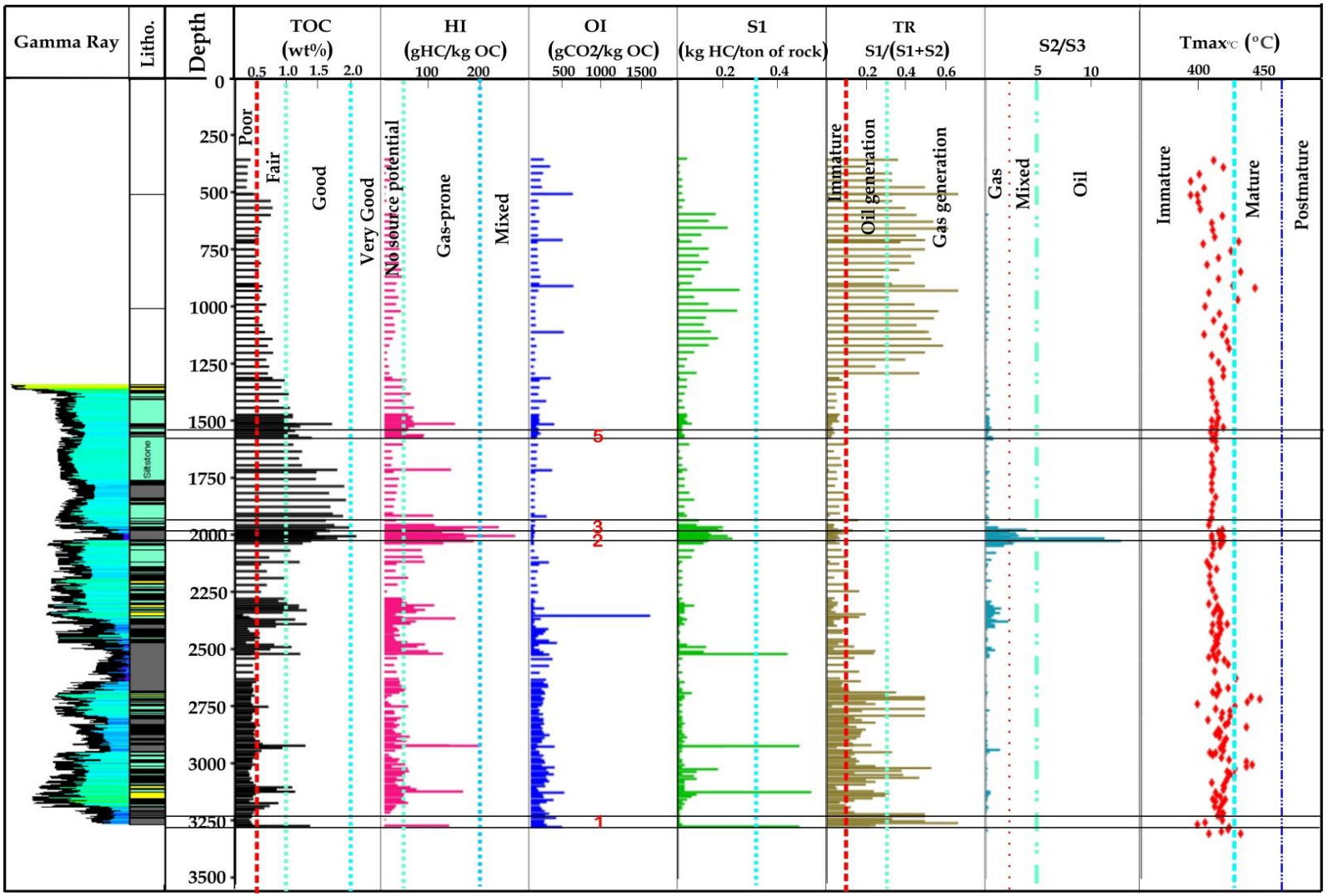

Figure 4.11: *Representative geochemical log, indicating the modelled source rock intervals determined from rock-eval parameters at present maturation levels, at the location of well Ga-Q1. Note: the encountered source rocks at the well are indicated by the numbers 1-5.*

http://etd.uwc.ac.za/

4.3 3D Basin Modelling Results

Presented here, is the breakdown of the sedimentary basin-fill, burial and thermal, maturation, generation, and expulsion events, throughout the basin's evolution history. The interpretations were mostly focused on 3D and results presented here will be highly focused on the main objective (not the side goals).

4.3.1 Calibration and Kinetics modelling

3D simulations for hydrocarbon maturity and generation incorporated the effects of paleo boundary conditions (such as paleo surface temperatures), rapid sedimentation and uplift on the transient temperature distribution. Presented below are the representative thermal calibrations established upon incorporation of the three paleo-heat flow peaks and associated erosion scenarios in the final thermal evolution model.

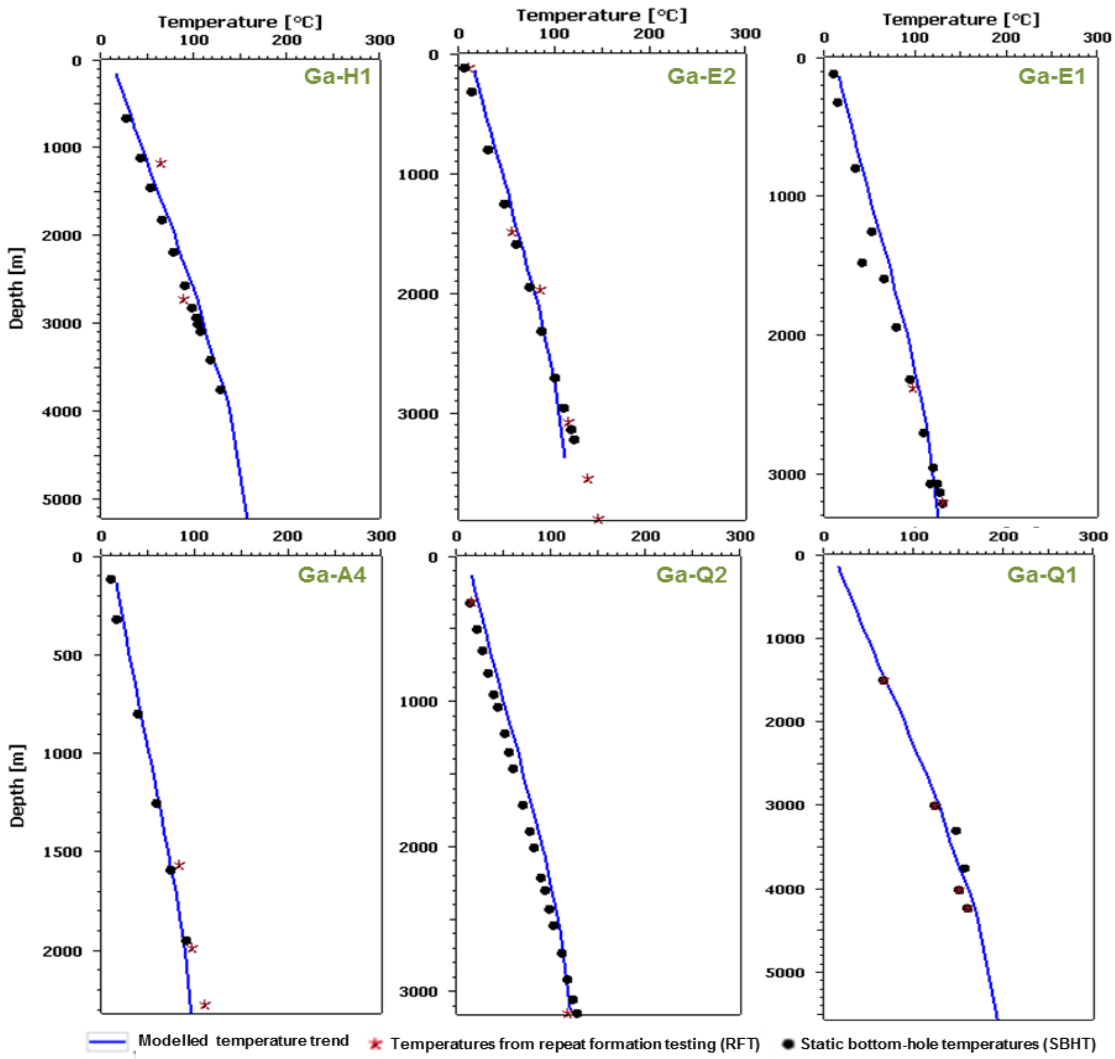

Figure 4.12: *Depth temperatures plots for all studied wells displaying the general reliability of the final thermal model with measured temperatures; the solid blue line indicating*

http://etd.uwc.ac.za/

modelled present-day geothermal gradient from the numerically simulated thermal evolution models; well locations are indicated in Fig. 3.1.

As revealed, the modelled temperature values match fairly well with measured values, within the area. Of all the well locations, the highest temperatures occur at well Ga-H1, Ga-Q1 and Ga-E2 (Fig. 4.12). Most notable is the gradual increase in geothermal gradients with increasing depths. Figure 4.13 reveals the best fit between measured and simulated vitrinite reflectance trends. Notable is the substantial mismatch between the modelled and actual vitrinite reflectance values as reflected by the profiles at most of the well locations. Thus, for thermal maturation modelling a general increase in vitrinite reflectance with depth was applied as the calibration trend for the source rock units.

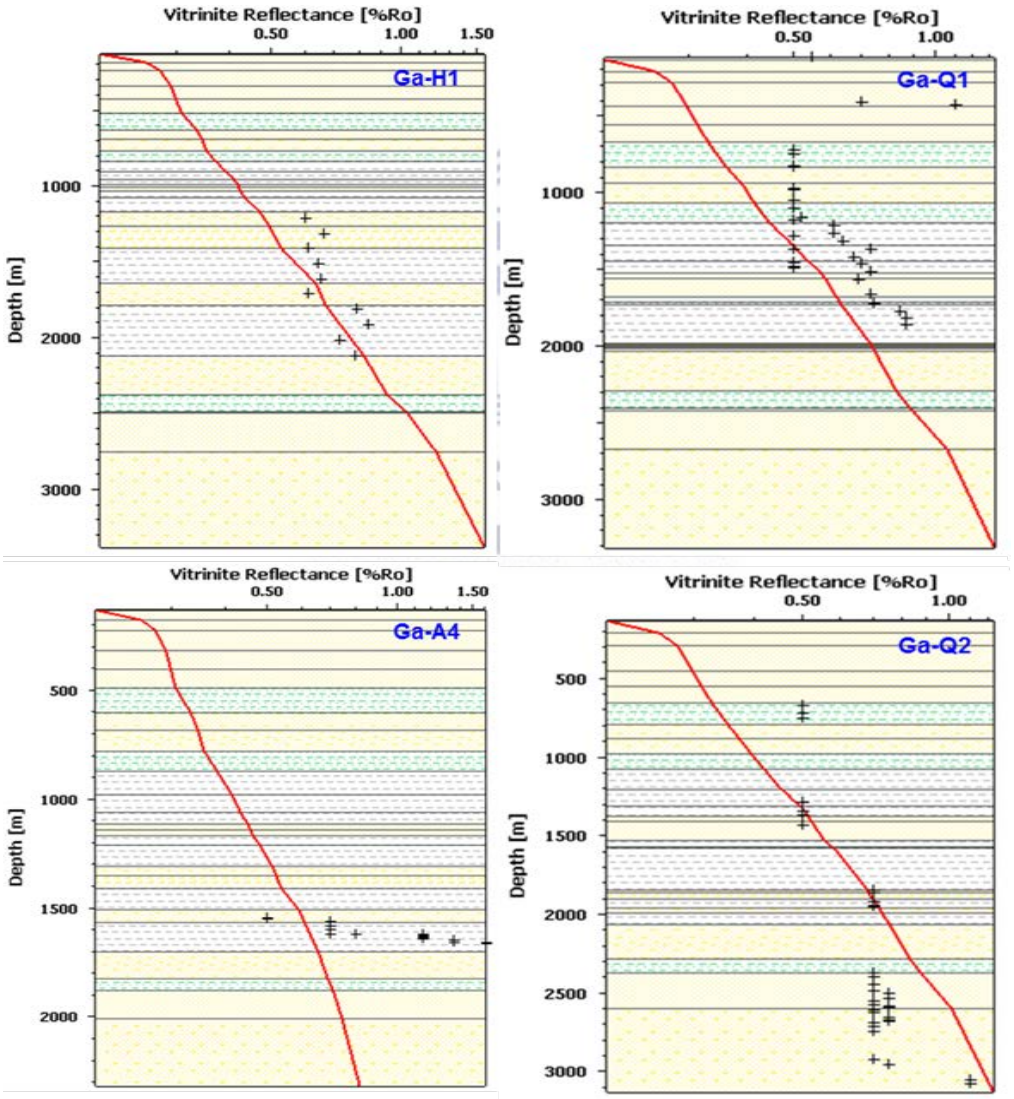

Figure 4.14: *Calibration of modelled present-day vitrinite trends (%VRo) against measured vitrinite reflectance data for 4 wells within the study area. Location of the wells is shown in Fig. 3.1.*

http://etd.uwc.ac.za/

4.3.2 Burial and Thermal History

The geo-history curves (Fig. 4.15a-c) generally reveal four main intervals of substantially increased sedimentation and subsidence during the Mesozoic – Cenozoic Evolution of the basin. The main sedimentation periods are observed during the Upper Jurassic (~ 160 – 145.5Ma), Lower-Mid Cretaceous (~ 129 – 120Ma, and ~103 –93Ma) times and Upper Cretaceous times (85 – 75Ma). These are followed by a relatively steady subsidence during the Paleogene. The last unconformity related major erosional event ended at ~ 67Ma, with resumed deposition of Cenozoic sediments. Maximum burial is observed to have occurred around 23.3Ma, after which the major uplift and erosion caused a substantial removal of sediments at the northern sub -domain.

The temperature fluctuations at different well locations follow the burial histories of the source rock formations during most of the geo-history, as can be seen in Figure 4.15a-c. The highest increase in vertical thermal gradients (temperature increase with depth) for the source rock units correlates temporally with tectonic erosional and/or thermal perturbation periods. Generally, the Southern locations display higher thermal gradients. The Kimmeridgian and Valanginian source rock units attained temperatures that range from ~ 56 - 180˚C and ~ 61-122˚C respectively during the rifting phase (~ 160-130 Ma). The Hauterivian, Aptian and Turonian source rock units are observed to have experienced periods of long-term thermal cooling and intermittent episodic renewed heating.

UNIVERSITY of the
WESTERN CAPE

Similarly, the heat flux trends within these units (Fig. 4.15d) also indicates smaller average values during the phases of renewed heating at ~ 80-70 Ma compared to those of the Kimmeridgian and Valanginian source rock units. Particularly notable, are the sedimentary infill heat flux peaks at each location associated with the late Cretaceous hotspot thermal anomaly at ~ 80-70Ma. These have values of 120, 165 and 250 mW/m², for the Northern, Central and Sothern sub-domains, respectively. The trend increases in a generally N-S direction along the basin axis (with the greatest values observed at well Ga-E2; Fig. 4.15c). This decreasing heat flux trend follows the measured and/or observed VRo profiles trends for the three representative well locations (Fig. 3.6).

Presented in Figure 4.16 are the present-day heat flow distribution maps for the syn-rift (Fig. 4.16a and b) and post-rift (Fig. 4.16c - e) source rocks. The maps show that the temperatures increase in a southerly direction and away from the Superior High for all the source rocks with the deeper (older) source rocks attaining the highest temperatures as expected.

http://etd.uwc.ac.za/

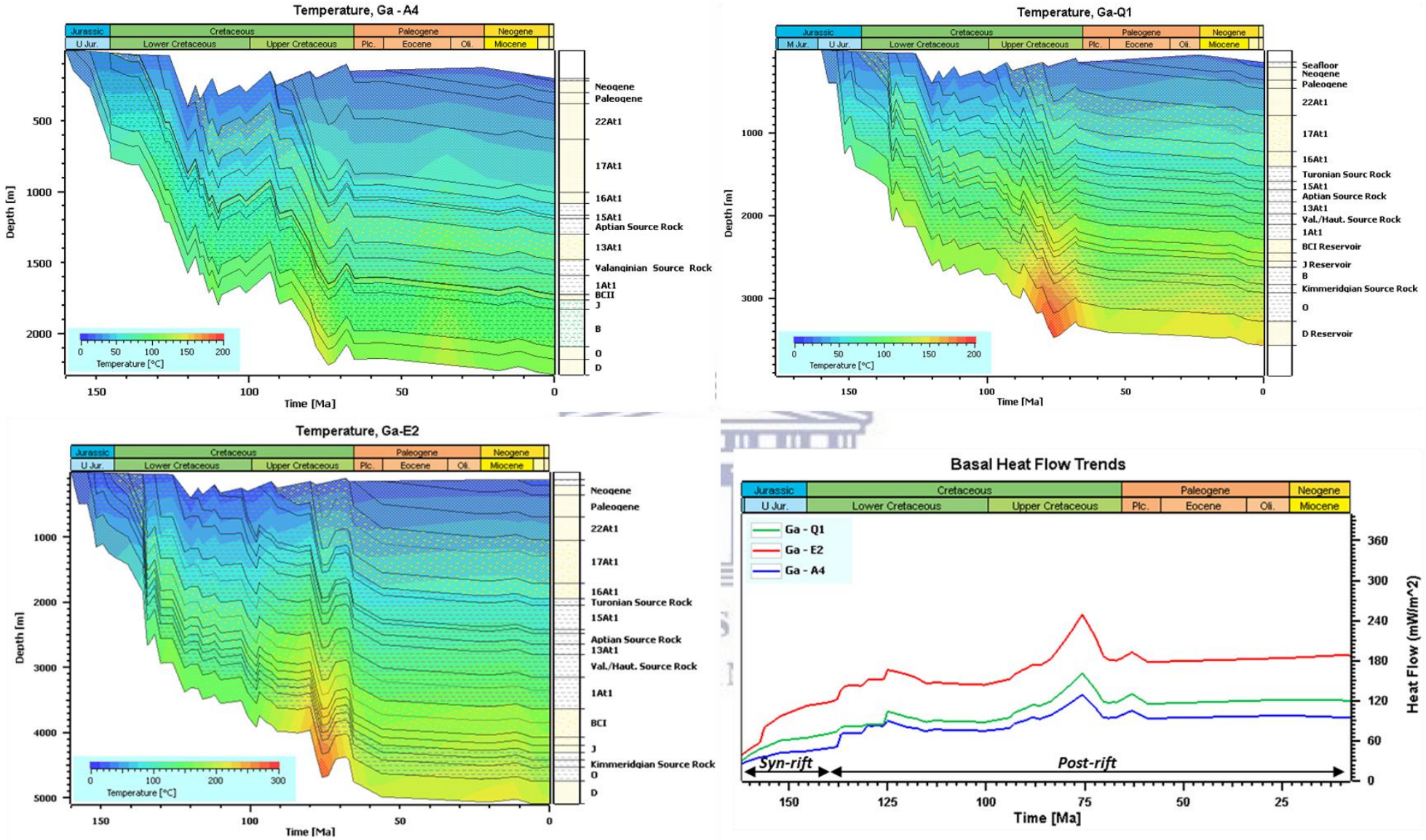

Figure 4.15: *Burial and thermal histories at representative well locations from (a) the Northern – Ga-A4, (b) central – Ga-Q1 and (c) Southern – Ga-E2. Plus (d) the Mesozoic – Cenozoic basal heat flow evolution at the abovementioned wells. Note: basal heat fluxes are considerably higher for Northern domains.*

http://etd.uwc.ac.za/

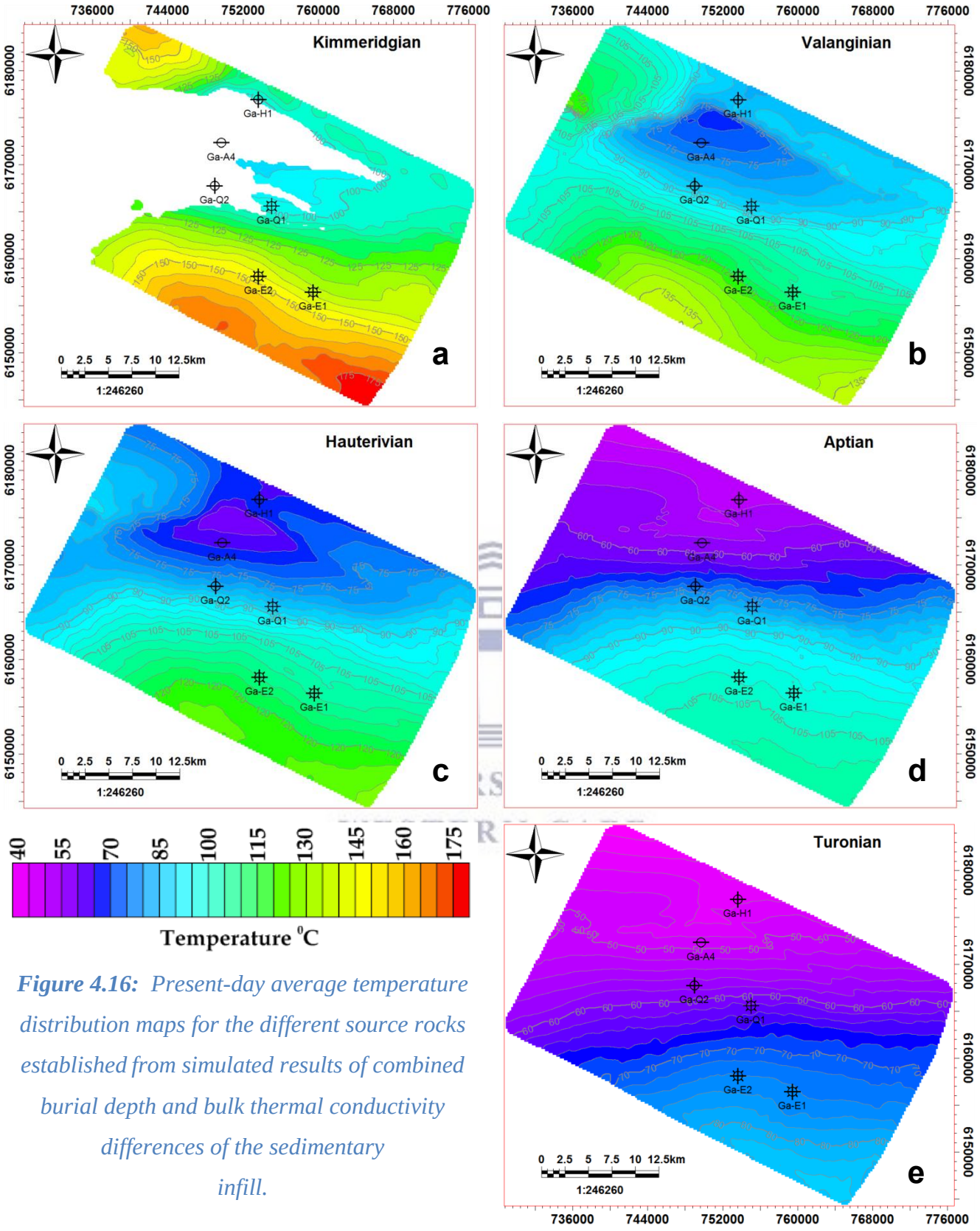

Figure 4.16: *Present-day average temperature distribution maps for the different source rocks established from simulated results of combined burial depth and bulk thermal conductivity differences of the sedimentary infill.*

http://etd.uwc.ac.za/

4.3.3 Maturation and Hydrocarbon Generation Evolution

This section exhibits the source rock maturity evolution trends as a function of burial and thermal variations, along with the transformation ratios that provide information on the generation potentials. Moreover, the hydrocarbon generation timing and efficiencies of the various source rock units are also disclosed. The values for vitrinite reflectance were calculated for all stratigraphic units, whereas the transformation ratios were calculated only for the source rock units.

Maturity and Transformation Ratio Evolution

Figure 4.17 illustrates extracted present-day 1D maturity modelling results in the form of calculated vitrinite reflectance at the 3 selected well locations (others present in Appendix D). The simulated maturity histories (Fig. 4.17) reveal that onset of maturity was at ~ 130 Ma. The largest increase in maturity occurred in the mid to late Upper Cretaceous following the thermal uplift and the subsequent onset of thermal subsidence. The modelled source rocks are observed to be at their maximum depth of burial at present-day as depicted by the extracted 1D and a 2D cross-section of the simulated 3D maturity model (Figs. 4.17 and 4.18).

Maturity evolution levels for the different source rocks from inception to present-day (Figs. 4.17 – 21; Figs. 6 - 8 Appendix D) are deduced to have varied generally as follows: early oil (0.5% - 0.7% VRo) and dry gas (2.0% - 4.0% VRo) windows for the Kimmeridgian and Valanginian, immature (0% - 0.55% VRo) to wet gas (1.3% - 2.0% VRo) for the Hauterivian and Aptian, and immature (0% - 0.55% VRo) to main oil (0.5% - 0.7% VRo) for the Turonian. Mostly, these variations in source rock maturity timing for the different wells can be attributed to topographic effects, i.e. the source rocks become more mature away from the Superior High (Fig. 4.18). Details of the widespread maturity increases are provided by the map views which signify the spatial evolution of the different source rock units (Figs. 4.20; 4.21; Appendix D).

http://etd.uwc.ac.za/

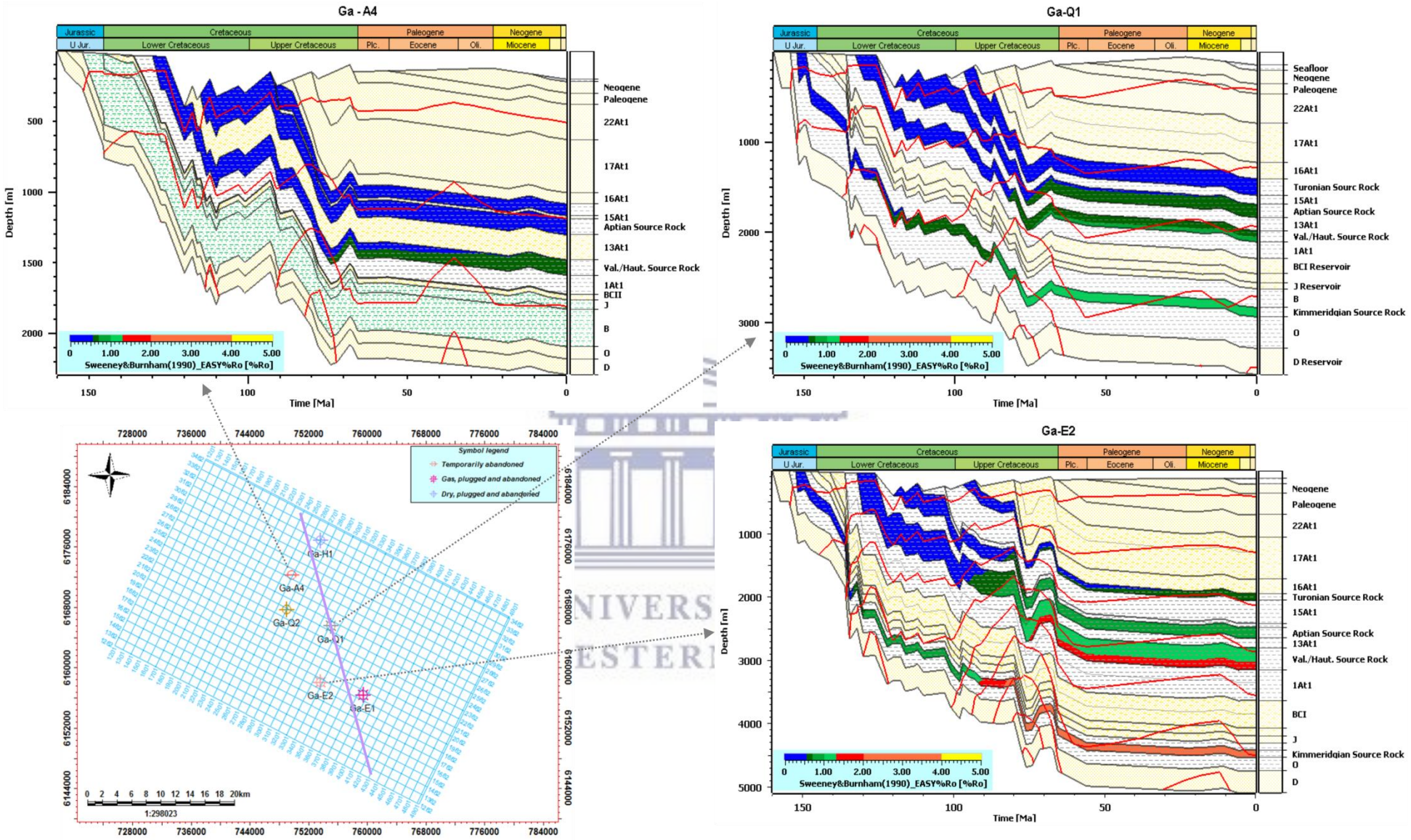

***Figure 4.17**: Modelled maturity evolution (a, b, c) for the occurring source rock units at the three well locations. The maturity models utilized the proper Burnham (1989) TII and TIII kinetics for the hydrocarbon generation modelling of the formations.*

http://etd.uwc.ac.za/

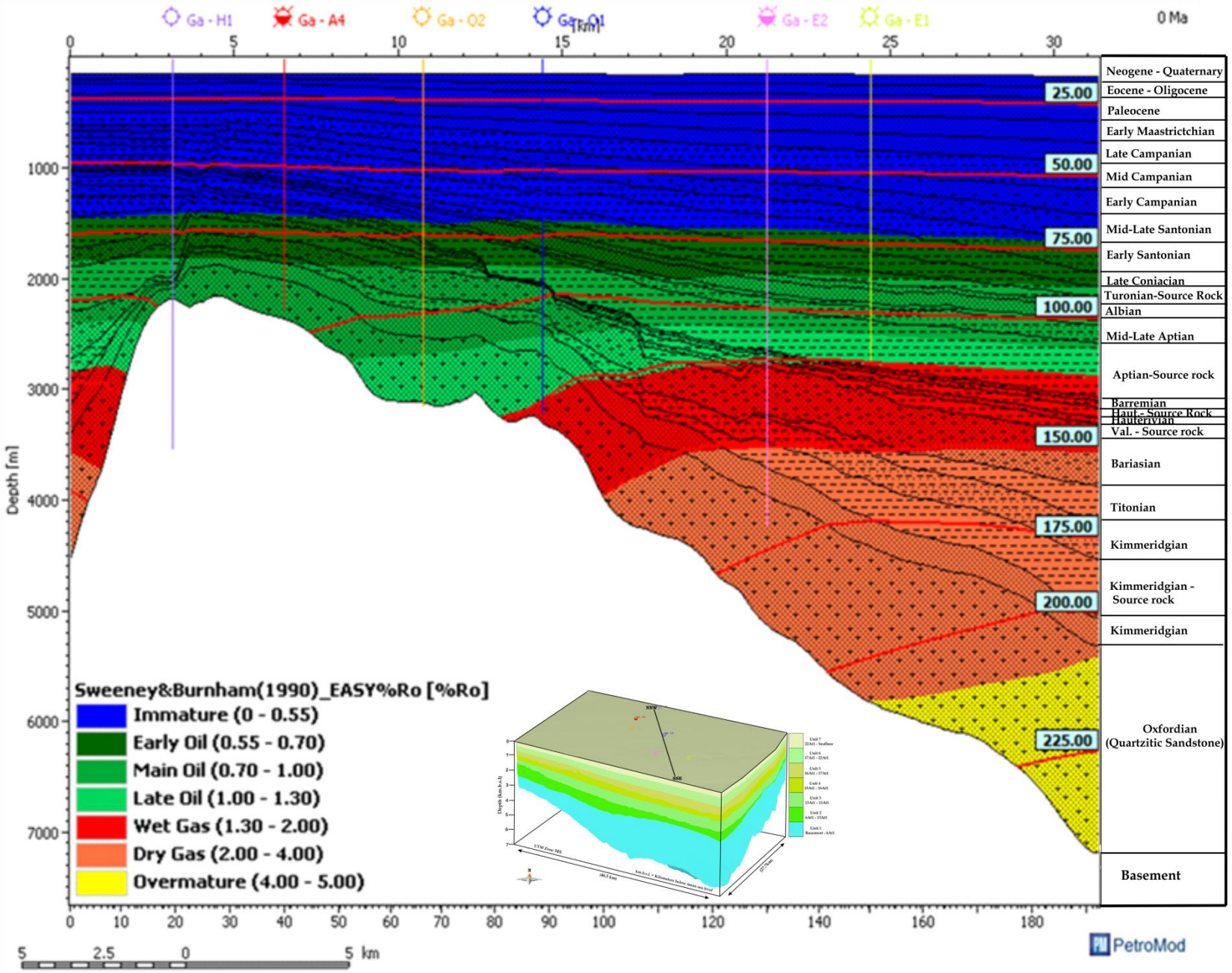

Figure 4.18: *A cross section indicating the present-day modelled maturity of the Mesozoic – Cenozoic sedimentary infill established from simulated results. Maturity is dependent on the formation depths, and becomes lower to the north where the formations become shallower. Red lines (isotherms) indicating temperature boundaries.*

http://etd.uwc.ac.za/

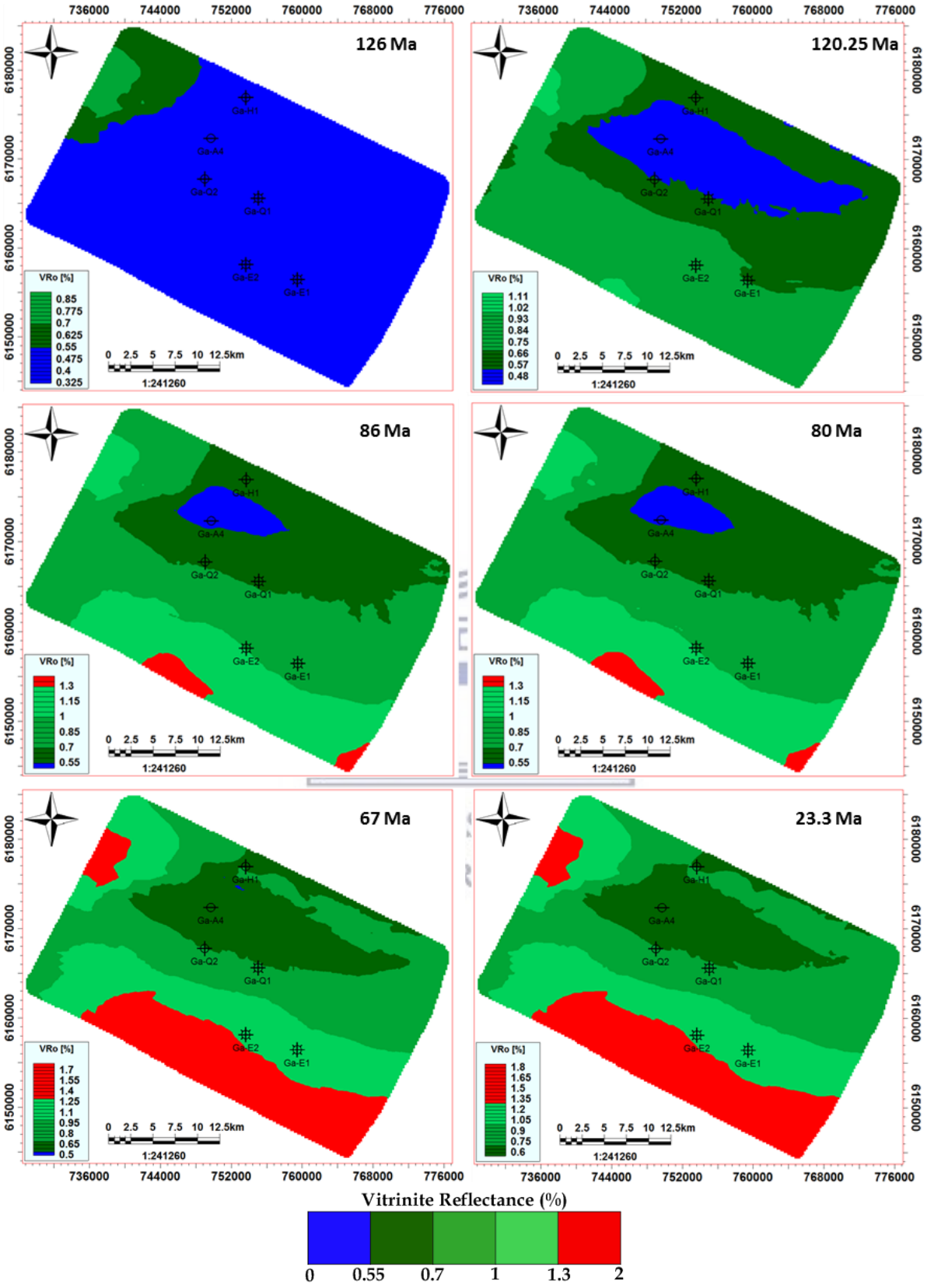

Figure 4.19: *Map (top) view of the simulated maturity history of the Valanginian (syn-rift) source rocks, from 126Ma - 23.30Ma. Ages depicted reflect the periods of tectonic significance (see Fig. 3) on the source rock maturity and hydrocarbon generation.*

http://etd.uwc.ac.za/

The Valanginian source rock reached the main- and late-oil windows at ~ 126 Ma and ~ 120.25Ma, respectively (Fig. 4.19). The source rock entered the gas window during the Upper Cretaceous at ~ 86Ma. In the same way Figure 4.20 shows that the Aptian source rock attained main- and late-oil conditions at ~ 86.0 Ma and 67Ma, respectively.

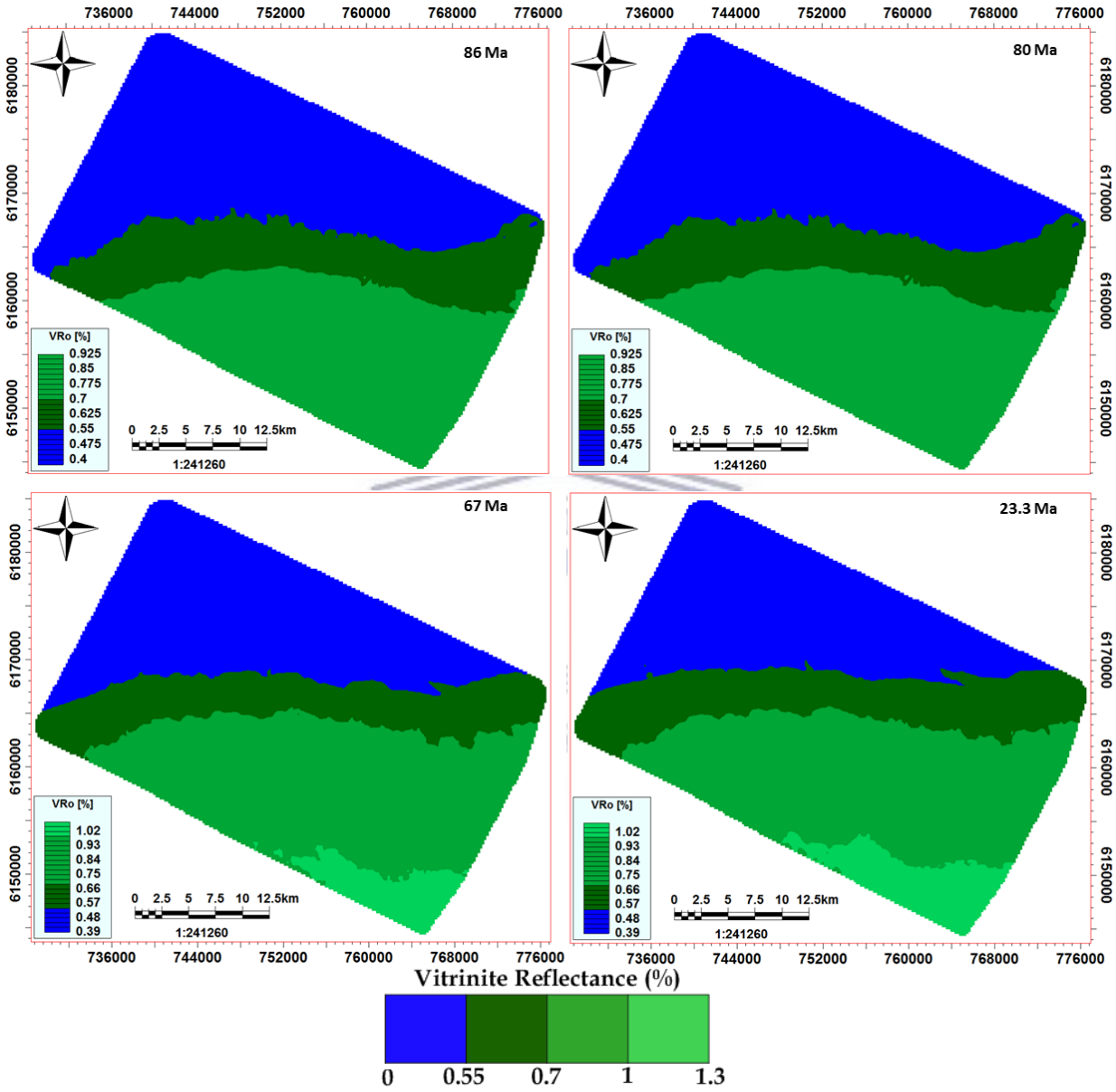

Figure 4.20: *Map (top) view of the simulated maturity history of the Aptian (post-rift) source rocks, from 86Ma - 23.30Ma.*

The simulated maturity evolutions of the other source rock units (i.e. Kimmeridgian, Hauterivian and Turonian) are shown in Figs. 6 - 8; in Appendix D. It is indicated that the Kimmeridgian unit experienced a rapid increase in maturity during the Lower Cretaceous (at ~ 134 - 132.9Ma). This led to maturity fluctuations that range from immature to wet gas windows at the north-western and south-eastern extreme locations. Moreover, it attained

http://etd.uwc.ac.za/

maturities within the dry gas windows as early as ~129.40Ma, with the entire unit being completely matured at ~ 110Ma.

The maturity evolution levels for the Hauterivian indicate that maturity onset was at ~ 120.25Ma. It remained in the early oil window up until ~ 103Ma, before entering the main oil window and only attained the late oil and wet gas windows at ~ 83.6Ma and 67Ma respectively. In the same way, maturity onset for the Turonian source rock was at ~ 72.30Ma. Since then it has only crossed the threshold into the main oil maturity window (0.55–0.70 %VRo) at ~ 23.3Ma. The maturity of the Aptian only attains wet gas conditions in its deepest portions, locally at the South-eastern border of the area (Figure 4.20).

Figures 4.21, 4.22 and 9 – 11; Appendix D, respectively demonstrates the transformation ratios evolution of the source rocks by means of extracted 1D models and map views.

Predicted present-day transformation ratios indicate that the onset of kerogen conversion was at the deepest portions as expected. For the Kimmeridgian source rock this was at ~ 132.9Ma. At ~113Ma the Northern portion and most parts of the southern portions had reached ~100% TR though the central parts were still in the 0 – 5% window. By ~80Ma major proportions of the Kimmeridgian source rock had already been completely transformed, although locations at the central east remained at ~ 70%. Some parts towards the centre only attained up to ~30% tranformation at ~ 67Ma, but at 23.3Ma were ~65 – 70% tranformed. At present-day, the unit has attained ~ 100% TR for the most part (Fig. 4.21).

UNIVERSITY of the
WESTERN CAPE

The onset of transformation for the Valanginian source rock was at ~126Ma (Fig. 4.22) A significant difference is observed in the ratio of transformation of the Valanginian source rock from northern to southern locations within the study area. Generally, the transformation ratio increases away from the Superior High which is in accordance with its maturity trend (Fig. 4.19). At 23.3Ma, the source rock has only reached ~ 75% in its NNW and S parts, and remained relatively the same until present-day (Fig. 4.21).

Analogous to that of the Valanginian, transformation for the Hauterivian (Fig. 4.23) source rock followed the maturation trend with onset at ~ 120.25Ma. It remained in the ~ 0-5% window untill ~ 103Ma, after which it slowly increased to ~ 85% in some parts of the southern sections. From ~ 67Ma, the southern parts attained ~ 90-100% transformation but the central - northern locations until present-day still remained within the ~ 0-5% window. As for the Aptian and Turonian source rocks, transformation onset was at ~ 89Ma and 23.3Ma respectively. The transformation ratio trends of these source rocks are parallel to those of

http://etd.uwc.ac.za/

maturation (e.g. Fig. 4.20), as by ~ 80Ma only the southern locations of the Aptian source rock had attained up to ~ 80- 85% transformation. The Northern – central locations and almost 90% of the Turonian source rock still remain immature to present day.

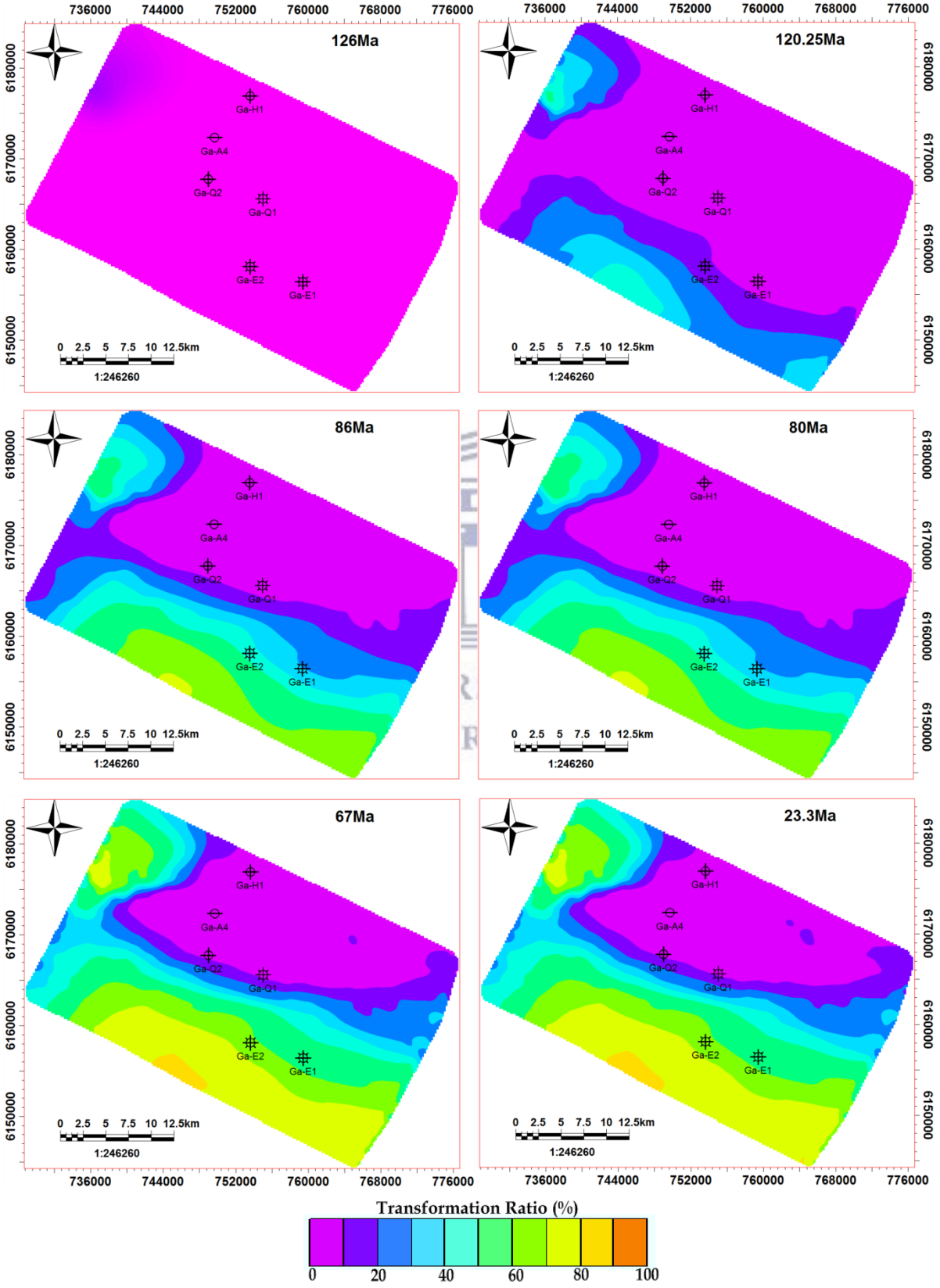

http://etd.uwc.ac.za/

Figure 4.21: *Map (top) view of the simulated of transformation ratio for the Valanginian (syn-rift) source rocks, from 126Ma - 23.30Ma.*

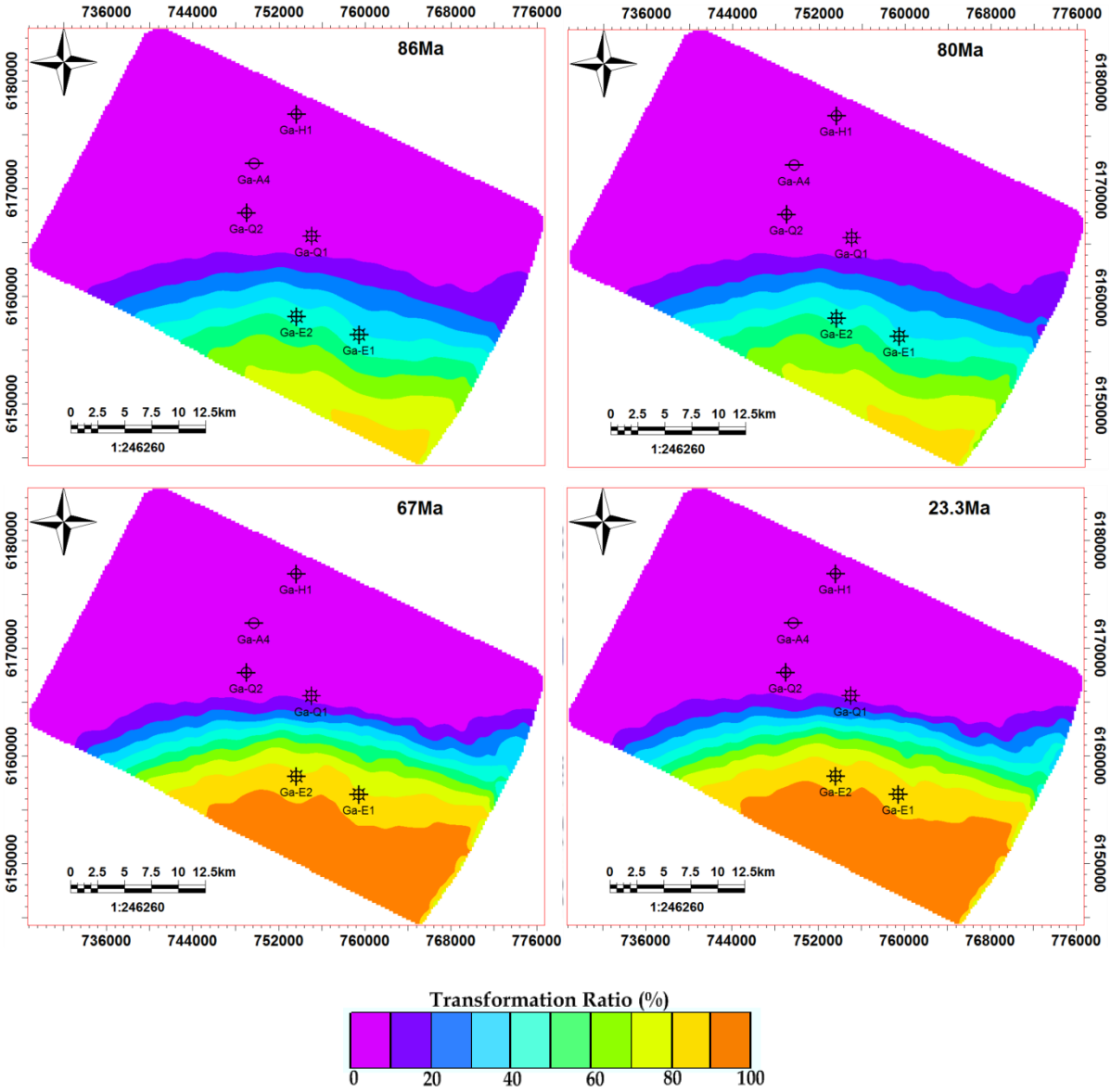

Figure 4.22: *Map (top) view of the simulated history of transformation ratio for the Aptian (post-rift) source rocks, from 86Ma - 23.30Ma.*

http://etd.uwc.ac.za/

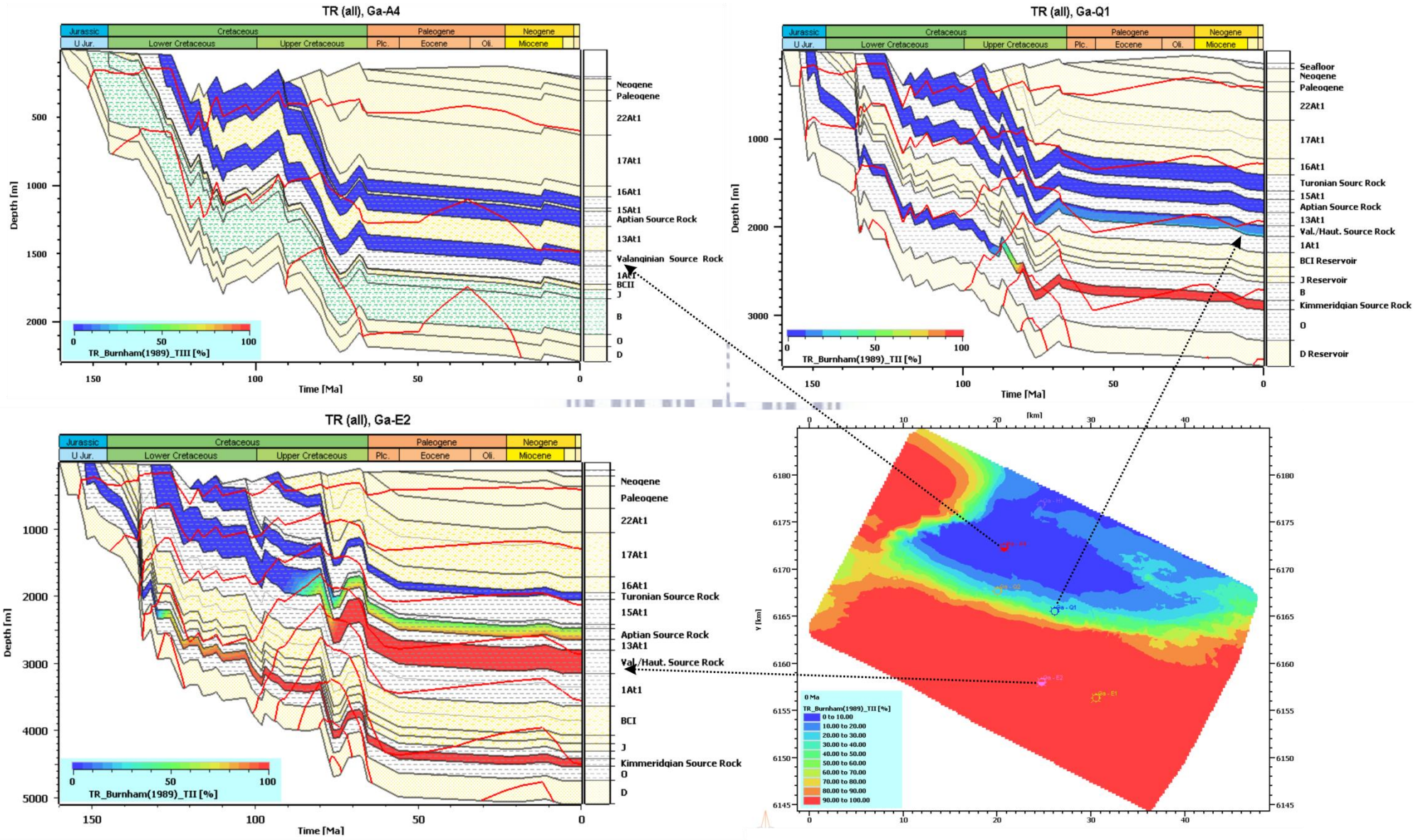

***Figure 4.23**: Modelled evolution of Transformation ratio (a, b, c) for the occurring source rock units, at the three well locations. They were established from simulations using the kinetic models of Burnham (1989).*

http://etd.uwc.ac.za/

Present-day Maturity and Transformation Ratio Distribution

The present-day maturities of the modelled source rock units and their corresponding transformation ratios are presented in Figure 4.24 and Figure 4.24. The trends generally reveal that the southern domains are more matured compared to the northern domains, and are in accordance with transformation ratios (TR) (Figs. 4.24 – 4.25). Of all the modelled source rocks, the Kimmeridgian stratum exhibits the highest transformation.

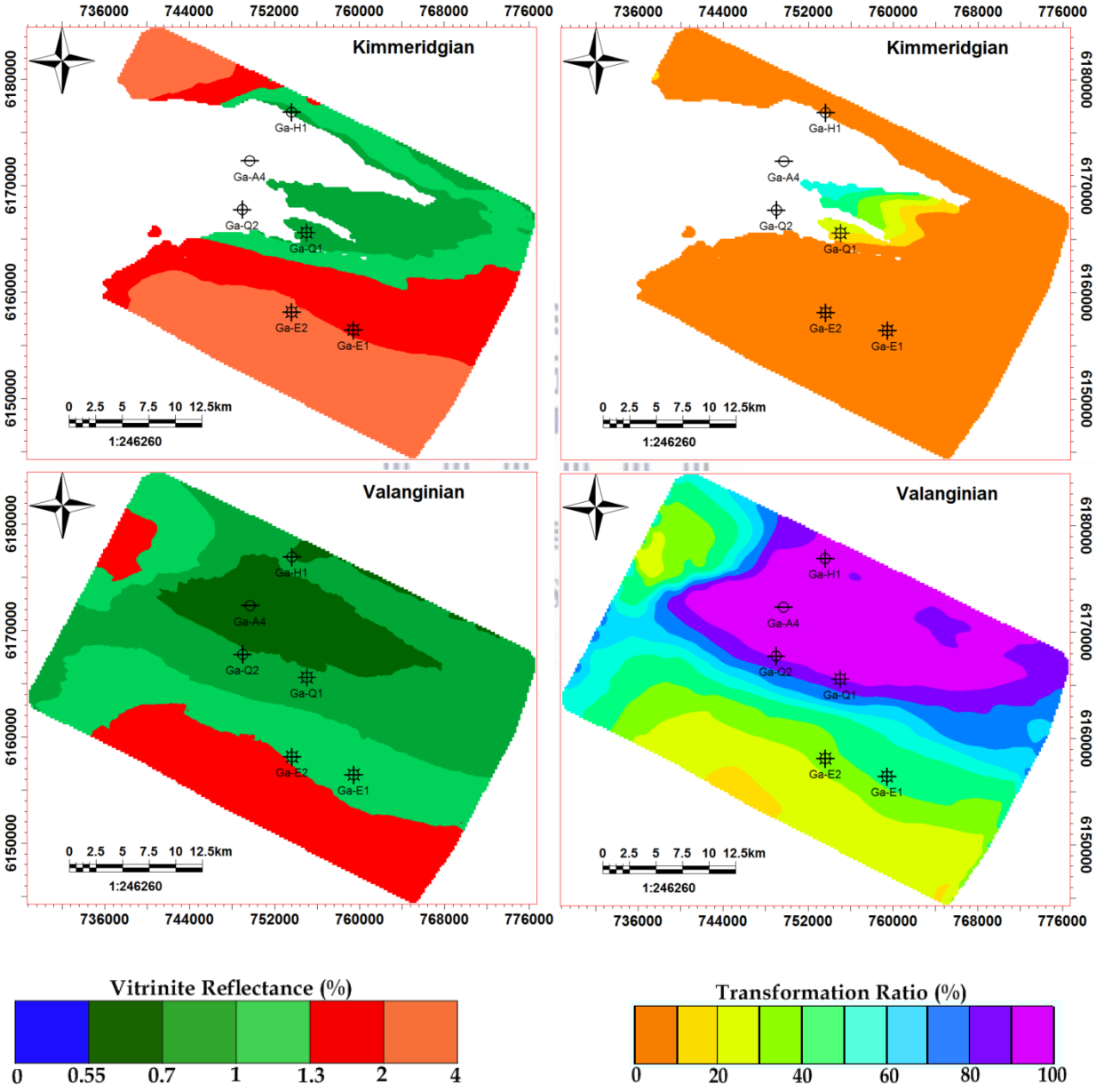

Figure 4.24: *Present-day maturity (VRo) and transformation ratio (TR) average distribution maps of the modelled Syn-rift (i.e. Kimmeridgian (a) and Valanginian (b)) source rocks.*

http://etd.uwc.ac.za/

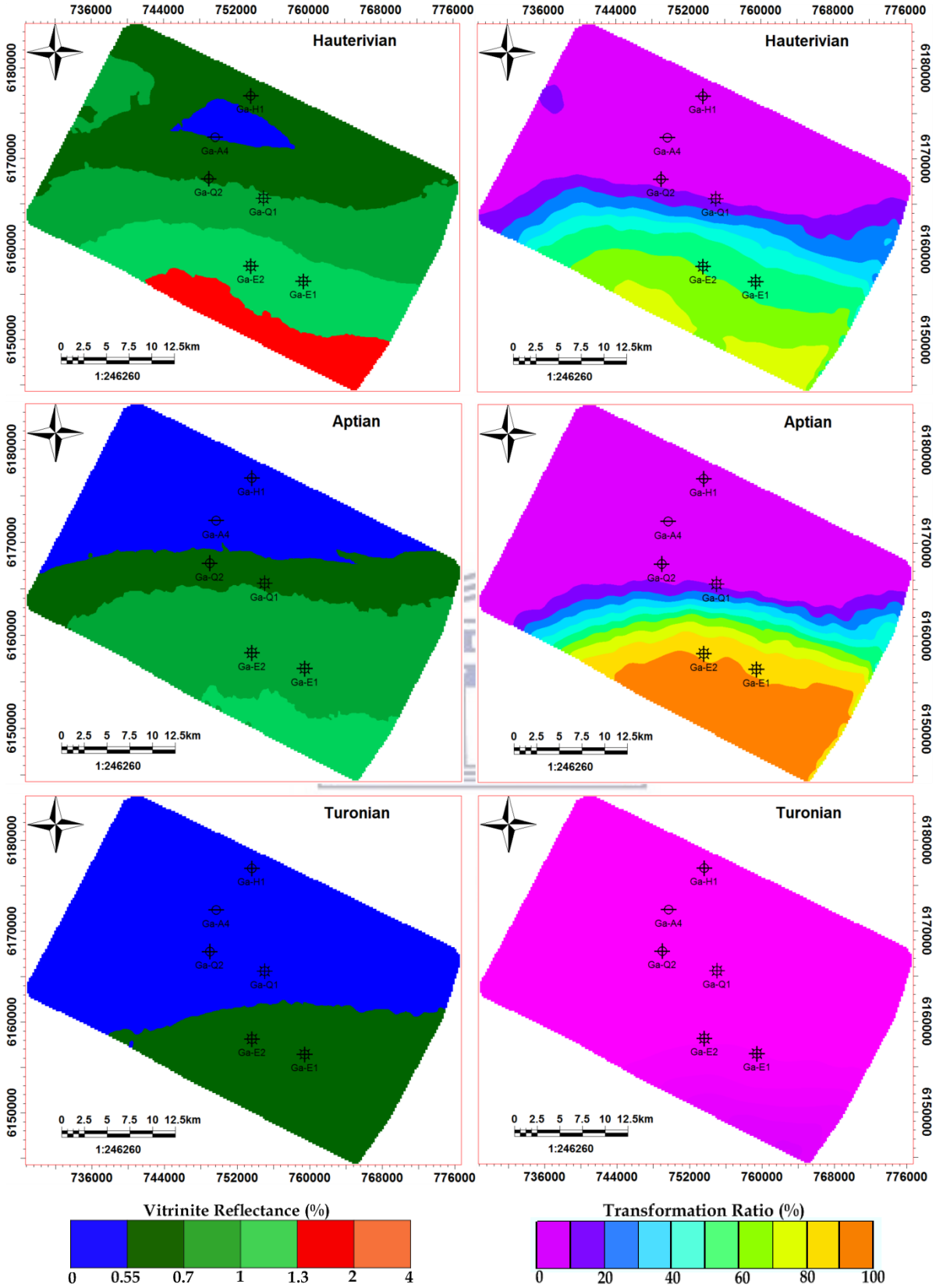

Figure 4.25: *Present-day maturity (VRo) and transformation ratio (TR) average distribution maps of the modelled post-rift (i.e. Hauterivian (c), Aptian (d), and Turonian (e)) source rocks. Note the generally increasing magnitudes towards the south of the basin.*

http://etd.uwc.ac.za/

Hydrocarbon Generation Potentials and Timing

The bulk hydrocarbon generation rates and generated fractions were established for the source rock units, using the Burnham (1989) kinetic model. As revealed by the transformation ratio distributions of the modelled source rocks; the northern Ga-H1 and Ga-A4, plus central Ga-Q1 and Ga-Q2 wells have present-day oil to wet gas generation potentials, while the southern Ga-E1 and Ga-E2 have a wet gas to dry gas present-day generation potential at present-day (Figs. 4.24 – 4.25).

The 3D simulation results of hydrocarbon generation are presented in Figure 4.26. These modelling results reveal that generation from the source rocks follow the maturation trend and there has been multiple phases of generation from the organic-rich source rocks. Accordingly, they suggest that substantial hydrocarbon generation from the source rocks typically occured from the lower Cretaceuos transitional phase, increasing slowly to the upper and Tertiary times of the basin. Generation began with the Kimmeridgian source rock at the extreme northern and southern locations, during the Lower Cretaceous (~ 135 Ma). This was followed by a slow increase in tranformation ratios until Late Creataceous times (~ 67 Ma) when peak generation was attained (Fig. 4.26). The onset of generation for the other four source rocks (Valanginian, Hauterivian, Aptian and Turonian) occurred in the Upper Cretaceous.

UNIVERSITY of the
WESTERN CAPE

The critical moments of peak hydrocarbon generation are represented as ~ 50% kerogen transformations for the individual source rocks and were derived from the deepest well location (Ga-E2; Fig. 3.1) where the highest maturity level was reached; these are depicted as the (red) dotted lines (Fig. 4.26). It is revealed that the Kimmeridgian source rock reached its critical moment at ~ 98Ma, the Valanginian and Hauterivian source rocks at ~ 80Ma and the Aptian source rock at ~ 60Ma. Moreover, it is worth noting that the Turonian source rock has not yet attained its critical moment, as it predominantly remains immature, as revealed by its present-day maturity and transformation ratio distributions (Figs. 4.25 and 4.26).

http://etd.uwc.ac.za/

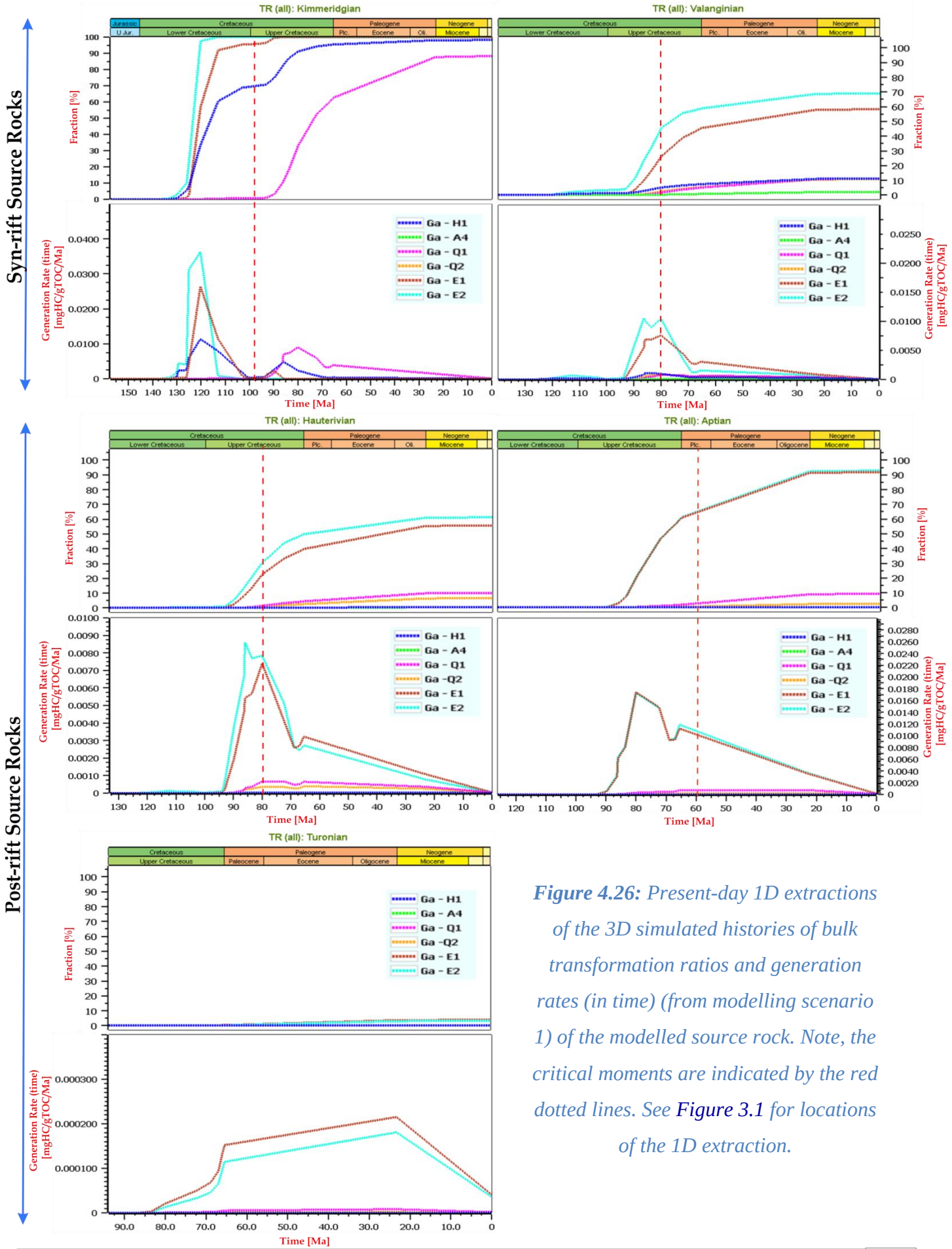

Figure 4.26: *Present-day 1D extractions of the 3D simulated histories of bulk transformation ratios and generation rates (in time) (from modelling scenario 1) of the modelled source rock. Note, the critical moments are indicated by the red dotted lines. See Figure 3.1 for locations of the 1D extraction.*

http://etd.uwc.ac.za/

Expulsion Efficiencies and Cumulative Mass

Figure 4.27 presents the histogram of estimated mass of generated, expelled, accumulated hydrocarbons as well as the remaining potential for the individual source rocks based on kinetic model predictions and their physical properties. For this study, expulsion efficiencies were estimated for the total petroleum using the generated and expelled hydrocarbon masses (Fig. 4.27) and these are reported in Table 5. The variable efficiencies can possibly be attributable to the source rock types.

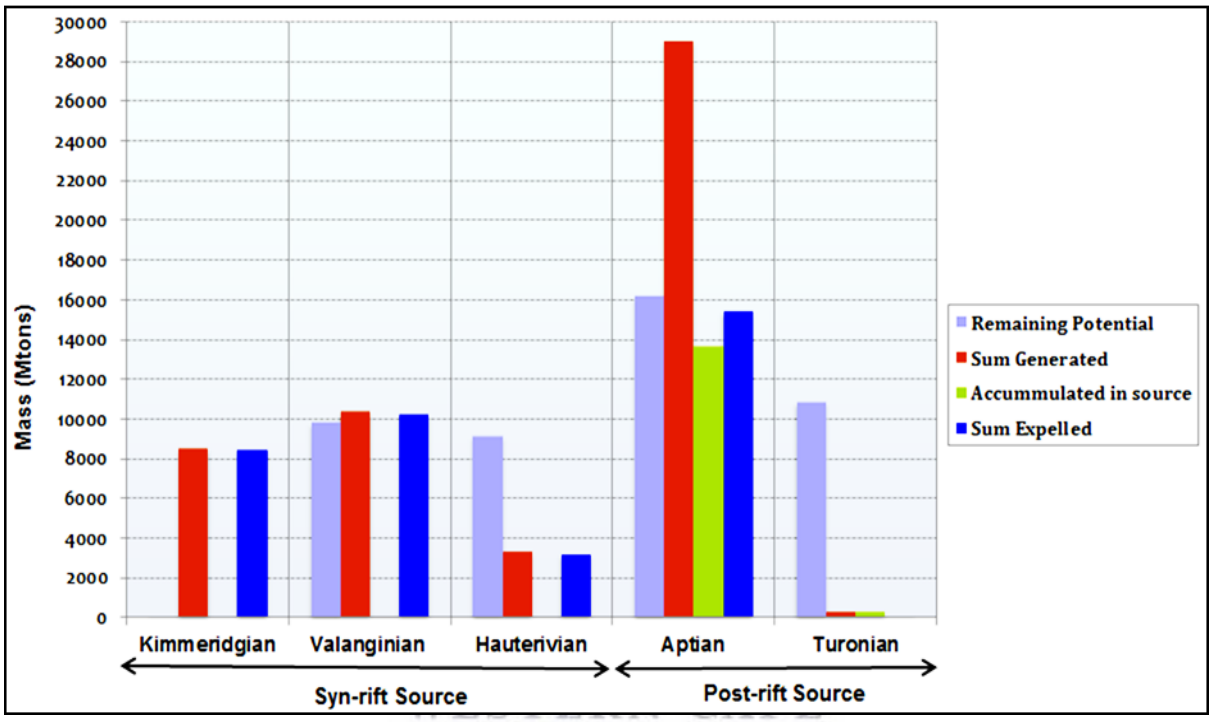

***Figure 4.27**: Cumulative generation and expulsion history plot showing the Total mass in Mt of hydrocarbons generated, accumulated and expelled by individual source rocks. The graphs were plotted from the simulated 3D- generation model of an area.*

***Table 5.** The established efficiencies derived from generated and expelled hydrocarbons masses over time from the simulated 3D- generation model.*

SOURCE ROCKS	SUM GENERATED	SUM EXPELLED	EFFICIENCY
Kimmeridgian	8517.05	8480.61	0.996
Valanginian	10375.14	10236.29	0.987
Hauterivian	3294.33	3191.15	0.969
Aptian	29079.57	15427.43	0.531
Turonian	303.61	32.52	0.107

http://etd.uwc.ac.za/

CHAPTER 5

Discussion

This study demonstrates one of the numerous benefits of combining geochemistry and subsurface mapping in basin evaluation. During the progression of the study, subsurface datasets were utilized. A number of diagrams and relationships between pyrolysis parameters were used to interpret the properties and hydrocarbon potential of the studied source rocks. The burial and thermal histories of the wells along with the maturation histories of the source rocks present within this study area were modelled, to understand their hydrocarbon generation and expulsion histories within the Southern Pletmos basin. Rock-Eval data and vitrinite reflectance values were used as source rock information and/or input for calibration processes. Present-day borehole measured temperatures (a combination of corrected SBHTs and DSTs), were used to validate the predicted temperature distributions. Basal-HF, PWD, and SWIT were used as boundary conditions due to their importance in defining the basic energetic conditions for thermal development and organic maturation through time.

5.1 Source Rock Characteristics

The ages of the analysed organic shales range from Kimmeridgian through to the Turonian (Fig. 2.2). Their stratigraphic depths from proximal-distal domains range between ~ 1500 to 3300m, with average thicknesses of approximately 50 - 100 metres (Fig. 4.11).

Results from Rock-Eval data analyses (Section 4.2), demonstrate that generally TOC values for the Aptian source rock are highest followed by the Hauterivian, Valanginian and Turonian, with the Kimmeridgian having the lowest. The TOC ranges for all five source rocks (Fig 4.6; Table 4) indicate that they meet the accepted standard for fair to excellent petroleum generating potential. Nonetheless, TOC content decreases northwards with a general southerly increase in conjunction with strata thicknesses along the modelled NNW – SSE axis (Fig. 3.5; Appendix D). S1 along with S2 values, generally demonstrate a fair to good petroleum potential with an exception of very good for the Valanginian and Aptian units. Furthermore, the sample distribution trend signposts a marginal to adequate petroleum potential with depth for the various source rock units. The petroleum potential trend of the source rocks increases (from marginal to adequate) with increasing depth, through a notable overlap within the three zones occurring between approximately 1500 to 3200m as samples amid this interval display a mixed hydrocarbon generating potential (Fig. 4.6).

http://etd.uwc.ac.za/

The TOC together with HI, Pyrolized S2 and vitrinite reflectance (%VRo) results (see Figs. 4.6 – 4.11; Section 4.2), summarises the qualities of the source rocks and maturity influences on the specific kerogen types. These quality and maturity indicators together demonstrate that the source rocks possess excellent gas potentials in addition to good remaining potentials (with an exception to the Kimmeridgian). Their estimated kerogen qualities based on HI values (and attained maturity levels) as indicated by existent organic matter, are in essence shown to be predominated by dispersed vitrinite macerals (Type III Kerogens). In view of their marine paleo-environments and fairly low HI values (Table 2), the Type III Kerogens are thought to be reworked organic debris. Thus, it is expected that because of the largely Type III organic matter predominance, the source rocks are considered as primarily gas-prone. Moreover, these decreased HI and S2 pyrolysis yields that indicate the higher gas-prone character, may have been influenced by maturity increases in response to the high existing thermal regime. Nonetheless, significant amounts of Type II Kerogens (liptinitic macerals of ~ 1–20%) are also present to a lesser extent.

Furthermore, it is worth noting that obtained Tmax values ranges between 409- 469ºC, essentially suggesting that the samples are in the early mature window. This indicates that the Tmax values are falsely low. Nevertheless, Tmax values are partly dependent on other factors (Peters, 1986; Peters and Cassa, 1994), and may have ensued either from suppression caused by bitumen or the presence of thermally labile (and sulphur-rich) kerogen in the samples types (Snowdon, 1995).

UNIVERSITY of the
WESTERN CAPE

5.2 Burial and Thermal History

The reconstruction of the burial and thermal history curves exhibits that during the periods of active rifting average sedimentation and subsidence rates were faster and more effective than post-rift times. Most diagnostic feature of the heat flow trends (Fig. 4.15) is the major peak in the Upper Cretaceous (~ 78Ma) which can be attributed to the hotspot-related thermal anomaly. Higher temperatures were observed in the southern parts and these values have been attributed to the increasing geothermal gradients towards the south due to greater burial depths and proximity to the main source of basal heat. The present-day temperature maps (Fig. 4.16) show that the temperature generally increases in a southwards direction which is in line with the burial and thermal history curves. The shallower locations (e.g. Ga-A4) show significantly lower present-day temperatures.

http://etd.uwc.ac.za/

5.3 Thermal Maturity History and Hydrocarbon Generation

5.3.1 Thermal Maturation

Maturity history modelling was based on the choice of kinetic model and on calibrating (or matching) as closely as possible the measured and the simulated vitrinite reflectance for each burial history location. This allowed for the estimating of the extent of hydrocarbon generation from the prospective source rocks. Assuming the onset of oil window maturity at 0.55% VRo, the syn-rift source rocks (Kimmeridgian and Valanginian) entered the oil window at ~ 135 and 98Ma, respectively. Gas maturity started at ~ 92Ma for the Kimmeridgian and 75Ma for the Valanginian source rock. The deeper post-rift source rocks (Hauterivian and Aptian) entered the oil window at ~ 98 and 83Ma, respectively. These source rocks remain in the oil window at present day. The Turonian source rock on the other hand only entered the first stage of oil maturity at ~70Ma and remains immature in most parts.

Anomalously high vitrinite reflectance values are observed on the vitrinite reflectance profile in the Tertiary sediments. In addition, both the Sweeney and Burnham (1989) and Pepper and Corvi (1995) kinetic models also showed significant deviations between the modelled and measured vitrinite reflectance trends. The most likely explanation for these can be rapidly increased heating rates caused by the abrupt burial of the source rocks during the Miocene times, evidenced by the geo-history curves (Fig. 4.15). As there is a well-documented thermal anomaly event (discussed in Chapter 2), called the 'African Superswell' during these periods, linked to the regional rapid high heat supplies (Davies, 1997; Nyblade, 2003; Sonibare et al., 2015).

Furthermore, the established maturity history maps (Figs. 4.19 – 4.22) reveal that during the late Cretaceous-Tertiary there was a rapid increase in vitrinite reflectance with hardly any increase in source rock maturity from Miocene (~ 5.3Ma) to present-day.

5.3.2 Hydrocarbon Generation

The 3D model permitted a first-order estimation of the mass of hydrocarbons generated through time. The extent of hydrocarbon generation is directly related to vitrinite reflectance values based on the Sweeney and Burnham (1989) kinetic model. The amount of hydrocarbon generation was further quantified on the basis of the transformation ratio (TR) which is dependent on the temperature and the maturation history of the source rocks.

http://etd.uwc.ac.za/

Generally, the degree of the transformation ratio differs considerably from the different source rocks. Present-day TRs for the syn-rift units indicate that the Kimmeridgian and Valanginian source rocks exhibit an overall diminished remaining petroleum potential along a NW-SE trend. Predicted present-day TR indicates that the most extensive petroleum generation occurred at the locations where the source rocks were most deeply buried (e.g. the southern parts), as expected. This is manifested in the Ga-E2 plot shown (Figs. 4.23 - 4.26) by vitrinite reflectance values greater than 1.3% VRo and TR values >80%. Central areas close to the Superior High (i.e. at well Ga-Q1) representing intermediate depths of burial display moderately extensive hydrocarbon generation. Moreover, the general transformation ratio trend exhibited by the post-rift source rocks is analogous to syn-rift maturation trends, as it increases from north to south in the modelled area (Figs. 4.23 and 4.26). The exception is that the shallower burial depths of the post-rift source rocks resulted in the least extensive hydrocarbon generation as some portions of these source rocks still remain immature.

The petroleum generation onset within the basin materialized during the early Cretaceous, between ~ 136.9-132.4Ma (Figs. 4.21 – 4.23). Following the generation onset, the expelled hydrocarbon quantities gradually increased onwards from the early transitional post-rift phase for all modelled source rock intervals. Three main stages of hydrocarbon generation are documented. The first, occurred at about ~ 132.4 – 120 Ma during the last stage of the syn-rift phase, and can be linked to the syn-rift heat flow peak (Fig. 4.15), believed to have resulted from rapid sedimentation and subsidence/ burial rates. The other two additional phases are associated to heat flow peaks and respective maximum burial depths during post-rift periods, as revealed in Figure 4.15. The cumulative peak of generation for the basin is revealed to have transpired at ~ 23Ma during the Late-Oligocene times, as a result of temperature increase linked to the aforementioned plume development (Burden, 1992; Roux, 2007) discussed in Chapter 2.

UNIVERSITY of the
WESTERN CAPE

5.4 Timing of Generation and Expulsion Efficiencies

In this study, a TR of 50% was used to predict the timing of the main hydrocarbon generation phase. Values were derived from the Ga-E2 well location (southerrn portion of the study area) where the five source rocks reached the highest maturity (and transformation) levels. Consequently, the Kimmeridgian source rock attained ~50% transformation at ~98Ma; the Valanginian and Hauterivan at ~80Ma; the Aptian at ~60Ma; and the Turonian has not yet reached its main stage of hydrocarbon generation as it remains largely immature at present-

http://etd.uwc.ac.za/

day, as previously mentioned. Clearly, the timing of generation followed the expected order of older source rocks generating before younger ones at any given location.

The expelled hydrocarbons through time were approximated by the 3D model and aided in the prediction of the present-day expulsion efficiencies of the different source rock units. The expulsion efficiency is hereby defined as the amount of expelled hydrocarbons over the amount of generated hydorcarbons for each source rock unit. The Kimmeridgian, Valanginian and Hauterivian source rock units have an expulsion efficiency close to 1. For this reason in conjunction with the greater burial depths and high VRo and TR at present day, the Kimmeridgian can be classified as a 'relic effective source rock'. Nonetheless, the Valanginian and hauterivian are classified as 'active source rocks' due to their present-day maturities and transformation ratios. The Aptian shale is classified as an 'active source rock' and is moderately thermally mature within the distal locations, and remains broadly immature at the proximal locations. The Turonian shale remains highly immature within the proximal and central domains and it is, therefore, classified as a 'Potential source rock'.

5.5 Uncertainty and Sensitivity Modelling

As aforementioned (Section 3.3.3), the effects of different kinetic models and input parameters on the source rock maturation, transformation, hydrocarbon generation timing, type and masses/volumes were tested using two (Pepper & Corvi (1995) _TII (B) and Pepper & Corvi (1995) _IIIH (DE)) kinetic models. These simulations adopted the boundary conditions (i.e. HF, PWD and SWIT), uplift and erosion periods (Fig. 3), and the listed set of source rock parameters (mainly TOC and HI) in Table 4. Notably, the kinetic model choice had the most dominant effect on the type of hydrocarbons generated and expelled, as well as on the timing and bulk generation rates of the source rocks.

Furthermore, increasing the heat flow will result to increased maturity and transformation ratios of the source rocks, accelerate the onset of hydrocarbon generation (at shallower depths), and the amount of gas generation compared to oil. Increasing TOC and HI mostly results in increasing generated masses/volumes of hydrocarbons, leading to rapid saturations and expulsion. Higher TOC and HI increases source rock hydrocarbon saturations, with increase in HI (particularly), resulting to an increasing amount of oil generation compared to gas. Varying the PWD only has a marginal effect on the model; interrelated to the oil and gas masses/volumes i.e. it increases or reduces the generated amount of oil compared to gas.

http://etd.uwc.ac.za/

Regarding evolution modelling, the main uncertainty pertains to the geo-history, regarding the assumed erosional thicknesses, particularly those related to the major uplift events (Fig. 3). Increasing or decreasing strata/unit thicknesses may influence the hydrocarbon generation timing and generation rates of the source rocks, but has no major effect on their burial depths and temperature distributions at present-day.

UNIVERSITY of the
WESTERN CAPE

http://etd.uwc.ac.za/

Conclusion

The following conclusions can be drawn, based on the evaluations of the spatial/structural configuration, source rock characteristics (e.g. TOC content and quality), Mesozoic - Cenozoic thermal maturation, petroleum generation and - expulsion in the study area:

- The Upper Cretaceous mantle-related hotspot and Miocene post-rift heat flux peaks (revealed to be associated to the events of uplift and erosion, and margin uplift during these times) seem to have had the greatest influence on the maturities of the source rocks.
- The modelled source rocks all display present-day maturity trends that increase in a southerly direction, which reflects a large influence of maximum thicknesses and burial depths towards the south.
- Present-day maturation windows range between late oil - dry gas (for syn-rift source rocks) and early oil - wet gas window (for post-rift source rocks) for southern domains, whereas at northern domains it ranges between main oil - wet gas (for syn-rift source rocks) and immature - early oil (for post-rift source rocks).
- The established maturity evolution trends, demonstrate that conditions seem to have been appropriate for hydrocarbon generation from the syn-rift source rocks, particularly the Kimmeridgian, throughout its Upper Cretaceous-Cenozoic history. Likewise, favourable conditions still exist for hydrocarbon generation from the post-rift source rocks, as large areas of the units presently are within the immature - oil windows.
- Petroleum generation commenced during the Early Cretaceous, nonetheless, the initial two main phases of generation (i.e. at ~ 135 – 105 Ma and ~ 95 - 70 Ma) are sensitive to the rapid subsidence and heat flow peak during syn-rift, whilst the subsequent two phases (i.e. at ~ 93 - 67 Ma and ~ 56 - 23.3 Ma) are sensitive to the Late Cretaceous to Early Tertiary hotspot-transit mechanism and Miocene margin uplift associated pulses of heat flow.
- Sufficient generation could only be accomplished during Oligocene times at ~ 33.3 Ma following the last thermal subsidence. Cumulatively, the post-rift akin to syn-rift source rocks, have a higher remaining hydrocarbon potential. Grading from the highest - lowest from the Aptian - Kimmeridgian source rocks, respectively.

UNIVERSITY of the WESTERN CAPE

http://etd.uwc.ac.za/

- Likewise, the post-rift source rocks have generated the most (due to the influence of the Aptian source rock). Nonetheless, the syn-rift source rocks have contributed the most to the expelled petroleum due to their higher burial depths and maturation stages.
- The Kimmeridgian, Valanginian and Hauterivian source rock units have expulsion efficiencies close to 1, which indicates that part of the gas discoveries in the study area and Sub-basin at large may have been sourced from them.

In view of the abovementioned conclusions, it can be proposed that all the source sediments are still retaining part of their generative potentials. These results confirm the viability of hydrocarbon plays within the basin, provided all other petroleum system elements and processes are in place.

UNIVERSITY of the
WESTERN CAPE

http://etd.uwc.ac.za/

Recommendations for Future Work

The research undertaken in this study highlighted a number of subjects on which supplementary investigation would be beneficial.

In particular, there is a need to develop a petrographic classification to validate the organic matter classification and provide additional value to source rock evaluation. The petrographic analysis will identify individual components that make up the kerogens, their organic characteristics, and depositional conditions which can then be used to cross check geochemical results. Moreover, the organic petrology can effectively identify the inertinite content and its effects on geochemical results, which is difficult to define based on Rock Eval pyrolysis techniques alone.

There are numerous additional areas for future research with regards to thermal maturity indicators. Whilst this thesis successfully defined the thermal maturity trends within the study area based on available data, additional thermal maturity indicators would yield valuable insights into the determination of the timing of erosion events and quantification of single heating events. In this regard, Apatite Fission Track Analysis and Fluid Inclusion studies would be beneficial. Nonetheless, these should be accompanied by elemental analysis and biomarker maturity ratios, so as to effectively describe the thermal maturity of the organic matter and hydrocarbon generative potential.

The choice of the kinetic model has a major influence on the timing and rates of hydrocarbon generation from source rocks. Thus, the effect of using different models could be further studied in a separate project in future. This would give a better impression of overall model performance, and allow comparison between the results.

Lastly, the modelled area represents the southern Pletmos Basin. Thus, additional effort should be devoted to modelling the other parts of the basin in order to establish a regional trend distribution of the source rocks and thermal maturity. The techniques used in this research could be usefully applied in this regional assessment.

UNIVERSITY of the WESTERN CAPE
http://etd.uwc.ac.za/

References

Allen, P.A. and J.R. Allen., 2005, *Basin Analysis: Principles and Applications*, 2nd edn. Blackwell Publishing, pp. 549

Al-Hajeri, M.M., Al Saeed, M., Derks, J., Fuchs, T., Hantschel, T., Kauerauf, A., Neumaier, M., Schenk, O., Swientek, O., Tessen, N., Welte, D., Wygrala, B., Kornpihl D. and Peters. K., 2009, '*Basin and petroleum system modelling'. Oilfield Review*, Summer 2009, pp. 1-16.

Bally, A.W. and Snelson, S., 1980, '*Realms of subsidence'*, In: A.D. Miall (Editor), Facts and Principles of World Petroleum Occurrence. *Can. Soc. Pet. Geol., Mem.*, **6**: 9-94.

Baskin D.K.,1997, '*Atomic H/C Ratio of Kerogen as an Estimate of Thermal Maturity and Organic Matter Conversion'. Am. Assoc. Petrol. Geol.* Bull. **81**:1437-1450.

Bate, K.J. and Malan, J.A., 1992, '*Tectonostratigraphic evolution of the Algoa, Gamtoos and Pletmos Basins, offshore South Africa'*. In: M.J. de Wit and I.G.D. Ransome (Editors), Inversion Tectonics of the Cape Fold Belt, Karoo and Cretaceous Basins of Southern Africa. *Balkema*, Rotterdam, pp. 66-76.

Brink, G.J., Brown, L.F., Jr., Keenan, J.H.G., 1994, '*Deposition of fourth-order post-rift Lower Cretaceous sequences and sequence sets (Lower Valanginian to Mid-Aptian), Pletmos Basin, Southern Offshore, South Africa'*, In: P. Weimer and H. Posamentier (Editors), Siliciclastic Sequence Stratigraphy. Recent Advances and Applications. *Am. Assoc. Pet. Geol. Mem.* **58**: 43-69.

Broad, D.S., Jungslager, E.H.A., Mclachlan, I.R., and Roux, J., 2006,'*Geology of the offshore Mesozoic basins'*. In: *The Geology of South Africa* (Ed. by M. R. Johnson *et al.*) pp. 553–571, Geol. Soc. South Africa, Pretoria.

Broad, D.S., 2004,'*Activities and Opportunities in South Africa*'. Unpublished Power Point Presentation to PetroChina.

Brown, L.F., Jr., Benson, J.M., Brink, G.J., Doherty, S., Jollands, A., Jungslager, E.H.A., Keenan, J.H.G., Muntingh, A., and van Wyk, N.J.S., 1996, '*Sequence stratigraphy in offshore South African divergent basins: An atlas on exploration for Cretaceous lowstand traps by Soekor (Pty) Ltd'*, Am. Assoc. Pet. Geol., *Studies in Geology*, **41**, 184 pp.

Burden, P.L.A., 1992, '*Soekor, partners explore possibilities in Bredasdorp Basin off South Africa*'. *Oil and Gas Journal*, **90**:109-112.

Burnham, A.K. & Sweeney, J.J., 1989, *A chemical kinetic model of vitrinite maturation and reflectance*'. *Geochimica et Cosmochimica Acta*, **53**, 2649–2657.

Campher, C.J., di Primio, R., Kuhlmann, G., van der Spuy, D., and Domoney, R., 2010, '*Geological Modelling of the Offshore Orange Basin, West Coast of South Africa'*, *AAPG International Conference and Exhibition,* Cape Town, South Africa.

http://etd.uwc.ac.za/

Chinn, E., W., 1991, '*The role of organic geochemistry in petroleum exploration*: *Basin Research Institute Bulletin'*, Louisiana State University, Baton Rouge, LA, pp. 15–23.

Davies, C.P.N., 1997a, '*Hydrocarbon evolution of the Bredasdorp Basin, offshore South Africa: from source to reservoir'*. Unpublished PhD Thesis, University of Stellenbosch, pp. 286.

Davies, C.P.N., 1997b, '*Unusual biomarker maturation ratio changes through the oil window, a consequence of varied thermal history'*. *Org. Geochem.*, ***27(7/8)***, 537-560.

Davies, C.P.N., 1990, '*Quantification of oil generation and expulsion from source rocks in the offshore Bredasdorp Basin'*. Abstract, Geocongress 90: *Geol. Soc. S. Afr., Abstr*. Vol., pp. 119-122.

Davies, C.P.N., 1991, 'Geochemistry section: calcimetry analyses - accuracy and repeatability testing'. SOEKOR unpubl. rept., 17pp.

De Wit, M.J., Ransome, I.G.D., 1992. '*The Cape Fold Belt; a challenge for an integrated approach to inversion tectonics*', In: de Wit, M.J., Ransome, I.G.D. (Eds.), Inversion Tectonics of the Cape Fold Belt, Karoo and Cretaceous Basins of Southern Africa. *Balkema*, Rotterdam, pp. 3–14.

Dingle, R.V., Siesser, W.G. and Newton, A.R., 1983, '*Mesozoic and Tertiary Geology of Southern Africa*'. *A.A. Balkema*, Rotterdam, pp. 375.

Duncan, R.A., 1981, *'Hotspots in the Southern Ocean- an absolute frame of reference for motion of the Gondwana continent'. Tectonophysics*, ***74***, 29-42.

Duran, E.R., Di Primio, R., Anka, Z., Horsfield, B., Stoddart, D., 2013, *'3D-basin modelling of the Hammerfest Basin (southwestern Barents Sea): A quantitative assessment of petroleum generation, migration and leakage'. Marine and Petroleum Geology, **45***, 281–303.

Edwards, J.D. and Santogrossi, P.A., 1990, '*Summary and conclusions'*, In: J.D. Edwards and P.A. Santogrossi (Editors), Divergent/Passive Margin Basins. *Am. Assoc. Pet. Geol.* Mem., **48**: 239-248.

Espitalié, J. and Bordenave, M.L., 1993, '*Rock-Eval pyrolysis'*, In: Bordenave, M.L. (ed.), Applied petroleum geochemistry. *Éditions Technip*, Paris, 237–261.

Espitalie, J., 1985, '*Use of Tmax as a maturation index for different types of organic matter comparison with vitrinite reflectance'*. In: Burrus J (ed) Thermal modeling in sedimentary basins. *Editions Technip, Paris*, pp. 475–496.

Gerrard, I., and Smith, G.C.,1982, '*Post-Paleozoic Succession and Structure of the Southwestern Africa Continental Margin*'. *Am. Assoc. Pet. Geol. Memoir* **34** (1), 49-74.

Gohl, K., and G. Uenzelmann-Neben., 2001, '*The crustal role of the Agulhas Plateau, southwest Indian Ocean: Evidence from seismic profiling'*. *Geophys. J. Int., 144*, 632 646, doi:10.1046/j.1365-246x.2001.01368.x.

http://etd.uwc.ac.za/

Goutorbe, B., F. Lucazeau, and Bonneville, A., 2008, '*The thermal regime of South African continental margins'. Earth Planet. Sci. Lett.*, ***267***, 256–265.

Gouws, H.J., 1990, *'The Ga-W prospect: a comparison of the seismic stratigraphic prognosis with drilling results'*. Geocongress 90: *Geol. Soc. S. Afr*., Abstr. Vol., pp. 181-184.

Hadad, Y.T., Hakimi, M.H., Abdullah, W.H., Makeen, Y.M., 2016, *'Thermal maturity history reconstruction and hydrocarbon generation/expulsion modelling of the syn-rift Rudeis and Kareem source rocks in the Red Sea Rift Basin, Sudan'. Arab. J. Geosci.*, 9, 442pp.

Hantschel, T., and Kauerauf, A.I., 2009,'*Fundamentals of Basin and Petroleum Systems Modelling'. Springer-Verleg* Berlin Heidelberg, p. 476.

Hartnady, C. J. H., and Partridge T.C., 1995, '*Neotectonic uplift in Southern Africa: a brief review and geodynamic conjecture'*. In Centennial Geocongress 95: *Geol. Soc. S. Afr*. Extended Abstracts, Vol. 11, pp. 456-459.

Haq, B.U., Hardenbol, J. and Vail, P.R., 1988, '*Mesozoic and Cenozoic chronostratigraphy and eustatic cycles of sea level change'*, In: Wilgus, C.K. et al. (Eds), Sea Level Change: an Integrated Approach. Spec. Publ. Soc. Econ. Palaeont. & Mineral., pp. 42, 71 - 108.

Hood, A., Gutjahr, C.C.M., Heacock, R.L., 1975, *'Organic metamorphism and the generation of petroleum'. Am. Assoc. Petrol. Geol*. Bull **59**: 986-996.

Hunt J. M., 1996, '*Petroleum Geochemistry and Geology'*. W.H. Freeman and Company, New York, 743 pp.

IHS Basin Monitor, 2010, *International Exploration & Production Database, Outeniqua Basin, South Africa*, viewed 2012 from https://www.ihs.com/products/oil-gas-basin-monitors.html.

International Union of Geological Sciences, 2015, 'T*he International Chronostratigraphic Chart*, viewed 2016 from http://www.stratigraphy.org/index.php/ics-chart-timescale.

Jarvie, D.M., 1991, *'Factors affecting Rock-Eval derived kinetic parameters'. Chemical Geology*, **93**, 79 – 99.

Johnson, M.R., Anhauesser, C.R. and Thomas, R.J., (Eds), 2006, '*The Geology of South Africa'. Geol. Soc. S. Afr*., Johannesburg, Council of Geoscience, Pretoria, pp. 691.

Law, C.A., 1999, *'Evaluating Source Rocks'*, In: AAPG special volumes. Volume treatise of petroleum geology/handbook of petroleum geology: exploring for oil and gas traps, 3.1–3.34.

Makeen Y.M., Abdullah, W.H., Pearson, M.J., Hakimi, M.H., Elhassan, O.M.A., Hadad, Y.T., 2016, *'Thermal maturity history and petroleum generation modelling for the Lower Cretaceous Abu Gabra Formation in the Fula Sub-basin, Muglad Basin, Sudan'. Mar. Pet. Geol.*, ***75***, 310–324.

Malan, J.A., 1993, '*Geology, potential of Algoa, Gamtoos Basins of South Africa'. Oil and Gas Journal*, **91**, pp. 74–77.

UNIVERSITY of the
WESTERN CAPE
http://etd.uwc.ac.za/

Martin, A.K. (1987), Plate reorganizations around Southern Africa, hotspots and extinctions. *Tectonophysics*, **142**, 309-316.

Martin, A.K. and Hartnady, C.J.H., 1986, '*Plate tectonic development of the south West Indian Ocean: a revised reconstruction of East Antarctica and Africa'. J. Geophys. Res.*, **91**: 4767- 4786

McCarthy, K., Rojas, K., Niemann, M., Palmowski, D., Peters, K. & Stankiewicz, A., 2011, *'Basic petroleum geochemistry for source rock evaluation'. Oilfield Review*, **23**(2), 32-43.

McLachlan, I.R. and McMillan, I.K., 1979, '*Microfaunal biostratigraphy, chronostratigraphy and history of Mesozoic and Cenozoic deposits on the coastal margin of South Africa'*. Geocongres 77, *Geol. Soc. S. Afr*. Spec. Publ., **6**: 161-181.

McMillan, I.K., Brink, G.J., Broad, D.S., Maier, J.J., 1997, '*Late Mesozoic sedimentary basins off the South Coast of South Africa'*, In: Selly, R.C. (Ed.), African Basins: Sedimentary Basins of the World 3. *Elsevier*, Amsterdam, pp. 319–376.

Magoon, L.B. and Dow, W.G., 1994, *'The petroleum system'*, In: *The Petroleum System From* Source *to Trap* (Ed. By L.B. Magoon, and W.G. Dow), *AAPG Memoir*, vol. **60**, pp. 3–24.

Moldowan, J. M., K. E. Peters, R. M. K. Carlson, M. Schoell, and M. A. Abu-Ali, 1994, Diverse applications of petroleum biomarker maturity parameters: *Arabian J. for Science and Engineering*, vol. **19**, pp. 273-298

Nyblade, A.A. and Robinson S.W., 1994, '*The African superswell'. Geophy. Res. Lett.* **21** *(9),* 765 - 768.

Nyblade, A.A., 2003, '*The origin of the African superswell'. American Geophysical Union*, Fall Meeting 2003, abstract #S51F-01.

Peters, K.E., Burnham A.K., and Walters, C.C, 2015, '*Petroleum generation kinetics: Single versus multiple heating ramp open-system pyrolysis*' *Am. Assoc. Pet. Geol. Bull.*, Vol. **99**, pp. 591 – 616.

Peters, K.E. & Cassa, M.R., 1994, '*Applied source rock geochemistry'*, Chapter 5, In: Magoon, L.B. & Dow, W.G. (eds), '*The petroleum system — from source to trap'. AAPG Memoir*, **60**, pp. 93-120.

Peters, K.E., and J. M. Moldowan., 1993, '*The Biomarker Guide, Interpreting molecular fossils in petroleum and ancient sediments*, Prentice Hall, 363 p.

Petroleum Agency South Africa – PASA, 2012, '*Petroleum exploration in South Africa: information and opportunities*'. PASA, Cape Town, pp. 30.

Poelchau, H.S., Baker, D.R., Hantschel, T., Horsfield, B. and Wygrala B., 1997, '*Basin simulation and the design of the conceptual basin model'*, In: Petroleum and basin evolution (Ed. by D.H. Welte, B. Horsfield and D.R. Baker), *Springer*, Berlin - Heidelberg - New York, pp. 5-70.

UNIVERSITY of the WESTERN CAPE

http://etd.uwc.ac.za/

Roux, J. and Davids, A., 2009, '*Barremian Basin Floor Fan Complex: An Untested Gas Play within the Northern Pletmos Basin*', In AAPG International Conference and Exhibition, Rio de Janeiro, Brazil, 2009, AAPG Search and Discover Article # 10234.

Roux, J., 2007, '*Republic of South Africa 2007 licensing round - Area C: Proximal Bredasdorp Basin*'. Petroleum Agency South Africa, pp. 26.

Roux, J., 1997, Soekor (Pty.) Ltd., *'Exploration and Production: Potential Outlined in Southern Outeniqua Basin'*, off S. Africa, *Oil and Gas Journal*, July 21.

Schmidt, S., 2004, '*The petroleum potential of the passive continental margin of South-Western Africa – a basin modelling study'*. PhD thesis, Rheinisch-Westfälischen Technischen Hochschule Aachen, pp.156.

Smith, M.R. and Bayliss, G.S., 1980, '*Source-rock evaluation I reference manual: GeoChem Laboratories'*, Inc. (Houston), pp. 60.

Sonibare, W.A., di Primio, R., Anka, Z., Scheck-Wenderoth, M., and Mikeš, D., 2015, '*Petroleum systems evolution within a transform-related passive margin setting: crustal scale 3D basin modelling of the Western Bredasdorp Basin (Area C/West Block 9), offshore South Africa'*. Marine and Petroleum Geology, (subm.).

Sonibare, W.A., Sippel, J. Scheck-Wenderoth, M. and Mikeš D., 2014, '*Crust-scale 3D model of the Western Bredasdorp Basin (Southern South Africa): data-based insights from combine isostatic and 3D gravity modelling'*. *Bas. Res.*, doi: 10.1111/bre.12064.

Sweeney, J.J. and Burnham, A.K., 1990, *'Evaluation of a simple model of vitrinite reflectance based on chemical kinetics'*. *Am. Assoc. Pet. Geol. Bull.*, **74**, pp. 1559 – 1570.

Thomson, K., 1998, '*When did the Falklands rotate*? *Mar. Pet. Geol.*, **15**, 723-736.

Tinker, J., De Wit, M.J. and Brown R., 2008, '*Linking source and sink: evaluating the balance between onshore erosion and offshore sediment accumulation since Gondwana break-up, South Africa'*. *Tectonophysics, 455*, 94–103.

Tissot, B.P. and Welte, D.H., 1984, '*Petroleum formation and occurrence'*. *Springer-Verleg* Berlin Heidelberg, pp. 679.

Van Der Merwe, R., and Fouché J., 1992, '*Inversion tectonics in the Bredasdorp Basin, offshore South Africa'*, In: *Inversion tectonics of the Cape Fold Belt, Karoo and Cretaceous basins of Southern Africa* (Ed. by M.J. De Wit & I.G.D. Ransome): *A.A. Balkema*, Rotterdam, pp. 49 -59.

Waples, D. W., 1985, Geochemistry in Petroleum Exploration: Boston, IHRDC, 232 p.

Wygrala, B.P., 1989, '*Integrated study of an oil field in the southern Po Basin, Northern Italy'*. PhD thesis: University of Cologne, Germany.

http://etd.uwc.ac.za/

Appendices

Appendix A

Table 1. General well information.

Well Name	Latitude	Longitude	KB	Bottom Depth	Potential
Ga – A4	34° 33' 36.07" S	23° 43' 17.05" E	26m	2302m	Commercial gas rates
Ga – E1	34° 33' 36.07" S	23° 43' 17.05" E	30m	2898m	Dry with gas shows
Ga – E2	34° 33' 36.07" S	23° 43' 17.05" E	30m	4396m	Dry with gas shows
Ga – H1	34° 33' 36.07" S	23° 43' 17.05" E	26m	3575m	Dry with no gas shows
Ga – Q1	34° 33' 36.07" S	23° 43' 17.05" E	26m	3243m	Commercial gas rates
Ga – Q2	34° 33' 36.07" S	23° 43' 17.05" E	26m	3177m	Dry with gas shows

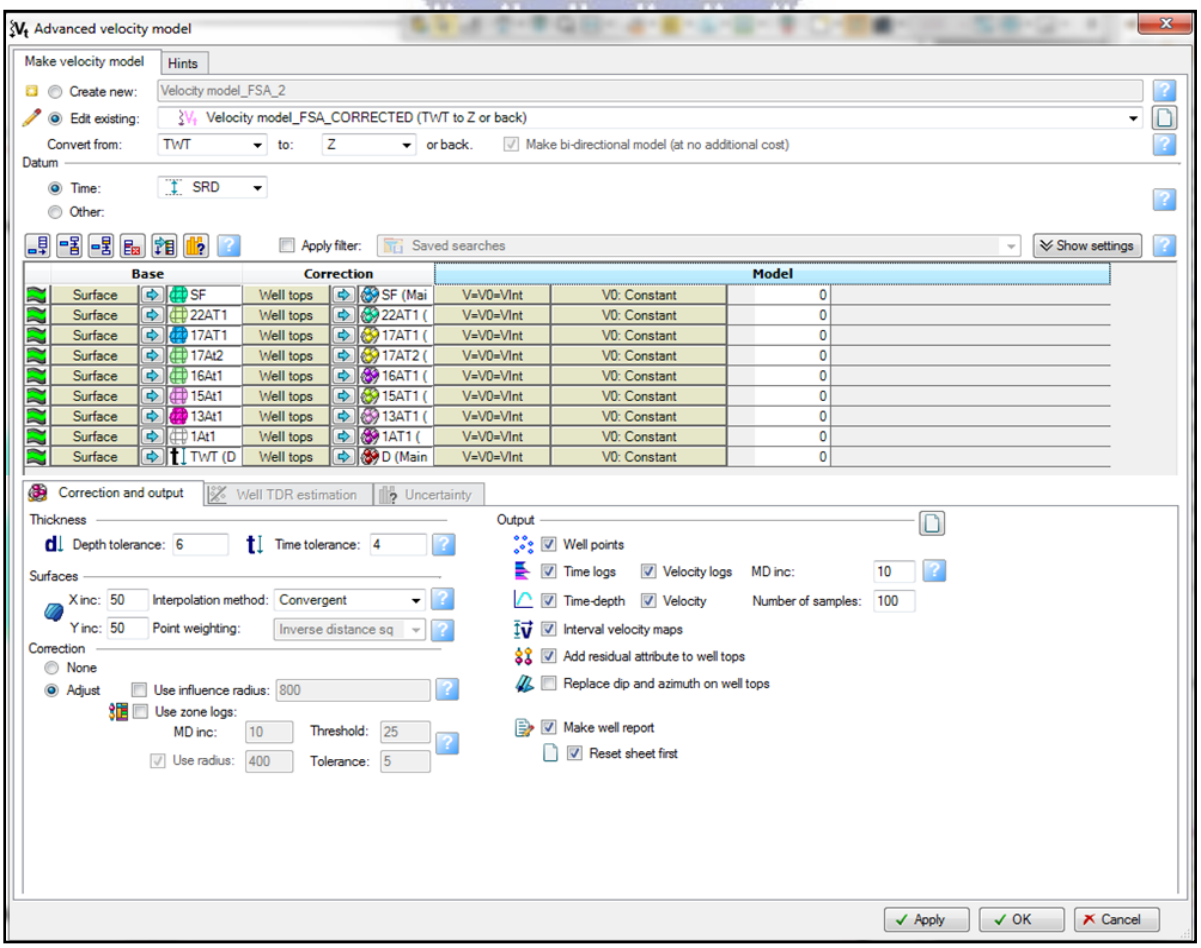

http://etd.uwc.ac.za/

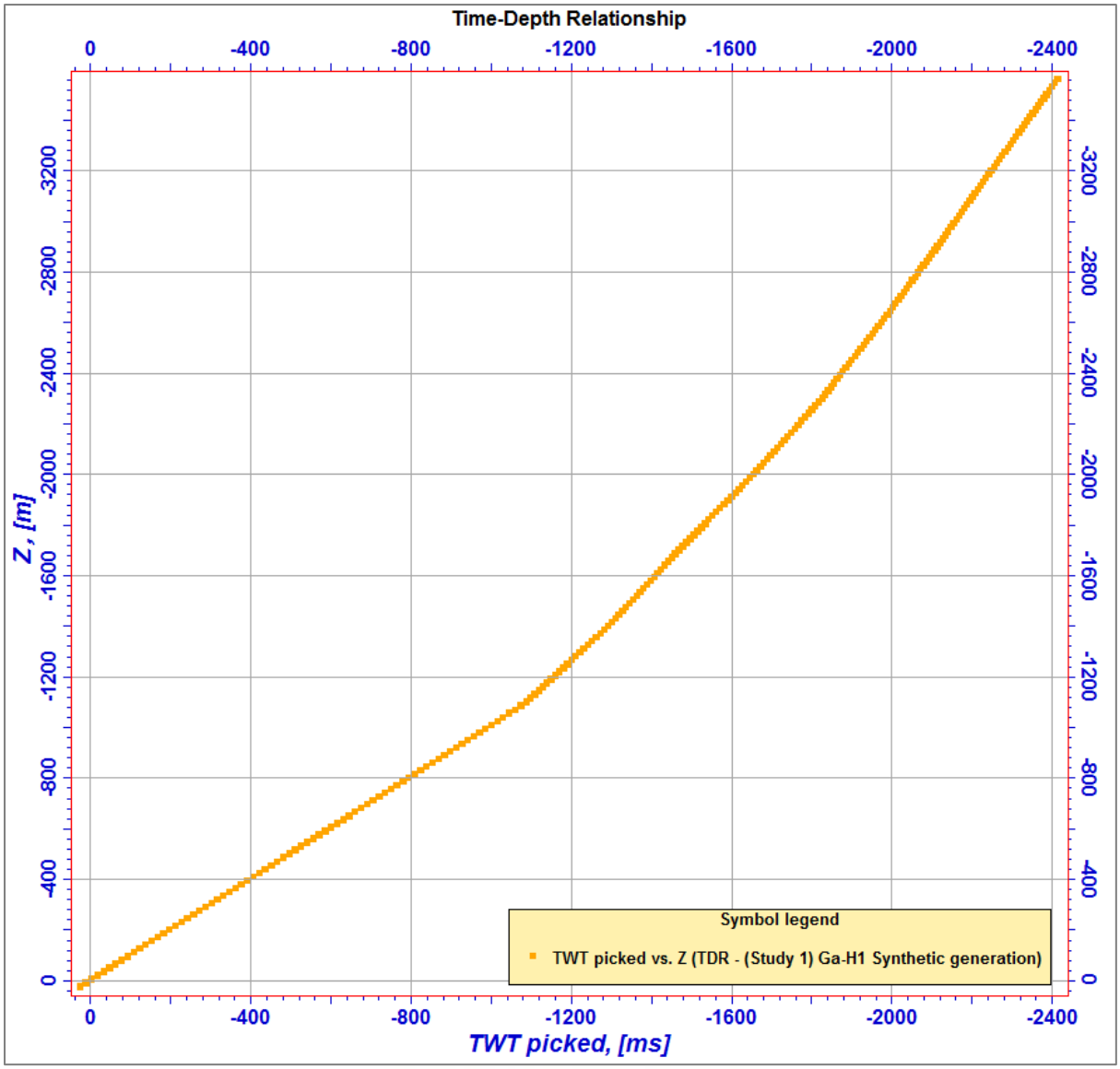

http://etd.uwc.ac.za/

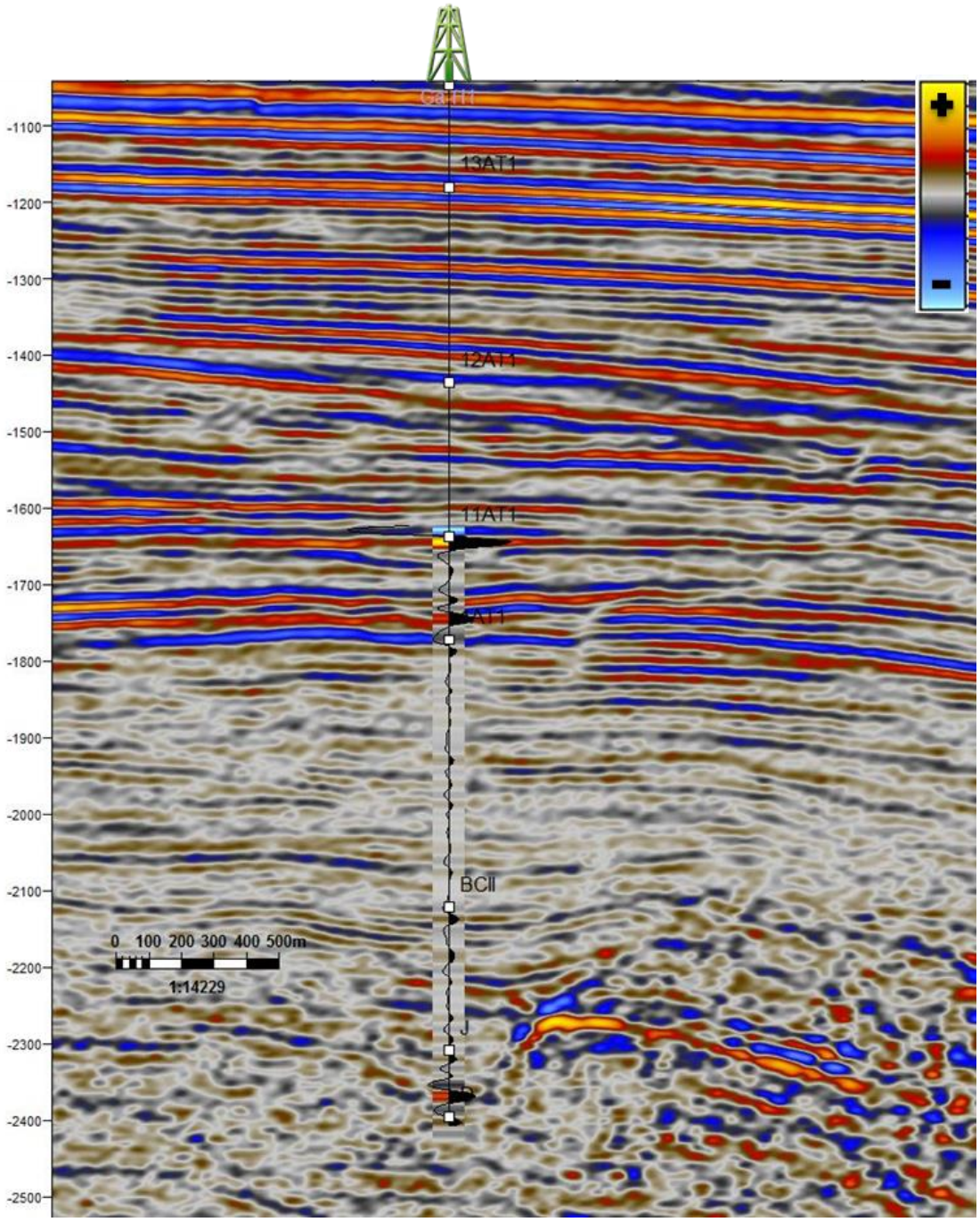

http://etd.uwc.ac.za/

Appendix B

Rock-Eval Pyrolysis Data

Well	Depth	Tmax	S1	S2	S1+S2	S3	S2/S3	TOC	HI	OI	TR
Ga-E1	2003.3	434	0.04	1.11	1.15	0.7	1.6	1.19	93.28	58.82	0.03
Ga-E2	2008.5	431	0.09	6.15	6.24	0.55	11.2	2.21	278.28	24.89	0.01
Ga-H1	1080	425	0.08	0.59	0.67	1.92	0.3	1.04	56.73	184.62	0.12
Ga-Q1	1530	428	0.02	0.55	0.57	1.33	0.4	1.04	52.88	127.88	0.04
Ga-Q1	1540	427	0.02	0.43	0.45	1.44	0.3	0.91	47.25	158.24	0.04
Ga-Q1	1550	424	0.03	0.97	1	1.25	0.8	1.1	88.18	113.64	0.03
Ga-Q1	1560	428	0.03	1.14	1.17	1.32	0.9	1.33	85.71	99.25	0.03
Ga-E1	2696	439	1.15	13.41	14.56	0.47	28.5	4.49	298.66	10.47	0.08
Ga-E2	2653	431	0.5	3.96	4.46	2.41	1.6	1.85	214.05	130.27	0.11
Ga-E2	2657	436	1.26	16.54	17.8	0.66	25.1	3.68	449.46	17.93	0.07
Ga-E2	2662	431	0.57	7.56	8.13	0.78	9.7	2.47	306.07	31.58	0.07
Ga-E2	2671	436	0.43	4.84	5.27	1.53	3.2	2.09	231.58	73.21	0.08
Ga-E2	2680	436	0.52	4.02	4.54	2.18	1.8	1.98	203.03	110.1	0.11
Ga-E2	2692	436	0.4	4.26	4.66	0.97	4.4	2.17	196.31	44.7	0.09
Ga-E2	2701	441	0.61	2.62	3.23	1.23	2.1	2.53	103.56	48.62	0.19
Ga-E2	2709	436	0.45	3.9	4.35	0.47	8.3	2.31	168.83	20.35	0.1
Ga-E2	2710	438	0.61	2.89	3.5	1.31	2.2	2.1	137.62	62.38	0.17
Ga-H1	1840	436	0.08	0.63	0.71	1.47	0.4	0.91	69.23	161.54	0.11
Ga-H1	1860	431	0.12	1.07	1.19	1.47	0.7	1.18	90.68	124.58	0.1
Ga-H1	1880	435	0.13	1.07	1.2	1.58	0.7	1.19	89.92	132.77	0.11
Ga-Q1	1700	425	0.04	2.54	2.58	5.61	0.5	1.77	143.5	316.95	0.02
Ga-Q1	1710	424	0.02	0.35	0.37	1.2	0.3	1.41	24.82	85.11	0.05
Ga-Q1	1740	424	0.03	0.5	0.53	1.19	0.4	1.4	35.71	85	0.06
Ga-Q1	1770	424	0.03	0.62	0.65	1.32	0.5	1.89	32.8	69.84	0.05
Ga-Q1	1800	428	0.05	0.5	0.55	1.39	0.4	1.63	30.67	85.28	0.09
Ga-Q1	1830	425	0.07	0.53	0.6	1.34	0.4	1.92	27.6	69.79	0.12
Ga-Q1	1860	424	0.03	0.42	0.45	1.31	0.3	1.65	25.45	79.39	0.07

UNIVERSITY of the WESTERN CAPE

http://etd.uwc.ac.za/

Ga-Q1	1890	424	0.03	0.4	0.43	1.27	0.3	1.69	23.67	75.15	0.07
Ga-Q1	1900	422	0.04	2	2.04	4.51	0.4	1.87	106.95	241.18	0.02
Ga-Q2	1830	426	0.04	0.64	0.68	1.41	0.5	1.62	39.51	87.04	0.06
Ga-Q2	1830	436	0.03	0.93	0.96	0.98	0.9	1.88	49.47	52.13	0.03
Ga-Q3	1840	426	0.07	1.34	1.41	1.1	1.2	1.94	69.07	56.7	0.05
Ga-Q2	1850	429	0.06	1.23	1.29	1.19	1	1.87	65.78	63.64	0.05
Ga-Q2	1860	433	0.1	1.64	1.74	0.96	1.7	1.96	83.67	48.98	0.06
Ga-Q2	1870	433	0.09	1.29	1.38	1.55	0.8	1.88	68.62	82.45	0.07
Ga-Q2	1880	433	0.09	1.38	1.47	1.55	0.9	1.89	73.02	82.01	0.06
Ga-Q2	1890	434	0.09	1.59	1.68	1.6	1	1.91	83.25	83.77	0.05
Ga-Q2	1900	434	0.09	1.42	1.51	1.33	1.1	1.95	72.82	68.21	0.06
Ga-Q2	1900	431	0.03	1.2	1.23	0.98	1.2	1.62	74.07	60.49	0.02
Ga-Q2	1910	429	0.1	1.42	1.52	1.32	1.08	1.88	75.53	70.21	0.07
Ga-Q2	1920	429	0.08	0.73	0.81	1.26	0.58	1.76	41.48	71.59	0.1
Ga-Q2	1930	426	0.1	1.35	1.45	1.49	0.91	1.79	75.42	83.24	0.07
Ga-Q2	1940	431	0.1	1	1.1	1.18	0.85	1.81	55.25	65.19	0.09
Ga-Q2	1940	431	0.04	0.83	0.87	0.24	3.46	1.42	58.45	16.9	0.05
Ga-Q2	1950	427	0.17	1.08	1.25	1.75	0.62	1.8	60	97.22	0.14
Ga-Q2	1960	429	0.09	1.12	1.21	1.49	0.75	1.81	61.88	82.32	0.07
Ga-Q2	1970	429	0.1	1.11	1.21	1.12	0.99	1.83	60.66	61.2	0.08
Ga-Q2	1980	429	0.11	1.04	1.15	1.25	0.83	1.74	59.77	71.84	0.1
Ga-Q2	1990	431	0.09	1.03	1.12	1.07	0.96	1.75	58.86	61.14	0.08
Ga-Q2	2000	431	0.26	2.95	3.21	5.8	0.51	2.02	146.04	287.13	0.08
Ga-Q2	2000	429	0.12	0.97	1.09	1.24	0.78	1.78	54.49	69.66	0.11
Ga-Q2	2005	424	0.19	1.36	1.55	0.29	4.69	2.03	67	14.29	0.12
Ga-Q2	2033	429	0.43	10.46	10.89	0.8	13.08	2.62	399.24	30.53	0.04
Ga-Q2	2040	431	0.21	3.11	3.32	1.37	2.27	1.85	168.11	74.05	0.06
Ga-Q2	2050	428	0.38	6.2	6.58	1.26	4.92	2.01	308.46	62.69	0.06
Ga-Q2	2060	431	0.22	4.3	4.52	1.6	2.69	1.68	255.95	95.24	0.05
Ga-H1	2180	432	0.09	0.64	0.73	1.12	0.57	0.63	101.59	177.78	0.12
Ga-H1	2210	431	0.1	1.21	1.31	0.53	2.28	0.66	183.33	80.3	0.08

UNIVERSITY of the WESTERN CAPE

http://etd.uwc.ac.za/

Ga-H1	2220	432	0.11	0.5	0.61	1.25	0.4	0.61	81.97	204.92	0.18
Ga-E2	2842	439	0.5	1.82	2.32	1.26	1.44	1.99	91.46	63.32	0.22
Ga-E2	2851	441	0.79	3.9	4.69	0.91	4.29	1.95	200	46.67	0.17
Ga-E2	2851	455	0.52	1.59	2.11	0.88	1.81	1.91	83.25	46.07	0.25
Ga-E2	2860	440	0.59	2.22	2.81	0.69	3.22	2.11	105.21	32.7	0.21
Ga-E2	2872	436	0.88	3.46	4.34	0.6	5.77	2.39	144.77	25.1	0.2
Ga-E2	2884	439	0.62	2.1	2.72	0.44	4.77	1.89	111.11	23.28	0.23
Ga-E2	2890	441	0.61	2.29	2.9	0.56	4.09	2.06	111.17	27.18	0.21
Ga-E2	2900	444	0.36	1.87	2.23	1	1.87	1.47	127.21	68.03	0.16
Ga-E2	2902	442	0.5	1.96	2.46	0.71	2.76	2.14	91.59	33.18	0.2
Ga-E2	2911	440	0.69	1.98	2.67	0.52	3.81	1.92	103.13	27.08	0.26
Ga-E2	2920	440	0.8	1.9	2.7	0.57	3.33	2.01	94.53	28.36	0.3
Ga-E2	2925	444	0.54	2.52	3.06	0.88	2.86	1.63	154.6	53.99	0.18
Ga-E2	2932	455	0.7	2.43	3.13	0.94	2.59	2.02	120.3	46.53	0.22
Ga-E1	2717	432	0.68	6.05	6.73	0.65	9.31	2.93	206.48	22.18	0.1
Ga-E1	2724	429	1.31	4.21	5.52	0.67	6.28	2.77	151.99	24.19	0.24
Ga-E1	2726	431	0.12	0.91	1.03	0.79	1.15	1.44	63.19	54.86	0.12
Ga-E1	2756	437	0.27	1.66	1.93	0.46	3.61	1.82	91.21	25.27	0.14
Ga-E1	2768	439	0.33	1.91	2.24	0.46	4.15	1.88	101.6	24.47	0.15
Ga-E1	2777	437	0.38	1.82	2.2	0.48	3.79	1.82	100	26.37	0.17
Ga-E1	2789	437	0.36	1.92	2.28	0.59	3.25	1.94	98.97	30.41	0.16
Ga-E2	3172	422	0.27	4.59	4.86	2.69	1.71	2.01	228.36	133.83	0.06
Ga-E2	3190	433	0.75	15.47	16.22	2.8	5.53	3.6	429.72	77.78	0.05
Ga-Q1	1980	433	0.14	2.38	2.52	0.89	2.67	1.39	171.22	64.03	0.06
Ga-Q1	1988	434	0.21	5.81	6.02	0.47	12.36	2.1	276.67	22.38	0.03
Ga-Q1	1990	436	0.13	2	2.13	0.95	2.11	1.44	138.89	65.97	0.06
Ga-Q1	1999	426	0.23	3.1	3.33	0.22	14.09	1.77	175.14	12.43	0.07
Ga-Q1	2000	433	0.14	2.68	2.82	0.84	3.19	1.56	171.79	53.85	0.05
Ga-Q1	2010	433	0.13	2.52	2.65	0.86	2.93	1.32	190.91	65.15	0.05
Ga-Q1	2020	426	0.11	1.5	1.61	0.76	1.97	1.17	128.21	64.96	0.07
Ga-H1	3221	427	0.44	1.65	2.09	1.22	1.35	0.79	208.86	154.43	0.21

UNIVERSITY of the
WESTERN CAPE

http://etd.uwc.ac.za/

Appendix C

Source Rock Analysis Materials

***Table 1**: Petroleum potential and TOC quantities of an immature source rock; after Peters and Cassa, 1994 and Law, 1999*

Petroleum Potential	Organic Matter		
	TOC	Rock-Eval Pyrolysis	
	(wt. %)	S1	S2
Poor	0.0 - 0.5	0.0 - 0.5	0.0 - 2.5
Fair	0.5 -1.0	0.5 -1.0	2.5 - 5
Good	1.0 - 2.0	1.0 - 2.0	5 - 10
Very Good	2.0 - 4.0	2.0 - 4.0	10 - 20
Excellent	>4.0	>4.0	>20

***Table 2**: Kerogen type classification, based on source material, hydrogen index and general depositional environments; after Peters and Cassa, (1994), Law, (1999) and McCarthy et al., (2011)*

Kerogen Type	Source Material	Hydrogen Index (HI) (mg HC/g TOC)	Predominant Hydrocarbon Potential	General Depositional Environment
I	Mainly Algae	> 600	Oil Prone	Lacustrine
II	Mainly Plankton, with some contribution from algae	300 - 600	Oil Prone	Dysoxic - Marine
II/III	Reworked Plankton - algae and Plants	200 - 300	Oil and Gas Prone	Marine
III	Mainly Higher Plants	50 - 200	Gas Prone	Terrestrial
IV	Reworked, Oxidized Material	< 50	Inert	Terrestrial (?)

http://etd.uwc.ac.za/

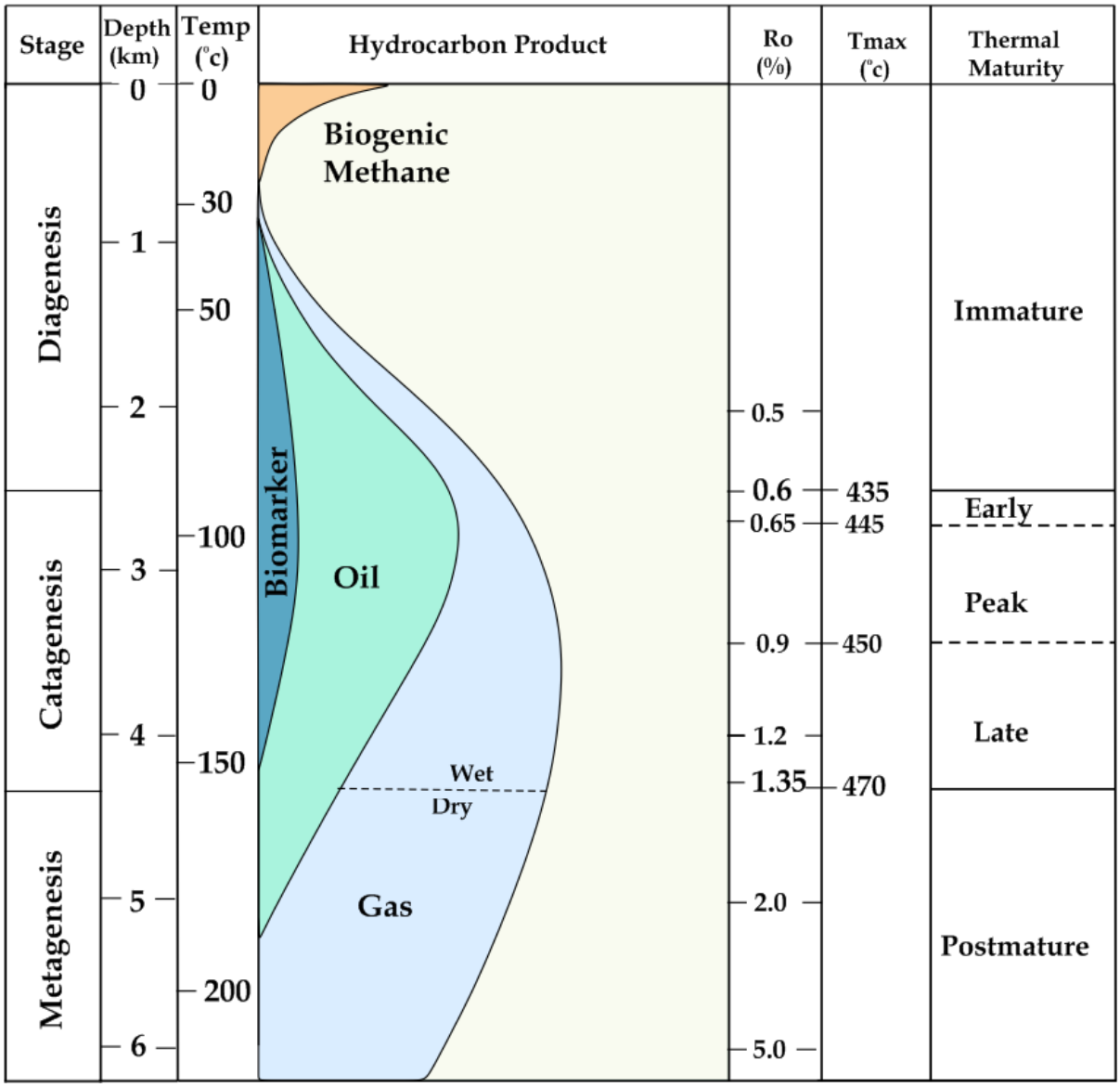

Figure 1: *General scheme of Kerogen transformation, maturation stages and hydrocarbon generation, with increase in burial depth and associated temperature, created after Tissot and Welte (1978).*

http://etd.uwc.ac.za/

Appendix D

Table 1. TOC range distribution values for the respective source rock intervals

Source Rock	TOC wt.%				Number of samples
	0.5 - 1.0	1.0 - 2.0	2.0 - 4.0	> 4.0	
Turonian	1	5	1	0	7.0
Aptian	1	34	9	1	45.0
Hauterivian	3	8	12	0	23.0
Valanginian	0	10	3	0	13.0
Kimmeridgian	1	0	0	0	1.0
	% values				
Turonian	14.3	71.4	14.3	0	7.0
Aptian	2.22	75.6	20	2.22	45.0
Hauterivian	13.0	34.8	52.2	0	23.0
Valanginian	0	76.9	23.1	0	13.0
Kimmeridgian	100	0	0	0	1.0

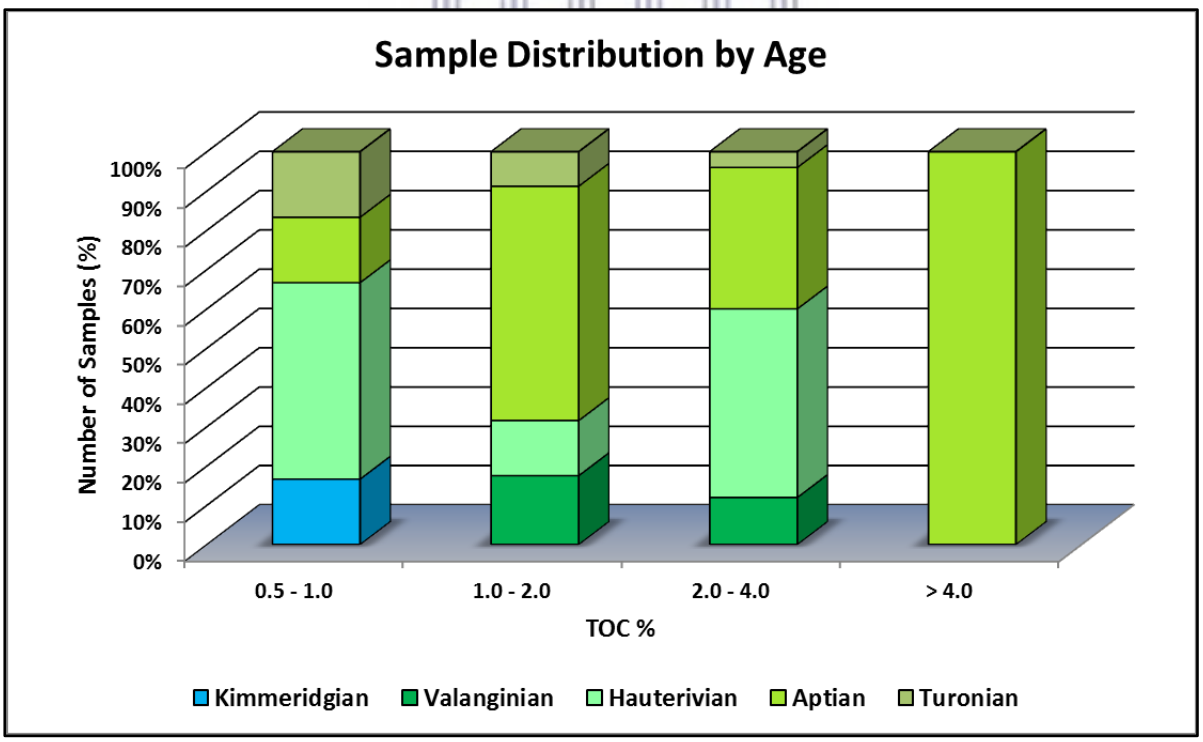

http://etd.uwc.ac.za/

- **Burial and thermal Plots with Property Overlay Maps**

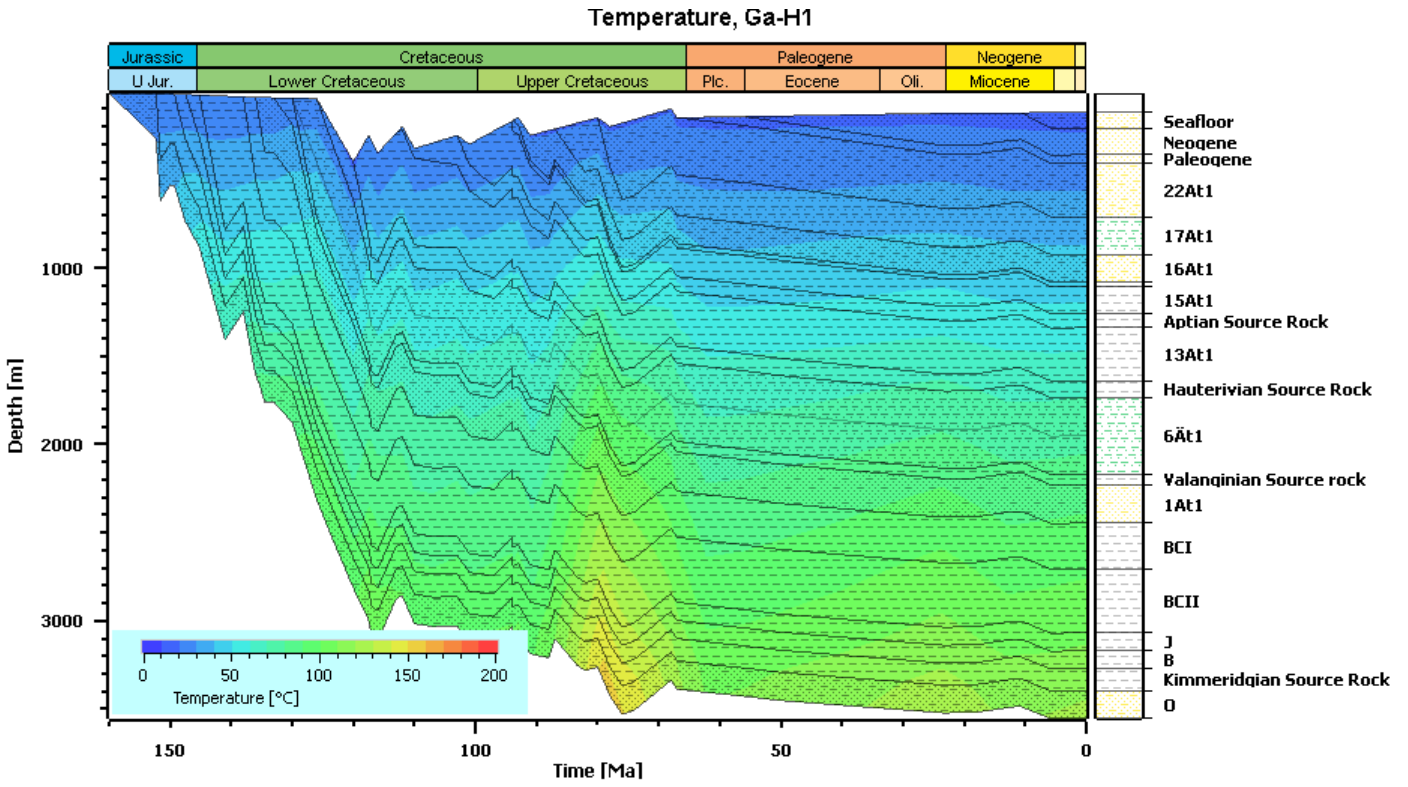

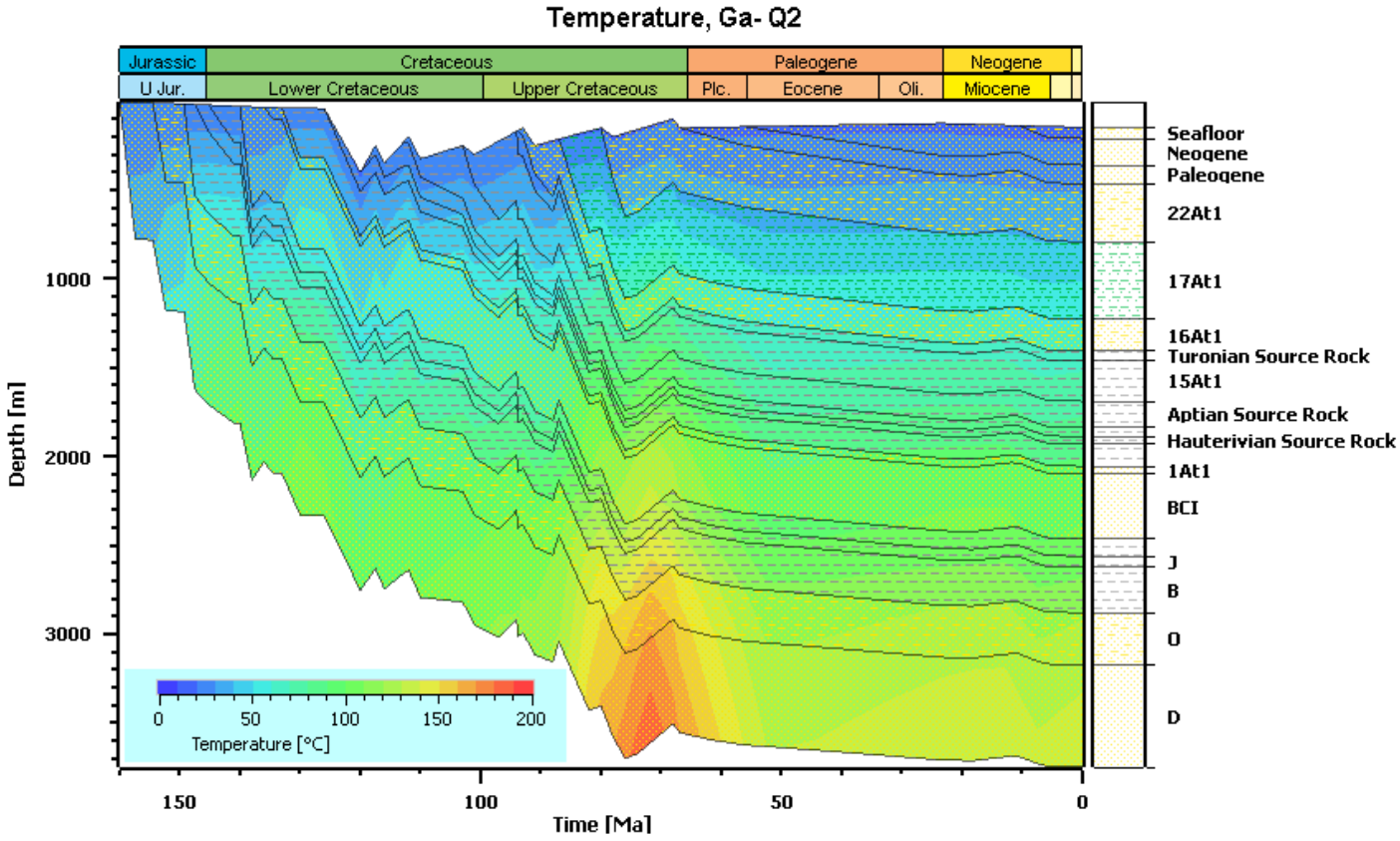

http://etd.uwc.ac.za/

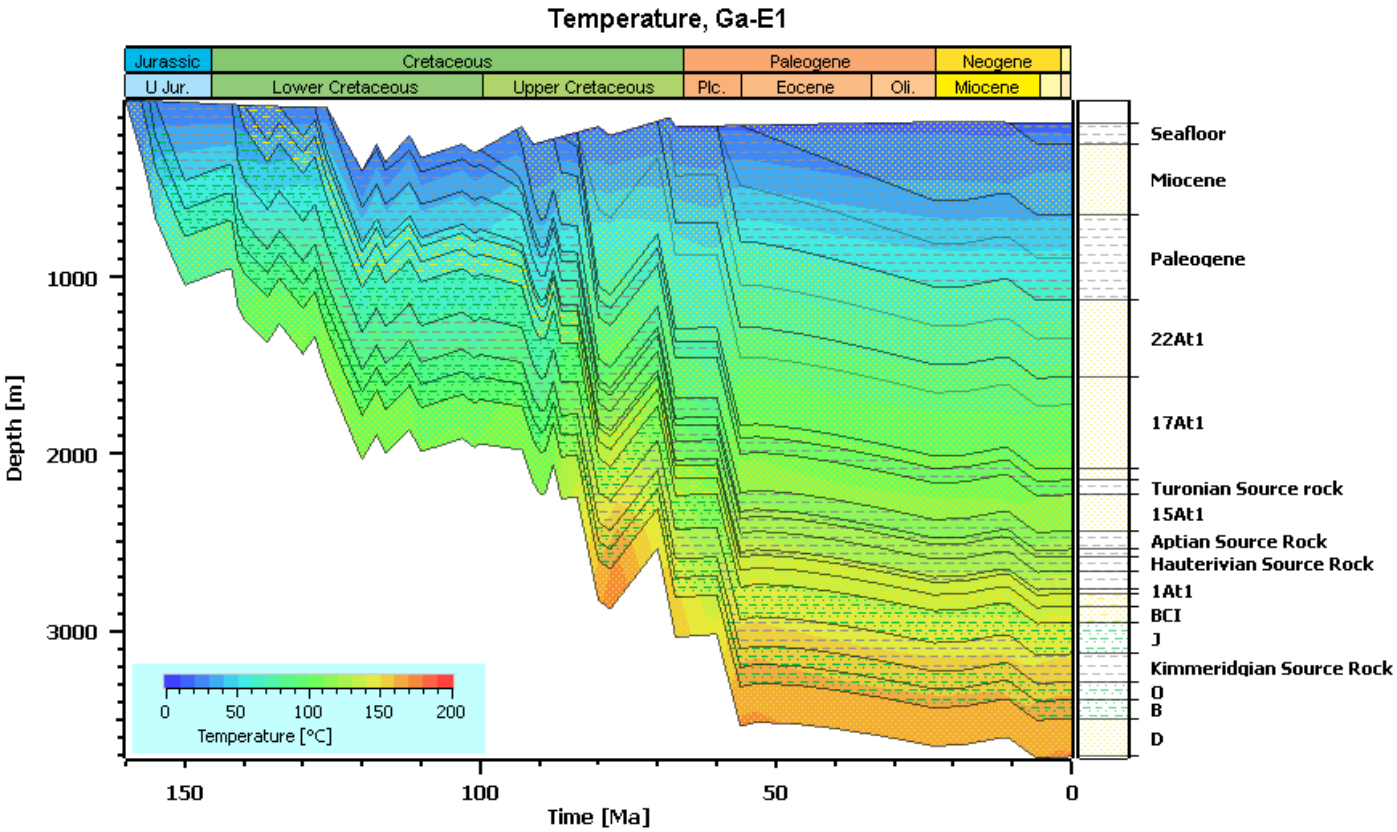

- **Thermal Maturation Plots**

UNIVERSITY of the
WESTERN CAPE

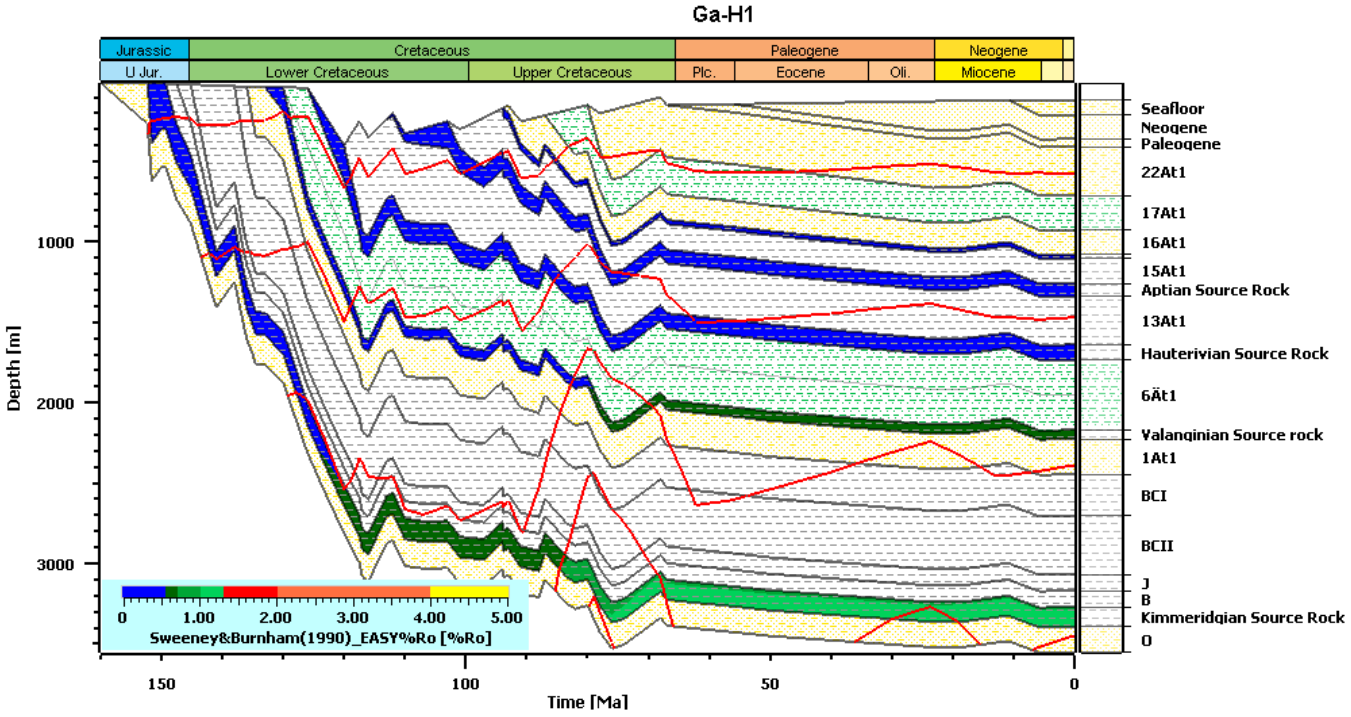

http://etd.uwc.ac.za/

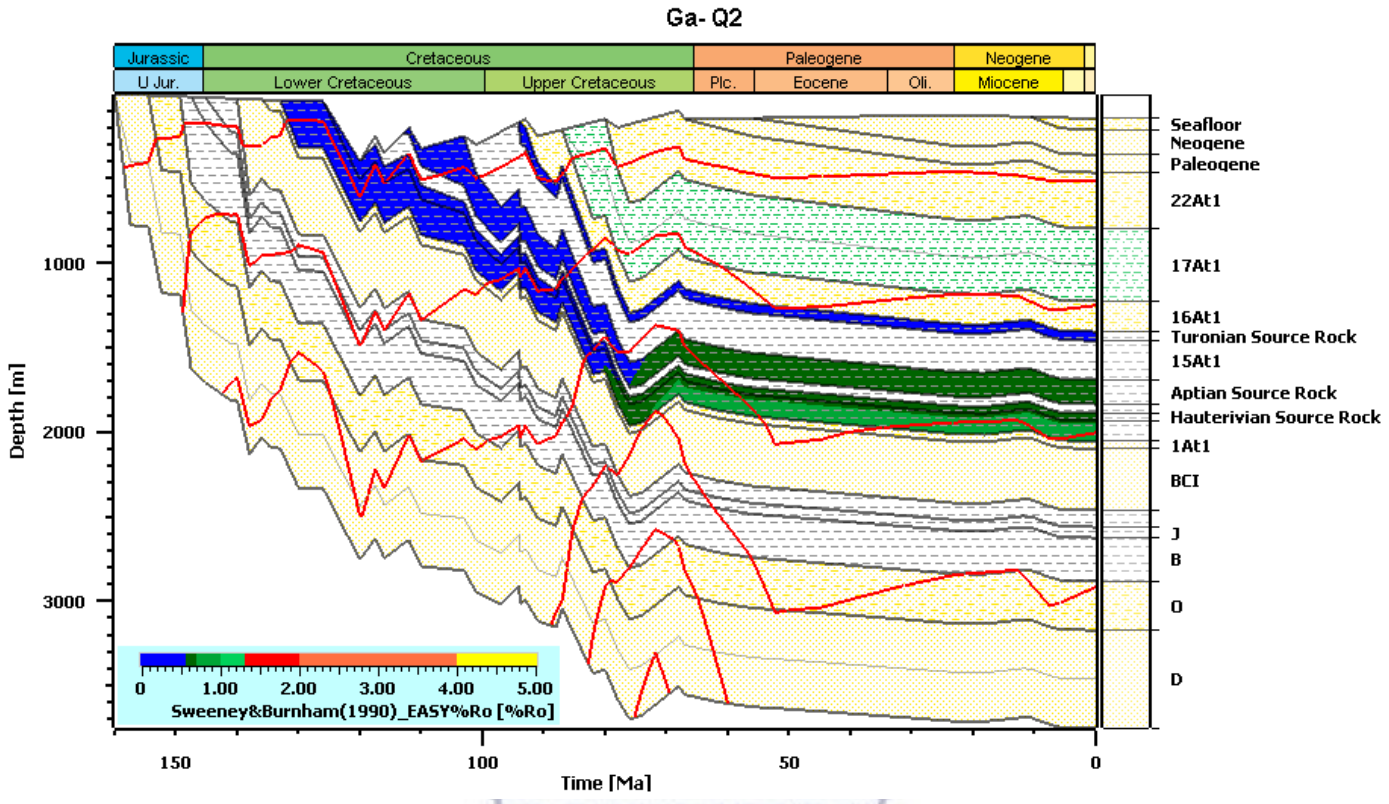

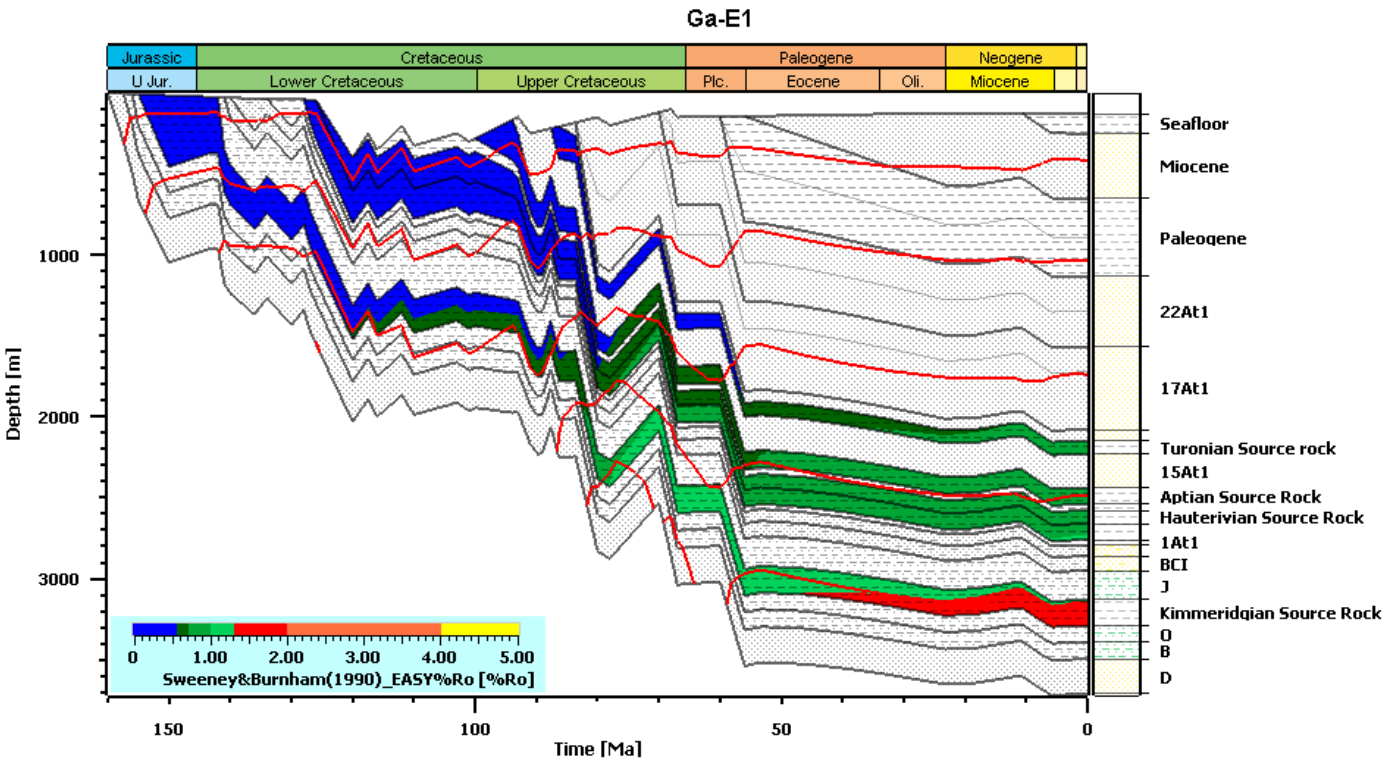

http://etd.uwc.ac.za/

- **Transformation Ratio**

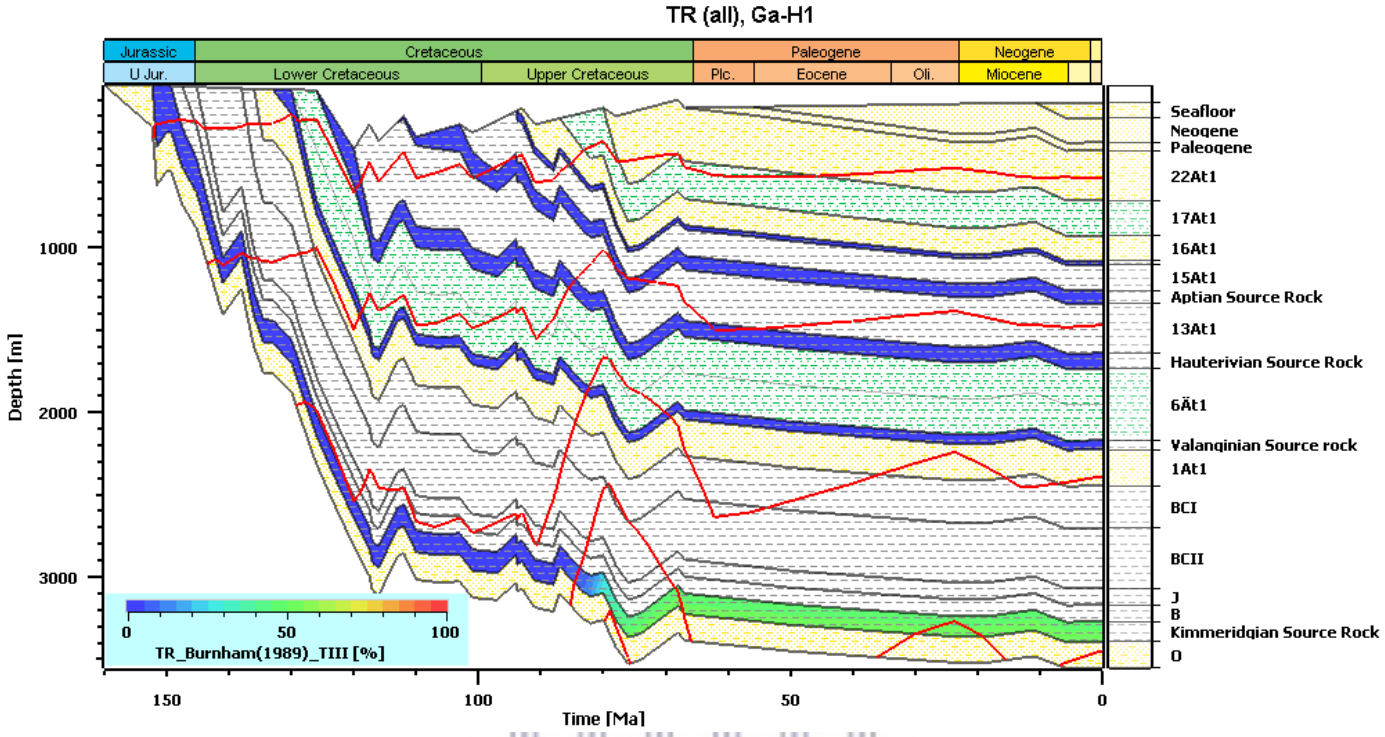

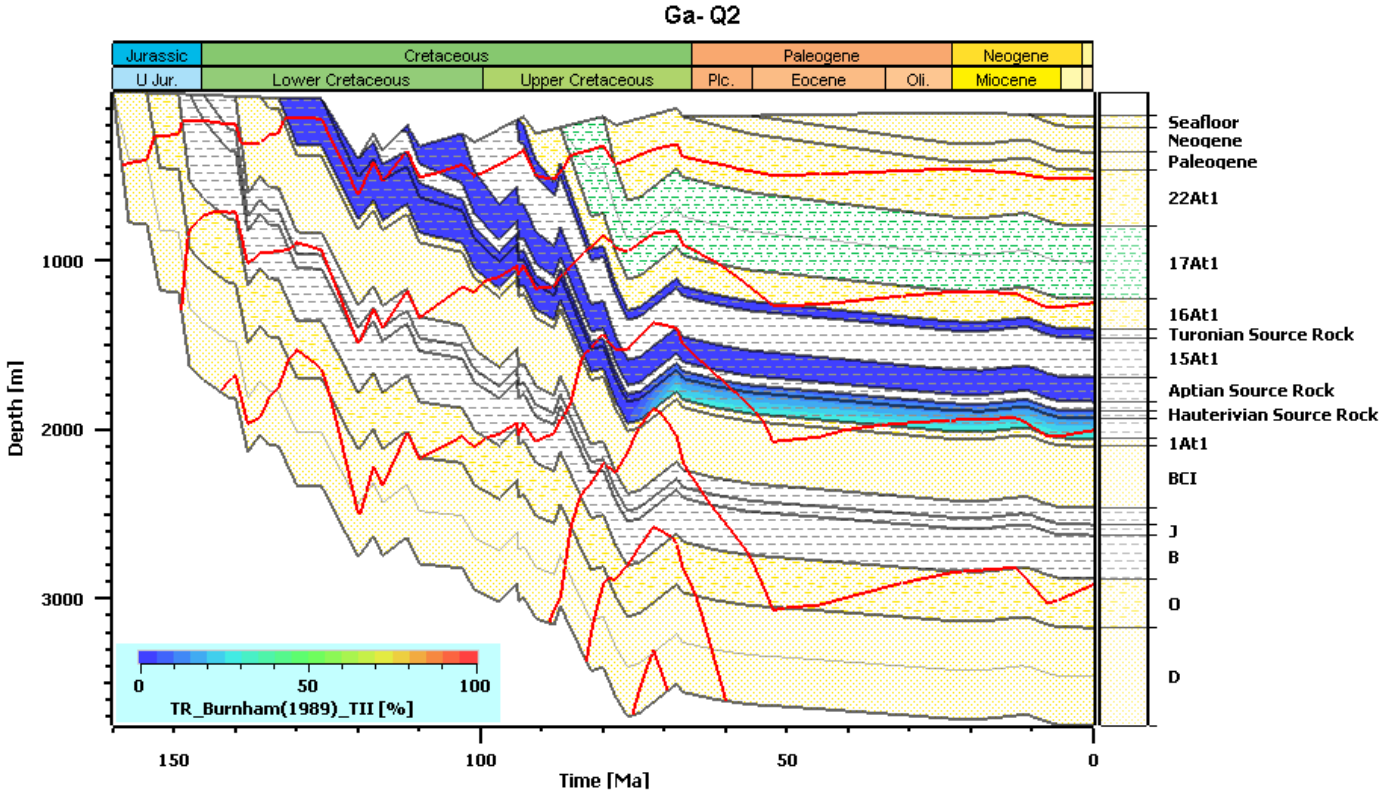

http://etd.uwc.ac.za/

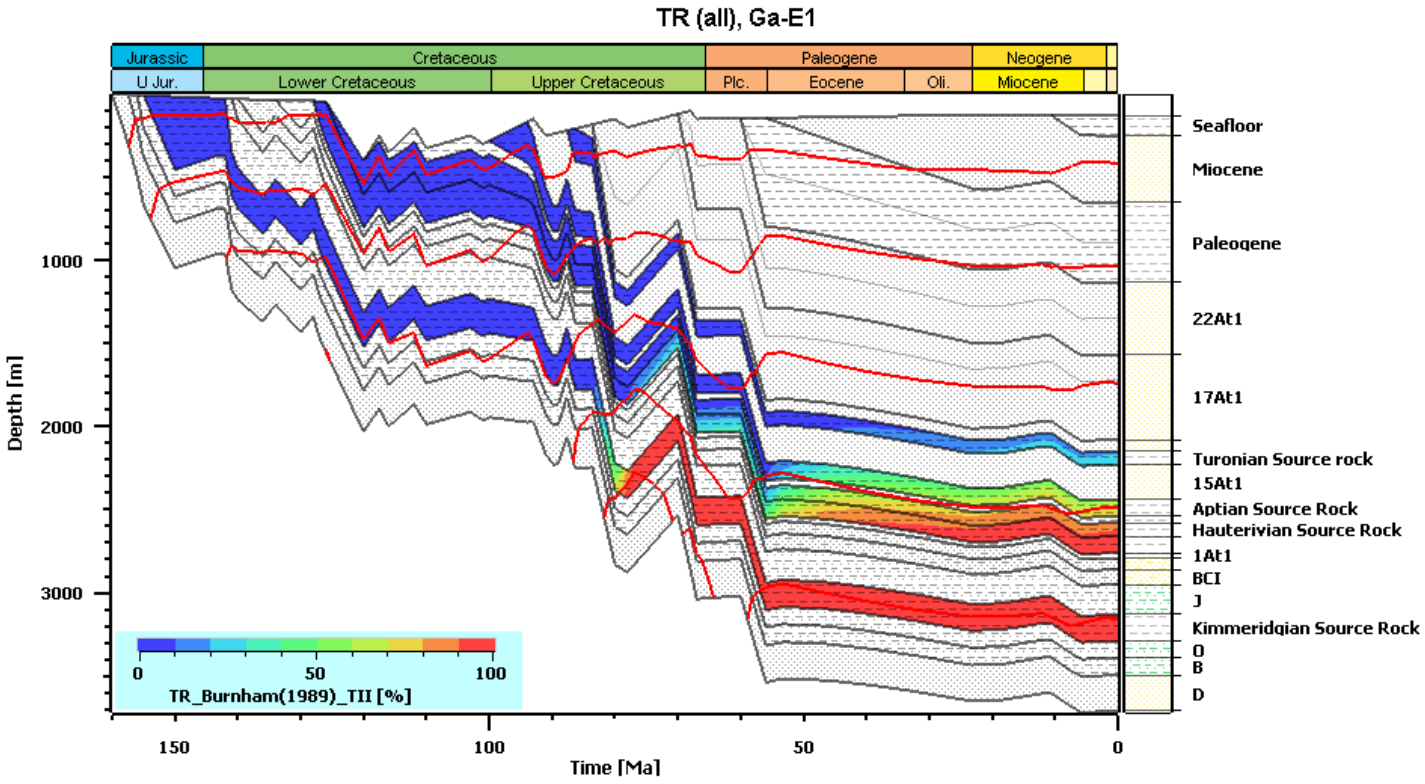

UNIVERSITY of the
WESTERN CAPE

http://etd.uwc.ac.za/